Deliverable 2.5: Uncertainties and environmental impact dependencies on array changes

University College Cork, France Energy Marines,

in collaboration with: Aalborg University, the University of Edinburgh, Sandia, ITPower

This project has received funding from the European Union's Seventh Programme for research, technological development and demonstration under grant agreement No 608597

D2.5: Uncertainties and environmental impact dependencies on array changes: the uncertainties and environmental impact dependencies on array changes.
Project: DTOcean - Optimal Design Tools for Ocean Energy Arrays
Code: DTO_WP2_ECD_D2.5

	Name	**Date**
Prepared	Work Package 2	08/12/15
Checked	Work Package 9	16/12/15
Approved	Project Coordinator	21/12/15

The research leading to these results has received funding from the European Community's Seventh Framework Programme under grant agreement No. 608597 (DTOcean).

DOCUMENT CHANGES RECORD			
Edit./Rev.	*Date*	*Chapters*	*Reason for change*
A/0	24/08/2015	Draft - All	New Document
A/1		Draft - All	First draft UCC-AAU-FEM
A/2		All	Review by UEDIN
A/3		All	Amendment_correction
A/4		All	Review 2 by UEDIN
A/5		All	Final document

Abstract

This report presents Deliverable 2.5 – Uncertainties and environmental impact dependencies on array changes: the uncertainties and environmental impact dependencies on array changes. This document includes content about wave and tidal uncertainties as well as environmental issues related to array design.

For wave uncertainties, this document describes the main theoretical limitations with particular regards to the inviscid and irrotational flow, water depth, linearized wave-structure interaction problem and wave field representation. The error analysis section deals with the influence of bathymetry in the wave resource as well as the influence of wave directional spreading in hydrodynamic interaction. Statistical and deterministic approaches are also described in order to address the environmental input uncertainties and how these uncertainties are reflected in the wave sub module output.

Theoretical limitations for tidal technology uncertainties are discussed considering flow field modelling, wake interactions, horizontal-boundary assumptions, vertical-dimension assumptions and device yawing. The error analysis is mainly based on the PerAWaT flume experiments.

Environmental issues are firstly discussed through a synoptic review of energy extraction, collision risks, turbidity, underwater noise, chemical pollution as well as potential beneficial effects such as reef effect, reserve effect and resting place. General and specific (based on a scenario) recommendations are then given in order to minimize environmental impacts. Finally, the Environmental Impact Assessment Module (EIAM) is also described with its main functions related to environmental impact dependencies on array changes.

TABLE OF CONTENTS

TABLE OF CONTENTS

TABLES INDEX

Description *Page*

FIGURES INDEX

Description *Page*

FIGURES INDEX

Description *Page*

1 INTRODUCTION - WAVE AND TIDAL MODEL UNCERTAINTIES

Content of this section refers to the WP2 hydrodynamic sub-package at beta development stage and therefore with reduced functionalities with respect to the final release of the DTOcean tool.

WP2 sub-package consists of a single interface capable of dealing with both wave and tidal scenarios. This section will describe what are the main theoretical limitations and assumptions that come from searching a trade-off between accuracy in representing at best the hydrodynamics and the need to keep the computational time low as the sub-package will be eventually embedded in the DTOcean global optimization algorithm.

The word uncertainties used thereafter is a broad definition and has to be understood as a number of investigations on the outcome of the model due to change of specific key input parameters (i.e. sensitivity analysis). This allows to gain a better understanding of the response of the model and to verify the goodness of the theoretical modelling choices made.

Sensitivity analysis tests are carried out for both wave and tidal scenarios.

For the wave model, the influence on power output of the bathymetry and spectrum directional spreading are investigated. Moreover a sensitivity analysis on the Array Annual Energy Production (AAEP) is performed by simply scaling the power input (i.e. scatter diagrams) within a fixed range. Also a simplified statistical model is applied in order to gain a better insight on what the influence of resource variability is on the AAEP. Data have been anonymised for confidentiality reasons.

For the tidal model, due to a lack of empirical data available for validation, a protocol of tests based on comparison to the PerAWaT project is described, should the PerAWaT data become available in the future. In similar fashion to the tidal model, a sensitivity analysis on AAEP is carried out varying two key resource parameters: turbulence intensity and tidal stream velocity.

2 WAVE MODEL

2.1 Wave Model Limitation and Uncertainties

In order to solve a large number of cases in a relatively small amount of time, the wave submodule has been built on a series of assumptions, detailed in D2.3, which constrain the field of validity of the solution. In the following, the known theoretical limitations are first given and detailed, then the error introduced by two limitations are further analysed using a code to code comparison.

2.1.1 Theoretical assumptions

In Table 2-1, the predominant theoretical limitations embedded in the formulation of the wave submodule are listed and further described hereafter.

Table 2-1: Limitations of the wave submodule stemming from the assumptions made in the theoretical formulation.

Assumption	**Limitation**
Inviscid flow.	Viscous forces are disregarded (only gravity forces).
Irrotational flow.	Vorticity is zero (thin boundary layer in good agreement with inviscid flow).
Constant water depth.	The bathymetric changes are disregarded.
Linearization of the boundary conditions on the free surface.	Amplitudes of the waves are much smaller than the wave length.
Linearization of the boundary condition on the WEC surface.	Amplitude of the WECs motion is much smaller than the wave length.
Wave field representation outside and immediate neighbourhood of a WEC in the array.	The wave field inside the enclosing cylinder is not valid. The cylinders enclosing the WECs do not overlap vertically.
Frequency domain analysis.	The PTO system is a linear damper. Nonlinear forces are disregarded.

2.1.1.1 Inviscid and irrotational flow

The viscosity of water is known to be low compared to other Newtonian fluids such as honey, oil or gasoline. Therefore, treating the flow of water as inviscid is usually well-accepted, which makes the wave-WEC array interaction problem easier to solve. However, since the water does have some viscosity, assuming inviscid flow will invariably introduce some inaccuracy in the results.

The viscous effects are confined within a region called the boundary layer, close to the fluid boundaries. In this region shear stresses will arise between fluid-fluid and fluid-solid contact surfaces with the consequent development of vortices (rotational flow) and a resultant integrated drag (friction drag) and lift forces on the solid.

For water-waves the boundary layer is known to remain thin and thus the developed flow is usually modelled as inviscid and irrotational. However, when water-waves interact with an array of WECs such assumption may no longer be valid.

The viscous effects on WECs are usually taken into account by means of a quadratic drag force approximation which involves a drag coefficient determined from experimental data. Hence, the user may choose the convenience of inviscid and irrotational flow assumptions by comparing the approximated drag force against the hydrodynamic forces from linearized potential flow theory (excitation and radiation forces).

It must also be mentioned that since the drag force is quadratic with the fluid-solid velocity and the WP2 tool solves the equation of motion in the frequency domain, the quadratic drag force is not considered herein.

2.1.1.2 Constant water depth

Bathymetric changes are not considered. This assumption is well agreed for deep water waves but it might not be valid when dealing with WECs set up in intermediate or shallow water depths. Therefore, the user may choose the convenience of constant water depth assumption by assessing the deviation between the input water depth and the actual bathymetry in cases of intermediate or shallow water waves.

2.1.1.3 Linearized wave-structure interaction problem

Linearization of the problem requires the waves and the WECs motion amplitude to be small compared with the wave length. The validity of this assumption can only be decided by the user. The user may choose the convenience of the assumption of linearity by comparing the actual waves in use for the analysis with a linear wave. In other words, if the actual waves are not well represented by cosine waves, the WP2 tool will produce inaccurate results.

2.1.1.4 Wave field representation

The wave field solution used in the WP2 tool to further compute wave forces on WECs is valid outside a virtual cylinder enclosing each WEC of the array. Therefore, the WECs throughout the array must not overlap vertically, otherwise the interaction forces between the intersecting WECs will come from an invalid wave field representation. The user should take into account that the virtual cylinders enclosing the WECs cannot intersect at any point.

2.1.2 Model limitations

Two of the previously mentioned limitations of the wave submodule are analysed below in order to quantify the error introduced into the solution. The error is evaluated from a code-to-code comparison due to a lack of validation data.

2.1.2.1 Influence of bathymetry in the wave resource

In order to deliver a fast-running tool, the estimation of the hydrodynamic forces for an array of WECs by the WP2 tool is based on the assumption of constant water depth. Therefore, the WP2 tool cannot

actually reproduce the wave transformations due to changes in water depth. Although this assumption is suitable for far-offshore arrays, it might not be valid for those arrays sitting close to the coast. For these arrays, the validity will be invariably related to the magnitude of change in water depth.

In order to assess the uncertainty of the predicted values by the WP2 tool due to varying water depth, a comparison of significant wave height (Hm0) values will be carried out between the WP2 tool and the MIKE 21 software. The MIKE 21 software solves the enhanced Boussinesq equations, which allows for the modelling of wave phenomena due to water depth variations.

The case study for the comparison to take place is an array of flap type fixed WECs, which span the water depth and which are hold fixed (i.e. they are not allowed to move). The flaps are modelled as rectangular boxes of dimension 10x2xh*m*, with h the water depth.

Three different bathymetric conditions are considered for comparison, which are reported in the following Table 2-2 :

Table 2-2: Description of the three different bathymetric cases used for the analyses.

MIKE 21 model	WP2 tool model
15*m* constant water depth.	15*m* constant water depth.
2.5% inclined bottom from 15*m* up to 11.9*m* water depth.	13.43*m* constant water depth.
5% inclined bottom from 15*m* up to 8.8*m* water depth.	11.87*m* constant water depth.

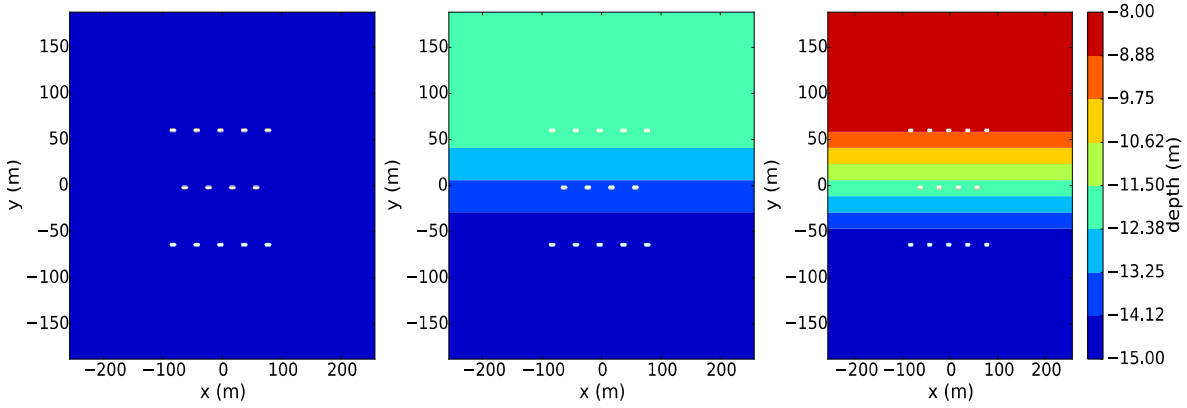

Figure 2-1: Water depth data for the three different bathymetric cases used for the analyses.

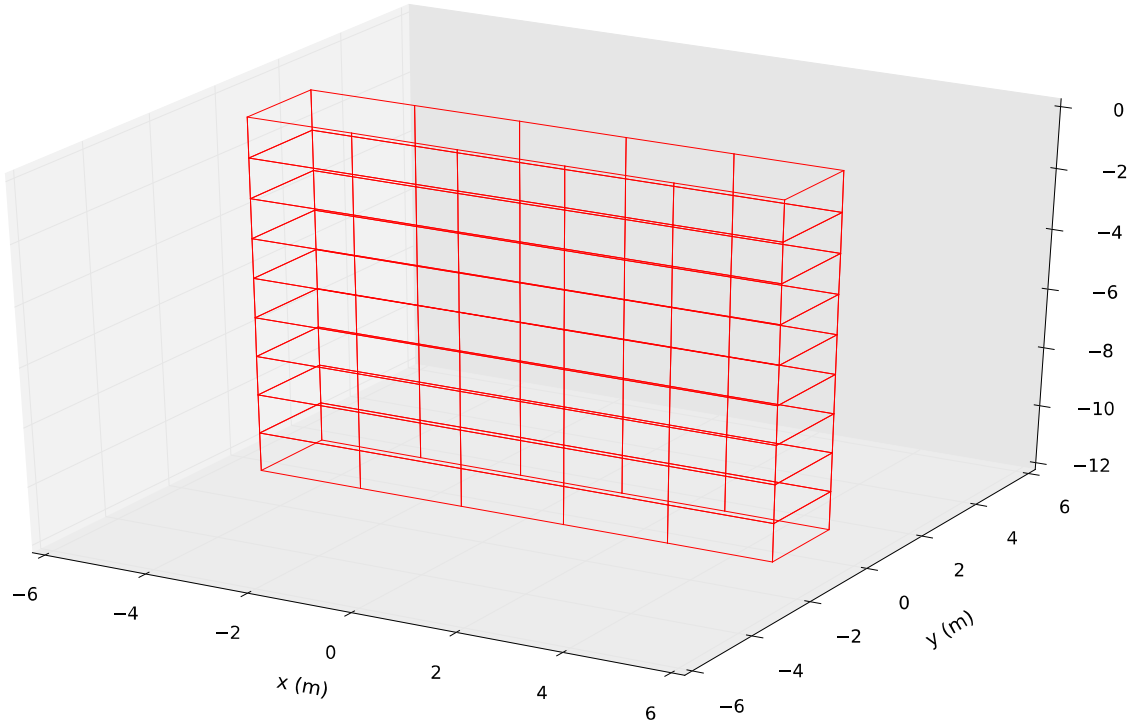

Figure 2-2: Mesh of the flap type WEC used to run the WP2 tool for the case of constant 15m water depth.

The mesh used to run the WP2 tool for the case of constant 15m water depth is shown in Figure 2-2 with the total number of panels being 108, regardless of the bathymetric case.

The rectangular cell size used to run the MIKE 21 software is 2x2m, so each flap takes exactly 5 cells. The flaps in MIKE 21 are modelled as fully reflective walls. With regard to the spatial discretization used to run the MIKE 21 software, this is illustrated in Figure 2-1.

The array consists of fourteen devices, equally-spaced by 40m and 62m towards the x and y–direction respectively. The array layout is staggered, made up by three rows of five-four-five devices with the central row shifted by 20m towards the x–direction. An illustration of the array layout can be seen in Figure 2-3.

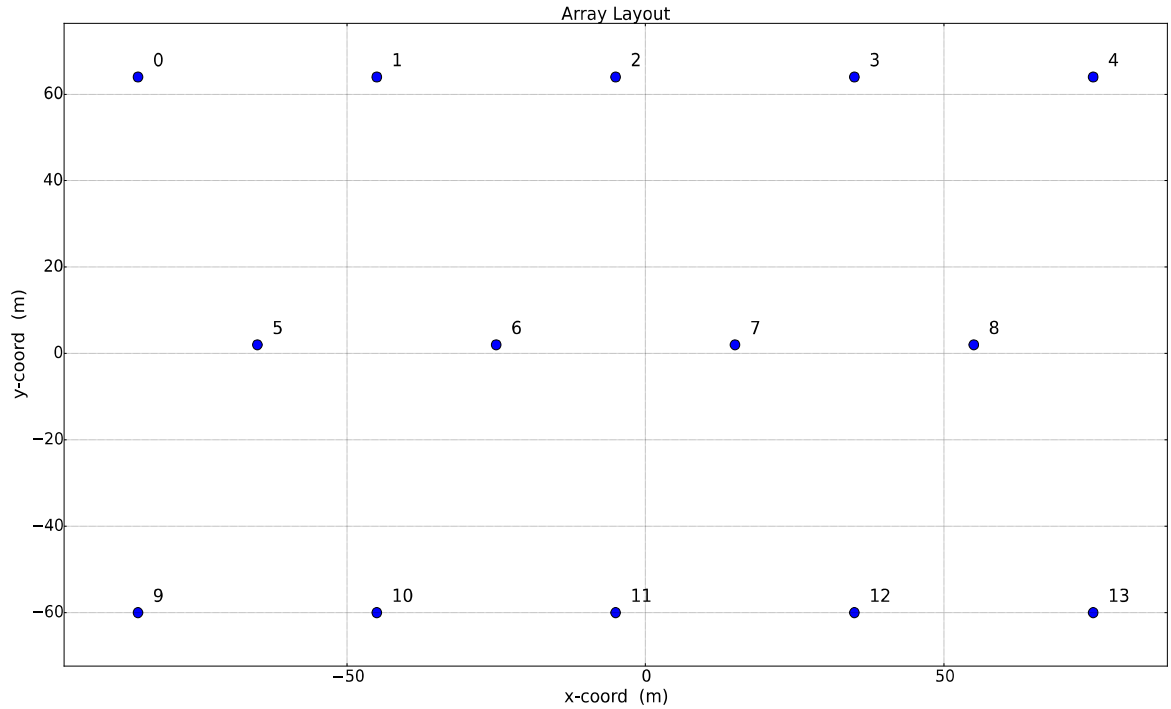

Figure 2-3: Array layout used for the analyses.

The y axis in Figure 2-1, Figure 2-2, and Figure 2-3 corresponds to the direction of propagation for the ambient waves, travelling from positive y to negative y, i.e. up-down in Figure 2-3

Besides the three bathymetric cases, five different sea state conditions will be studied. The ambient wave for each sea state condition will be generated using a Jonswap type spectrum, with Hm0 equal to 0.5 m, peak enhancement factor (γ) equal to 3.3 and peak periods 6, 7, 8, 9 and 10*s*. Moreover, a cut-off value for the maximum wave frequency is set at 1/4.39*Hz*, approximately 0.228*Hz*.

The spectral density values S_η for each of the sea state conditions are plotted in the following Figure 2-4:

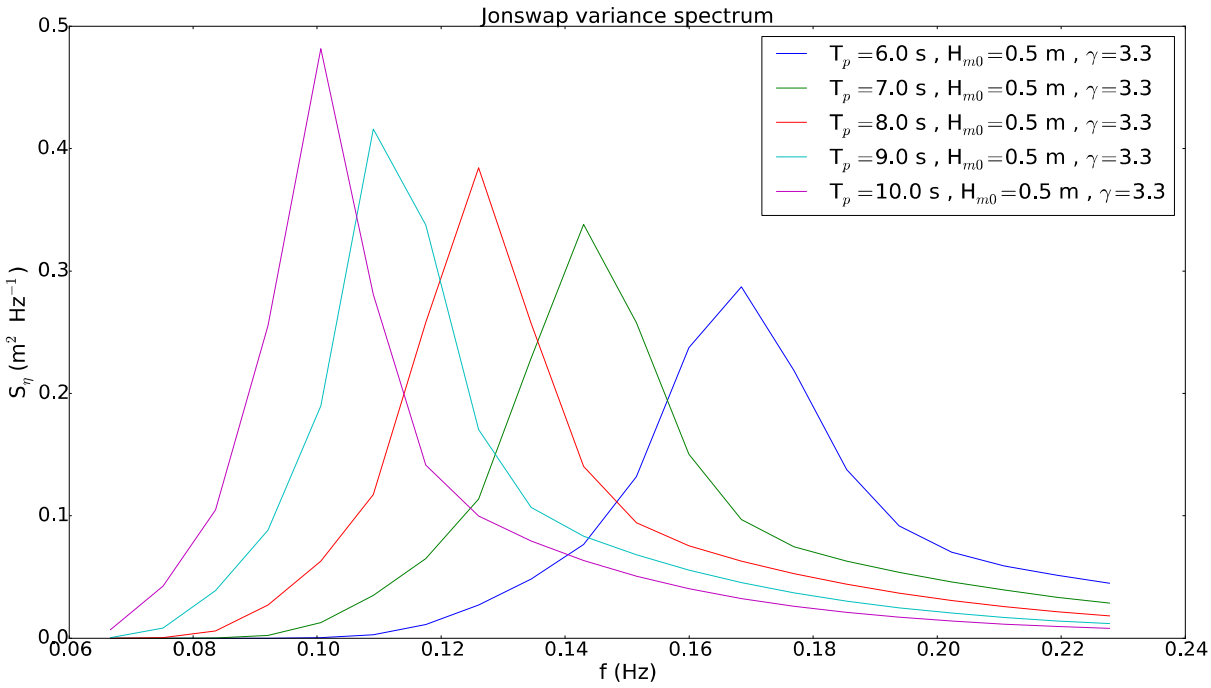

Figure 2-4: Jonswap variance spectrum for the five different sea states used for the analyses.

The wave data required to run the WP2 tool is reported in Table 2-3:

Table 2-3: Wave data used to run the WP2 tool.

Parameter	Initial Value	Final Value	Number of values	Units
Wave frequencies (frequency domain discretization)	0.067	0.228	20	*Hz*
Wave heading angles for the diffraction transfer matrix calculation	0	327,27	11	*deg*
Wave heading angles for the analyses	270	270	1	*deg*

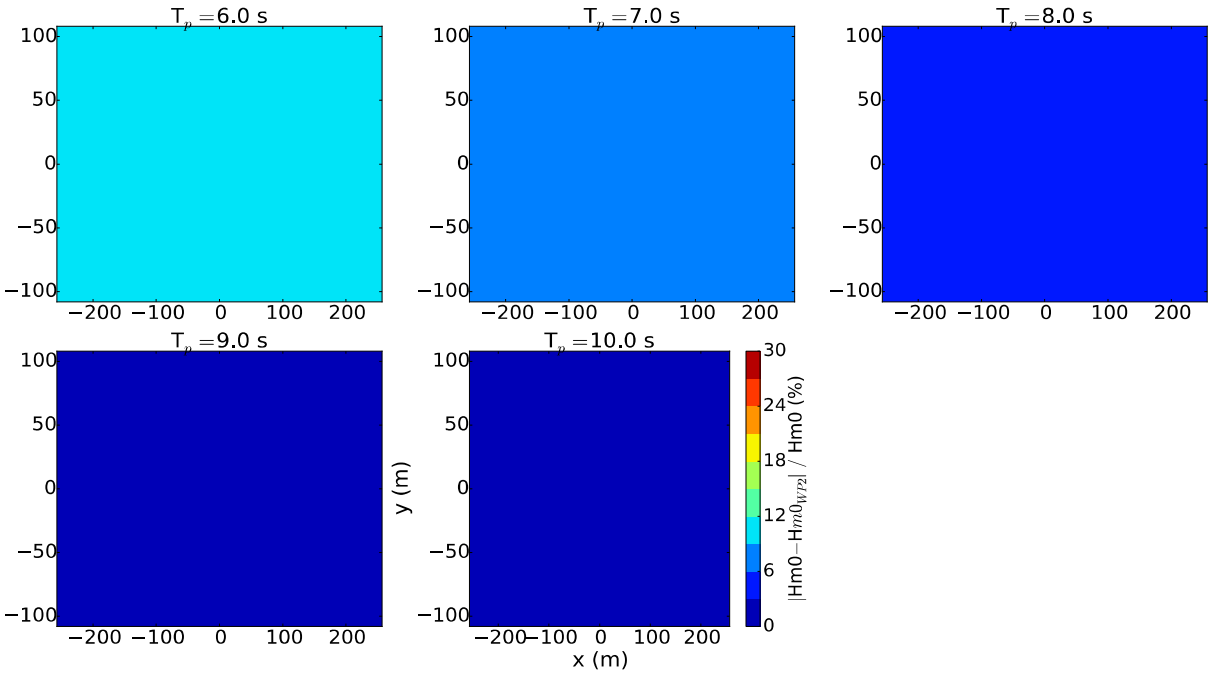

Figure 2-5: Relative error in the prediction of Hm0 by the WP2 tool for the case of constant 15m water depth and no WEC array.

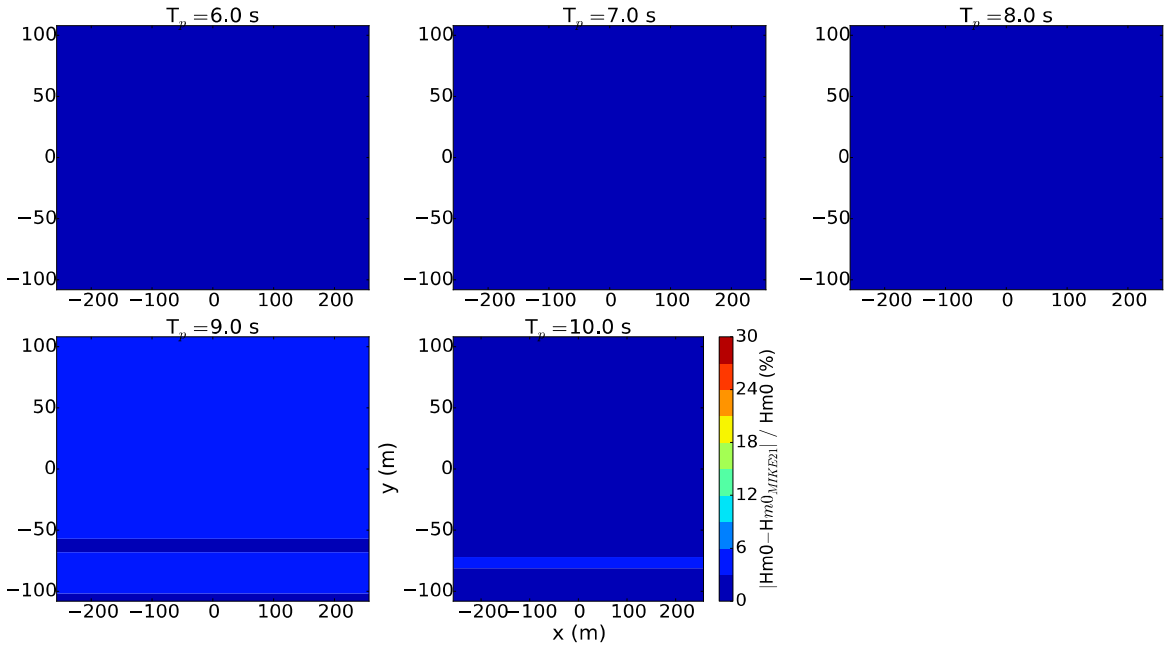

Figure 2-6: . Relative error in the prediction of Hm0 by the MIKE21 software for the case of constant 15m water depth and no WEC array.

The reader should notice that the fact of considering a cut-off for the maximum wave frequency will introduce some uncertainty into the input data (ambient waves) since some of the energy (area below the curve in Figure 2-4) will be disregarded in this way. To estimate how much this will affect the

comparison results between the WP2 tool and the MIKE 21 software, the predicted Hm0 for the case of constant 15m water depth and without the WEC array (only the ambient wave) is compared with the theoretical 0.5m. The difference will indicate the error produced in the generation of the ambient wave.

Figure 2-5 shows a maximum error (error $= |Hm0 - Hm0_{WP2}|/Hm0$) of around 12% for WP2 predictions for the 6s peak period wave, whereas the error (error $= |Hm0 - Hm0_{MIKE\ 21}|/Hm0$) is kept below 5% for MIKE 21 predictions for all wave cases, see Figure 2-6. This means, that the MIKE 21 software implements a mechanism to account for the energy loss due to the cut-off settings, which reduces the error produced in the prediction of Hm0 and which will invariably bias the comparison results presented hereafter.

Furthermore, the first bathymetric case (constant 15m water depth) will allow us to quantify how much uncertainty stems from other fundamental aspects than that of constant water depth assumptions. Indeed, ideally, the Hm0 given by the WP2 tool and the MIKE 21 software should be exactly the same for this very first bathymetric case.

Taking into account the observed bias on the input ambient wave was around 12% for the 6s peak period wave, one can see in Figure 2-7 that the error difference between the WP2 tool and the MIKE 21 software (error $= |Hm0_{MIKE\ 21} - Hm0_{WP2}|/Hm0_{MIKE\ 21}$) is mainly caused by such bias. Thus, the error difference in the following will mainly stem from the bias on the input ambient wave and the water depth variations.

Once the bias in the input ambient wave has been quantified and the error difference from other fundamental aspects have been seen to be small, the second and third bathymetric cases (Table 2-2) will serve to estimate the uncertainty in the WP2 tool results due to varying water depth.

From Figure 2-8 and Figure 2-9, it is readily seen that the case, which leads to the largest error difference is the one of 2.5% inclined bottom. These large errors are found just right behind the wake of the last row of devices, so that WP2 tool predictions diverges up to 25% MIKE 21 predictions within such areas. On the other hand, the predicted Hm0 appears to be less sensitive to water depth variations when it comes to 5% inclined bottom for this particular WEC array. For this bathymetric case, the error difference is seen not to exceed 12% the predictions done by the MIKE 21 software.

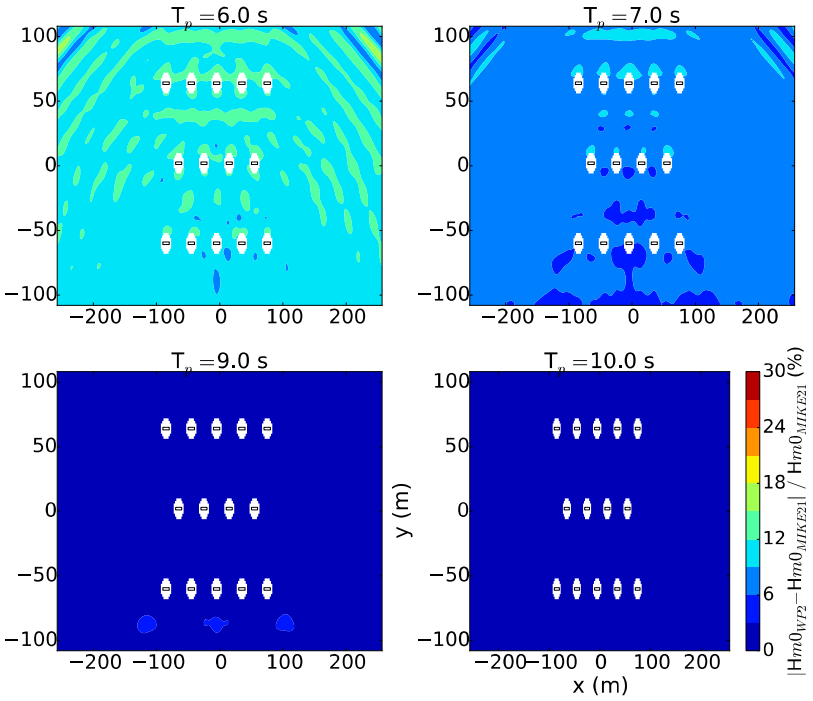

Figure 2-7: Error difference between the Hm0 predicted by the WP2 tool and the one predicted by the MIKE 21 software for the 15m constant water depth case [1].

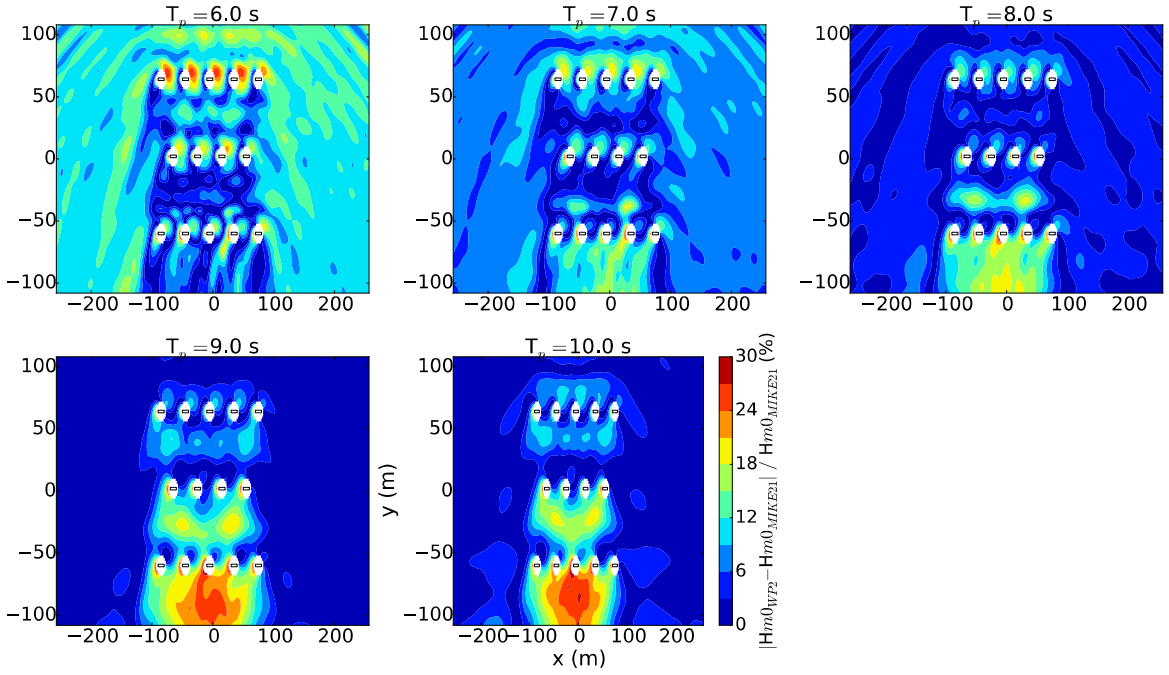

Figure 2-8: Error difference between the Hm0 predicted by the WP2 tool and the one predicted by the MIKE 21 software for the 2.5% inclined bottom case [1].

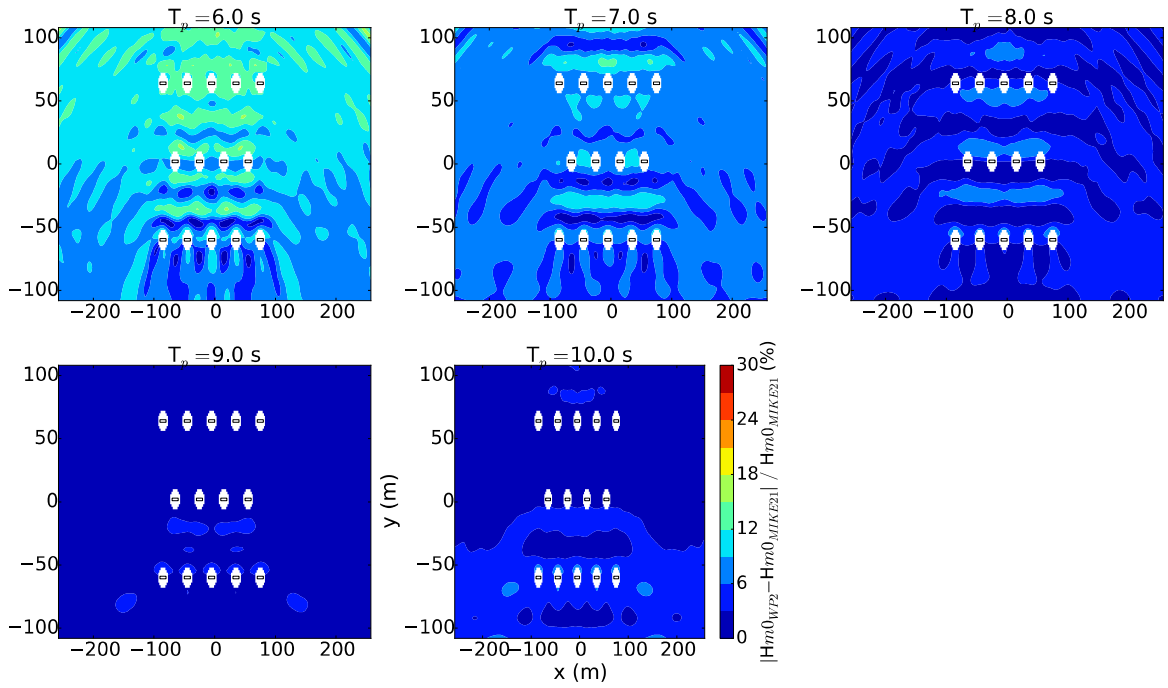

Figure 2-9: Error difference between the Hm0 predicted by the WP2 tool and the one predicted by the MIKE 21 software for the 5% inclined bottom case [1].

Overall, it is seen that wave transformations effects due to water depth variations can lead up to 25% uncertainty to Hm0 predictions. Since the Hm0 is a measure of the total wave energy content, it seems apparent that water depth variation effects play an important role when predicting the total power output of WEC arrays placed near the shore.

2.1.2.2 Influence of wave directional spreading into the hydrodynamci interaction

Another important limitation of the interaction theory based on BEM solutions is that the body is not assumed to move from the initial equilibrium position.

This assumption forces the relative position between bodies to be fixed, and therefore, within an array, highly destructive or constructive interaction can build up, even if not entirely realistic.

In a real scenario the bodies will move around the equilibrium position and most likely constrictive/destructive interaction will be averaged in time.

Since the model is built in the frequency domain it is not possible to include this type of non-linearity in the solution, and a simple approach to estimate this energy dissipation is to distribute the energy content around the main direction using a spreading function.

In this way, for each wave direction, the relative distance between bodies will vary, creating a smoothing effect on the constructive/destructive hydrodynamic interaction.

In order to analyse the influence of the directional spreading in the hydrodynamic interaction a simple case has been used.

The array is composed of two cylinders set 1000 meters apart from each other.

The cylinder is shown in Figure 2-10, along with the array layout used in the analysis.

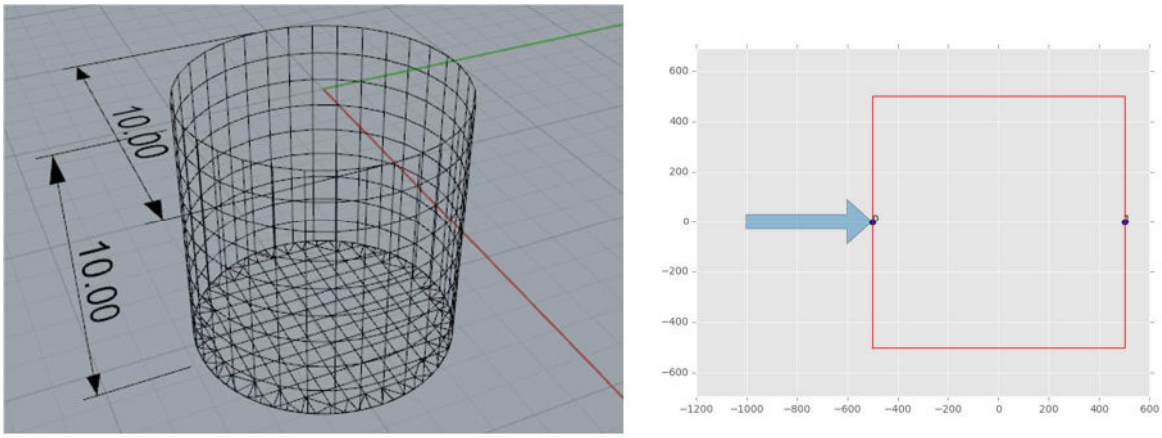

Figure 2-10: Left: Heaving cylinder used in the analysis. Right: Representation of the array layout and main direction.

The waves are travelling from West to East, and the wave period is ranging from 4 to 20 s. The wave height is fixed to 1 m.

Five different set-ups are used for the undisturbed waves:

1. Regular waves
2. Irregular waves, spectral shape JONSWAP, peak-enhancement factor 3.3.
3. Irregular waves, spectral shape JONSWAP, peak-enhancement factor 3.3. Directional spreading parameter 15.
4. Irregular waves, spectral shape JONSWAP, peak-enhancement factor 3.3. Directional spreading parameter 10.
5. Irregular waves, spectral shape JONSWAP, peak-enhancement factor 3.3. Directional spreading parameter 1.2.

The main results of the analysis are summarised in the following figures.

Figure 2-11 can be used to visualise the concept expressed above, regarding the problem of the fixed position of the devices. If regular waves are sent to the array, the devices wave length over the devices distance will assume only a narrow band spectrum of values, creating a high sensitivity to the position. The trend is more evident in the short period range, where a small variation of the wavelength will generate a great variation of the phases between devices. Already using a distribution of the wave

energy content over a spectrum of frequency has a smoothening effect of the problem. As shown in Figure 2-12, the variation of the q-factor is drastically reduced closer to the single device behaviour.

A directional spreading is added on top of the frequency spreading in Figure 2-13, Figure 2-14, Figure 2-15. The figures show an increasing range of angles added to the analysis.

As expected, the wave energy content is additionally spread in the directions axes, which has the effect to flat the q-factor further, reducing the hydrodynamic interaction to only a small amount.

Overall, it is possible to notice that the directional spreading has only a marginal influence, if compared with the long crested waves case, and since it require extra computational power to assess the additional waves direction, it should not be used in the first stage of analysis.

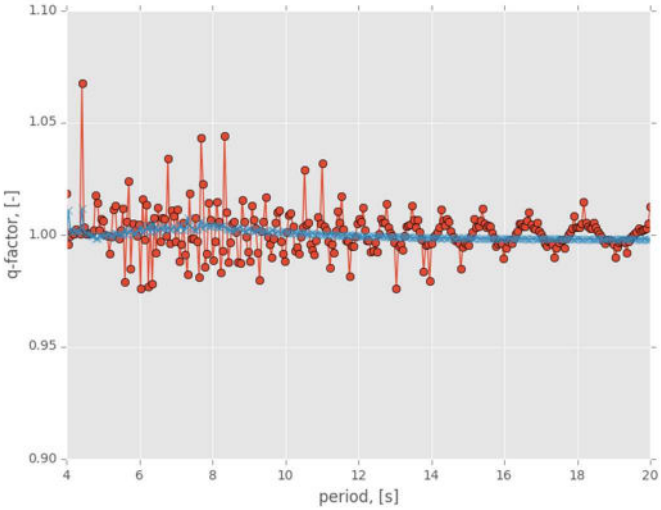

Figure 2-11: case 1, regular waves. q-factor in function of the wave period for the upwave body (red) and downwave body (blue).

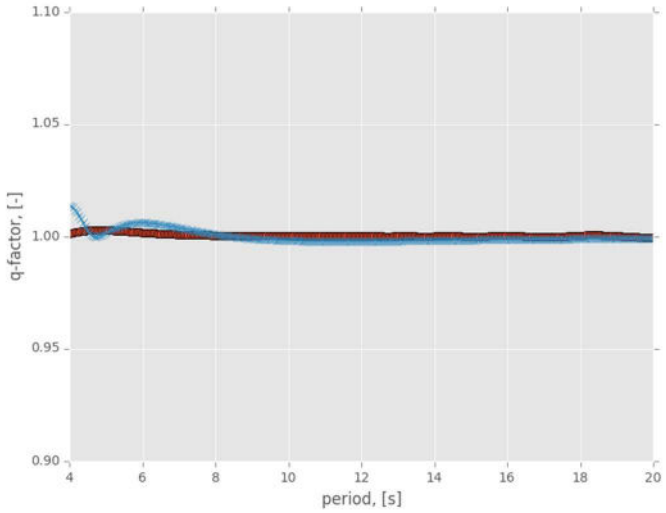

Figure 2-12: case 2, irregular long crested waves. q-factor in function of the wave period for the upwave body (red) and downwave body (blue).

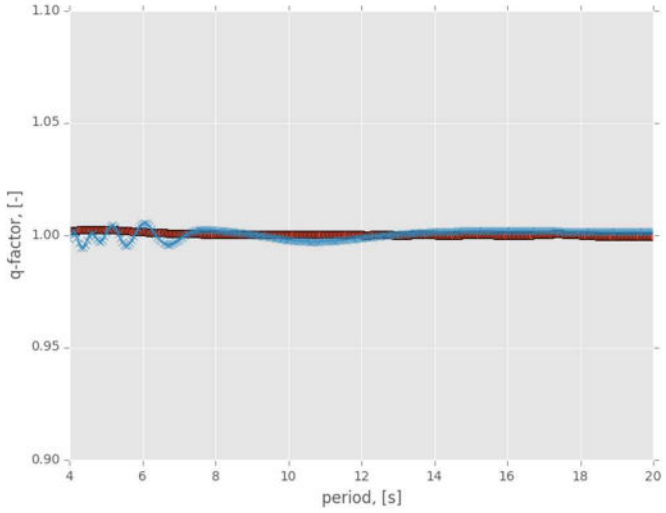

Figure 2-13 : case 3, irregular short crested waves with directional spreading parameter of 15. q-factor in function of the wave period for the upwave body (red) and downwave body (blue).

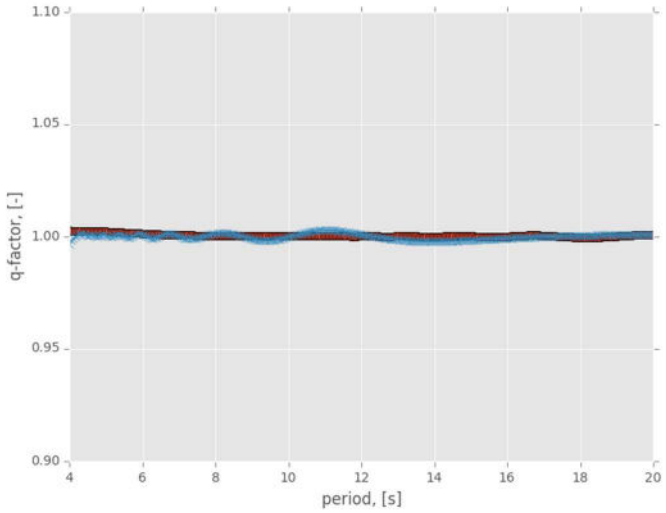

Figure 2-14: case 4, irregular short crested waves with directional spreading parameter of 10. q-factor in function of the wave period for the upwave body (red) and downwave body (blue).

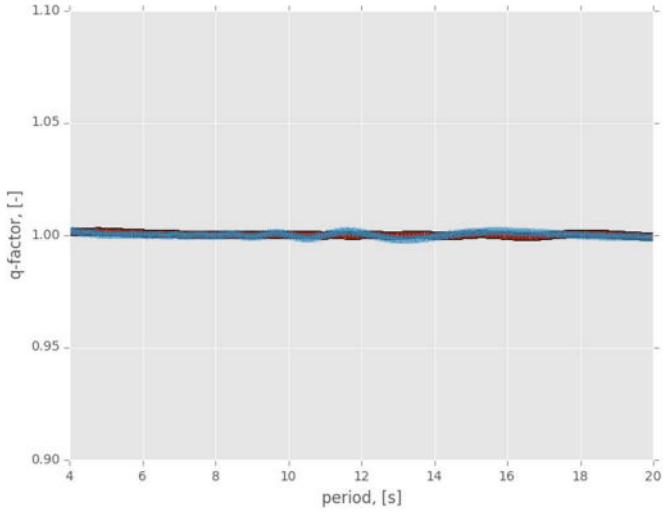

Figure 2-15 : case 5, irregular short crested waves, with directional spreading parameter of 1.2. q-factor in function of the wave period for the upwave body (red) and downwave body (blue).

2.1.3 Input/ Output uncertainties assessment

Changes in power production (WP2 model output) due to uncertainties of wave resource (WP2 model input) are addressed in this subsection. The general approach is to alter the wave time series or scatter diagram input to the WP2 sub-package (i.e. power input) in order to evaluate the influence on power output arising from such alteration. For confidentiality reasons only typical graphs/distributions and values of sea states will be shown hereafter.

Two different investigations are carried out:

- Statistical approach - Investigate uncertainties of the input scatter diagram
- Deterministic approach - Sensitivity analysis of the power input

The input uncertainties analysis will take place prior to the actual hydrodynamic analysis as shown in Figure 2-16 .

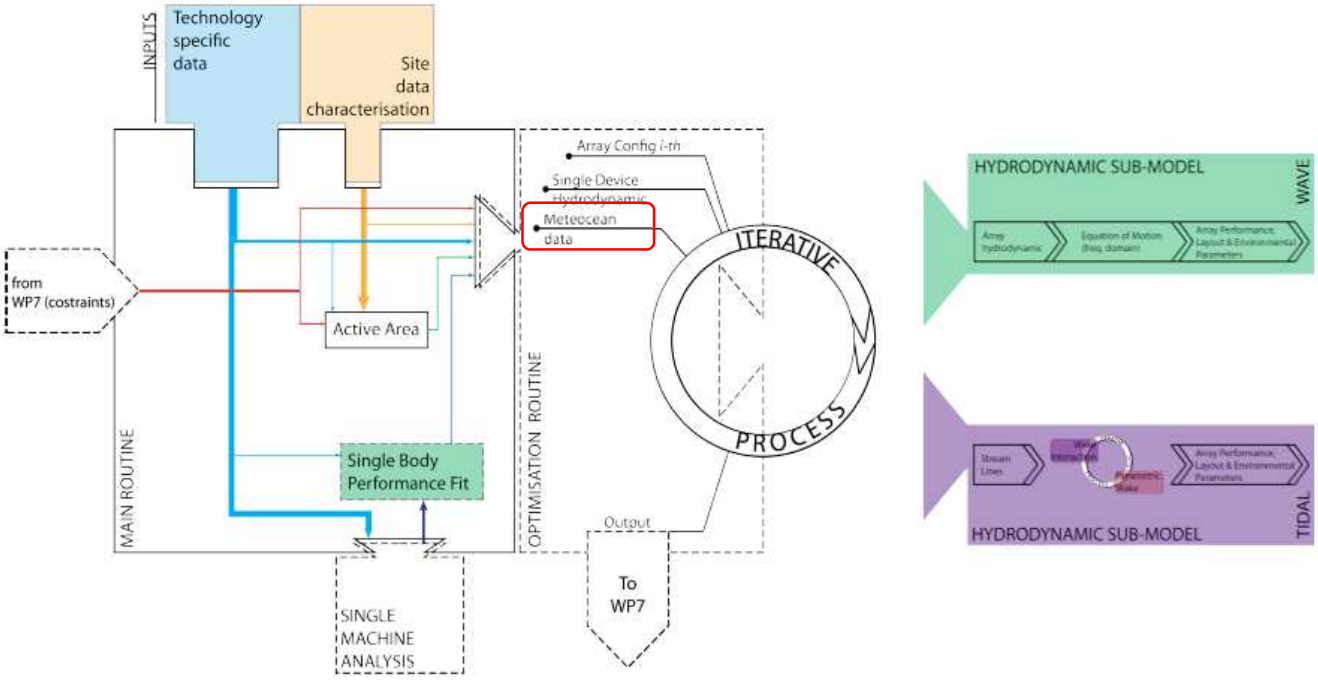

Figure 2-16: Global WP2 overview [2]

2.1.3.1 Deterministic approach:

The power output of the model is investigated by linearly scaling the scatter input diagram (i.e. scaling the number of waves in each bin) of a fixed quantity ranging between the boundaries of -30% and +30%. In doing so, non-integer number of waves will occur. Non-integer number of waves is unrealistic; however this expedient is only used for investigating the response of the model to linear changes in the input.

The wave input to the model has to be provided as directional wave scatter diagrams of T_e and H_{m0}. Eight different scatter diagrams representing eight sectors spaced 45° degrees (i.e. from 0° to 360°) have been fed to the model in order to represent omnidirectional sea states.

The beta version of the wave model has been tested investigating the change in the Array Annual Energy output yielded by linearly scaling the wave input. The number of waves in each single scatter diagram has been scaled by a fixed percentage ranging between the boundaries of -30% and +30% . That represents therefore a direct alteration to the energy input.

An example of linear scaling of scatter diagrams for the directional sector 270°-315° (i.e. the sector with highest energy content) is shown in Figure 2-17.

-

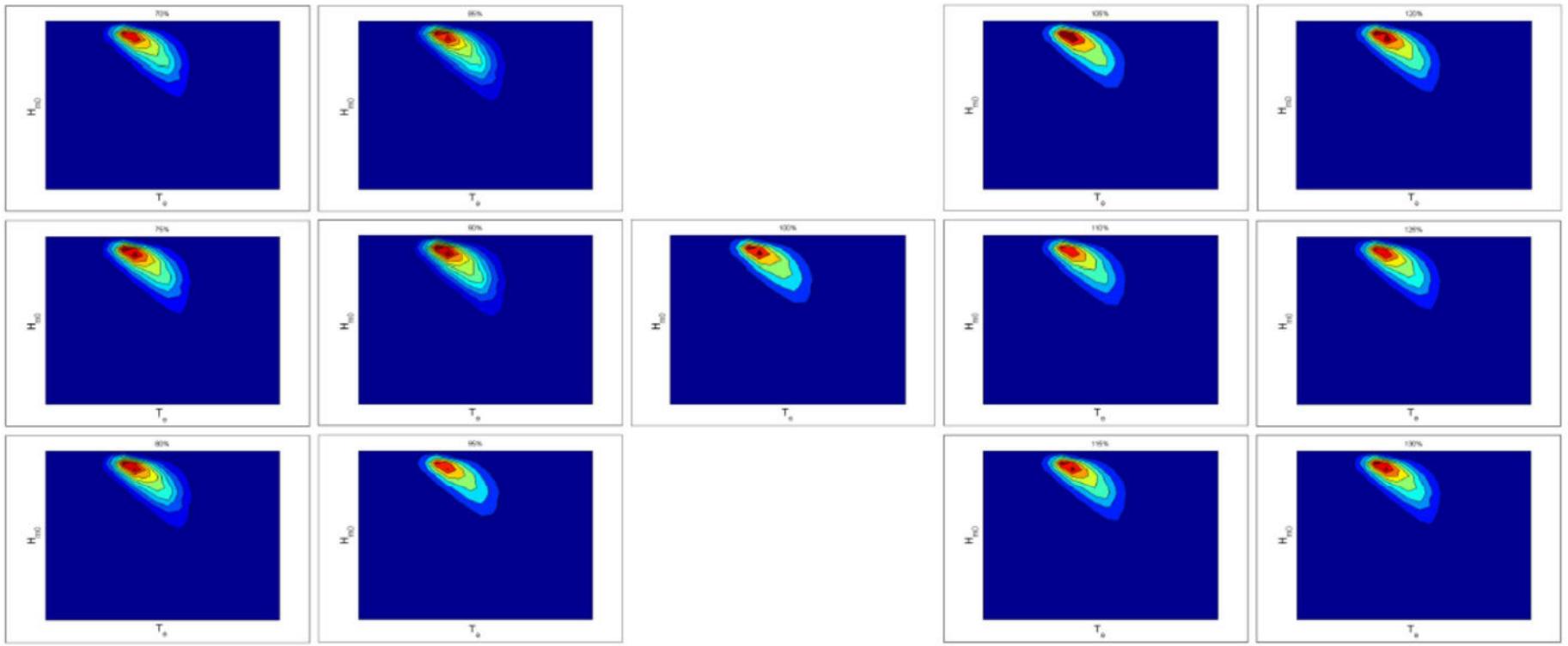

Figure 2-17: *In the middle the unaltered scatter diagram (i.e. 100%). Left and right hand side the altered scatter diagrams with lower and higher number of waves respectively.*

It is important to remark that since the model is at its beta version at the date of this, not all functionalities of the wave model have been activated.
Due to the approach used to solve the hydrodynamics (i.e. linear theory), it is expected that a linear change in the power input (i.e. number of waves) should be linearly reflected in the power output. Simple conditions for simulation have been set up in order to have an easy check on the outputs at the beta version stage.
Simulations with the following conditions have been run:

- Device: floating cylinder (Diameter: 8 m, Height: 10 m, Draft: 4 m). Figure 2-18.
- Generic Boundary lease area
- Bathymetry = flat, -50 m
- Minimum distance among devices = 20 m
- Installation depth constraints = None
- Optimisation threshold = 0.85 (The input defines the minimum q-factor allowed for the selected array layout. Any array with average q-factor smaller than this value will be considered unfeasible).

Power matrix = The device power matrix it is automatically generated by the model

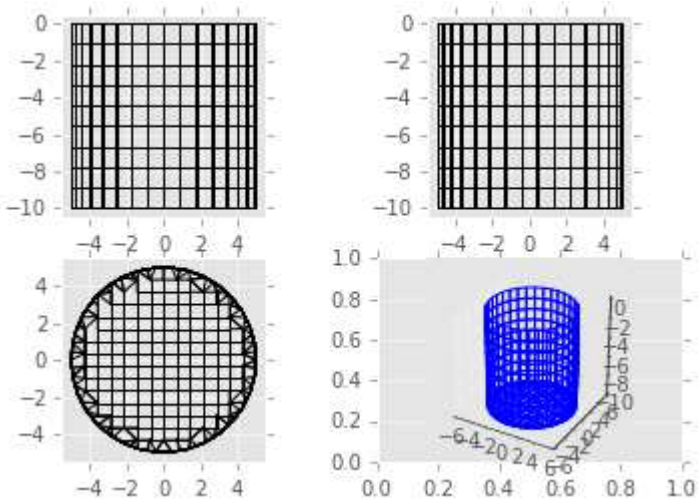

Figure 2-18: Mesh geometry for the cylinder simulated

The model finds an optimal layout solution of 19 devices within the lease boundary specified (Figure 2-19).

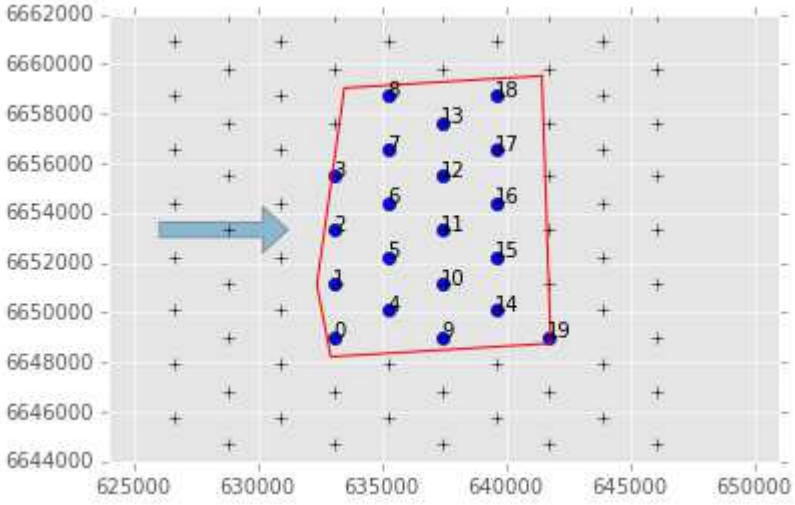

Figure 2-19 : Optimal WP2 found by the wave model solution

The arrow represents the direction of the scatter diagram with higher energy content (i.e. 270°-315° sector).

The simulations show the following Annual Energy Production per Device (Table 2-4) :

Table 2-4 : Table reporting the Annual Energy production associated to each device

Device Number	Annual Energy production per Device [W]
1	2865743.20
2	2862574.96
3	2855973.99
4	2869158.98
5	2875359.11
6	2882875.36
7	2880527.92
8	2866176.54
9	2862855.95
10	2859477.80
11	2874450.72
12	2873140.36
13	2882936.96
14	2889039.71
15	2857685.92
16	2856531.70
17	2864074.67
18	2874247.17
19	2876745.90

Table 2-5 shows the % variation of energy input with respect to the original scatter diagrams (i.e. eight directional scatter diagrams) and the relative computed power output:

Table 2-5: percentage variation of total number of waves in the original directional scatter diagrams and related computed output (i.e. Array Annual Energy Production). Marked in red the computed solution for the unchanged number of waves in the scatter diagrams.

% of number of Waves	Array Annual Energy Production [MWh]
70%	30911134.18
75%	33119072.33
80%	35327010.49
85%	37534948.64
90%	39742886.8
95%	41950824.95
100%	**44158763.11**
105%	46366701.27
110%	48574639.42
115%	50782577.58
120%	52990515.73
125%	55198453.89
130%	57406392.04

Table 2-5 and Figure 2-20 clearly shows the expected linear behaviour of the Wave model at its beta version:

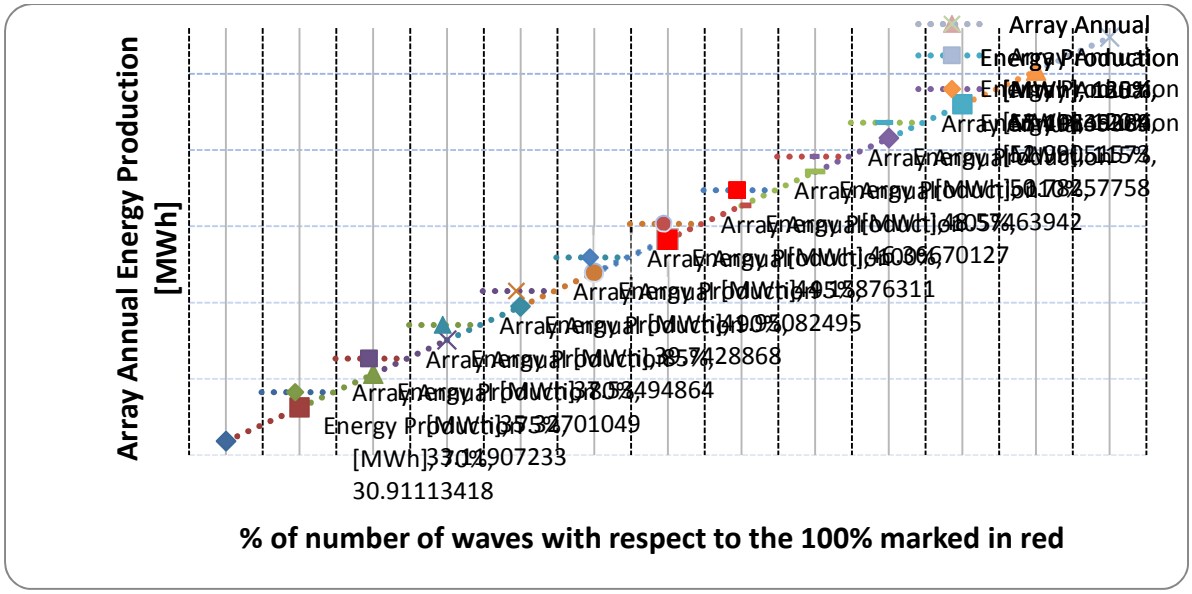

Figure 2-20 : Graphical representation of Table 2-5.

2.1.3.2 Statistical Approach:

This section addresses the influence of resource variability on the power outuput by means of a simplfied statistical apporach.

The WP2 wave hydrodynamic package takes a scatter diagram (i.e. H_{m0} , T_e) as input, produced by appropriate binning of the time series of spectral wave height H_{m0} and energy period T_e.

However, the time series represents only a limited sample of the population of H_{m0} and T_e. The size of the time series sample is denoted by N.

Some approaches exist to compute the joint distribution of environmental variables (e.g. Maximum Likelyhood Model, Conditional Modelling Approach) [3]. However, little is known about the joint distribution of H_{m0} and T_e .

Although energy period can be derived from the peak period if the sea spectrum is known [4], this adds an additional level of complexity and uncertainty when it comes to estimating the joint probability distribution of H_{m0} and T_e.

A simplified approach for the assesment of uncertainties in the sea state input is used in Task 2.6.

The key assumption is that the the variables H_{m0} and T_e are independent and therefore their joint probabilty distribution can be calculated as follows :

$$\boldsymbol{f_{H_{m0},T_e}(H_{m0},T_e) = f_{H_{m0}}(H_{m0}) \cdot f_{T_e}(T_e)}$$

As opposed to :

$$f_{H_{m0},T_e}(H_{m0},T_e) = f_{T_e|H_{m0}}(T_e|H_{m0}) \cdot f_{H_s}(H_{m0}) = f_{H_{m0}|T_e}(H_{m0}|T_e) \cdot f_{T_e}(T_e)$$

Therefore, the joint probaility density function (PDF) of H_{m0} and T_e can be calculated as the product of the respective marginal PDF. This will allow the recomputation of a scatter diagram without knowing the conditional distributions $f_{T_e|H_{m0}}(T_e|H_{m0})$ or $f_{H_{m0}|T_e}(H_{m0}|T_e)$.

A wave time series can be binned into equally spaced classes of H_{m0} and T_e, and the marginal frequency of occurrence of these variables can be drawn.

The number of bins N_b and their boundaries will be kept unchanged throughout the statistical approach. In the example that will be shown thereafter a bin spacing of 0.5m and 1s is used respectively for H_{m0} and T_e as advised by the IEC Standards [5]. The significant wave height bins range from 0m to 14m whereas the energy period goes from 0s to a maximum of 22s in order to capture all the seastates from the origainal data.

For demonstration purposes a 14 year timeseries (1980 - 2013) at hourly resolution of H_{m0} and relative T_p has been used. The peak period (T_p) has been converted to energy period by standard integration of the wave spectrum [4]. A parametrised Pierson-Moskowitz spectrum has been assumed [6]. Wave time series is relative to Scenario 1 – North West Lewis [7] at a nearshore point (exact coordinates cannot be shown for confidentiality reasons).

A typical wave rose for the North West Lewis location can be found in Deliverable 2.2 [8] from which it can be seen that the predominant wave direction is East/North-East. Therefore, a statistical approach for simplicity will only be applied to the directional sector 270°-315° N. Figure 2-21 shows the scatter diagram associated to this directional sector. For confidentiality reasons the actual data cannot be shown.

H_{m0} (m) \ T_e (s)	0 - 1	1 - 2	2 - 3	3 - 4	4 - 5	5 - 6	6 - 7	7 - 8	8 - 9	9 - 10	10 - 11	11 - 12	12 - 13	13 - 14	14 - 15	15 - 16	16 - 17	17 - 18	18 -19	19 - 20	20 -21	21 - 22
0 - 0.5																						
0.5 -1																						
1 - 1.5																						
1.5 - 2																						
2 - 2.5																						
2.5 - 3																						
3 - 3.5																						
3.5 - 4																						
4 - 4.5																						
4.5 - 5																						
5 - 5.5																						
5.5 - 6																						
6 - 6.5																						
6.5 - 7																						
7 - 7.5																						
7.5 - 8																						
8 - 8.5																						
8.5 - 9																						
9 - 9.5																						
9.5 - 10																						
10 - 10.5																						
10.5 - 11																						
11 - 11.5																						
11.5 - 12																						
12 - 12.5																						
12.5 - 13																						
13 - 13.5																						
13.5 - 14																						

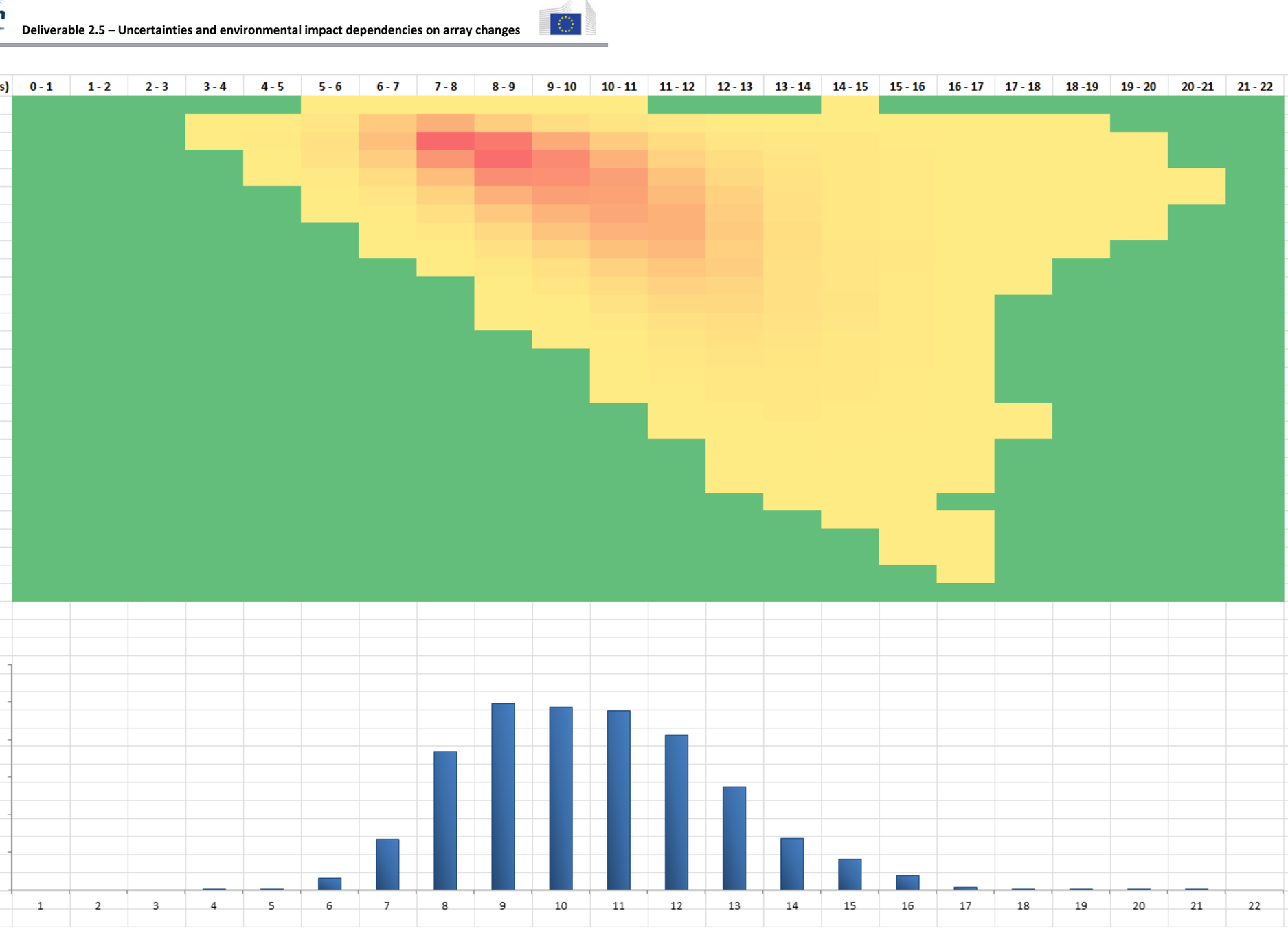

Figure 2-21: 270°-315° N Directional Scatter Diagram with related bar charts of Hm0 and Te. Each bin represents the number of waves. Actual data cannot be shown for confidentiality reasons.

A second assumption of this methodology is to assume that it is possible to fit the time series sample with a probability distribution for the variable H_{m0}. That is in theory always possible although the quality of the fit has to be verified as it may not be possible to adequately discriminate the tail behaviour. This method is also known as "the global model"[3] or "total sample method [9].

Opposite to H_{m0}, the T_e time series will not be fitted to any probability distribution and only its marginal frequency of occurrence will be used.

The H_{m0} sample time series is fitted to a probability distribution curve using standard methods (e.g. Graphical Fitting, Methods of Moments, Least Squares Methods, Maximum Likelyhood Estimations [3]. It is assumed that the sample probability distribution represents the "true" population probability distribution of the variable H_{m0} .

Hereafter is shown an example of the statistical approach to produce a scatter diagram that takes into account the statistical variability of the seastate. The scatter diagram thus generated will be fed to the WP2 subpackages and the output will be compared with the output resulting from applying the original (i.e. non-altered) scatter diagram.

For simplicity only a directional scatter diagram relative to the predomimnat wave direction is utilised. That wave sector is identified as 270°-315° N. The total number of waves considered is *N*.

Unless data indicates otherwise, a 3-parameter Weibull distribution can be assumed for the marginal distribution of significant wave height H_{m0} [3]. The example below shows a typical Weibull distribution:

$$P_{H_{m0}}(H_{m0)} = 1 - e^{\left[-\left(\frac{H_{m0}-\gamma}{\alpha}\right)^{\beta}\right]}$$

where α is the scale parameter, β is the shape parameter, and γ is the location parameter.The distribution parameters are determined from site specific data by a fitting technique [3].

Figure 2-22 shows a typical marginal frequency of occurrence as a % of the significant wave height (i.e. H_{m0}) time series. This marginal frequency of occurrence will be used to show how the new scatter diagram can be derived :

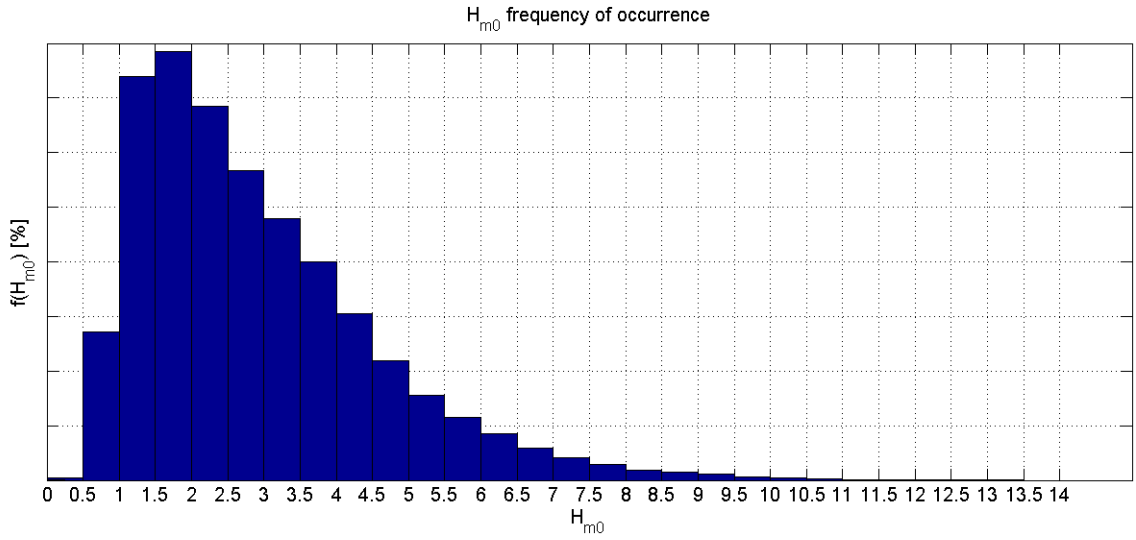

Figure 2-22: Typical Hm0 marginal frequency of occurrence (as a percentage)

The best fit returns the parameters that describe the CDF (or alternatevely the PDF). These parameters will be representative of the true CDF distribution. Figure 2-23 shows the Weibull CDF applied to the West Lewis time series:

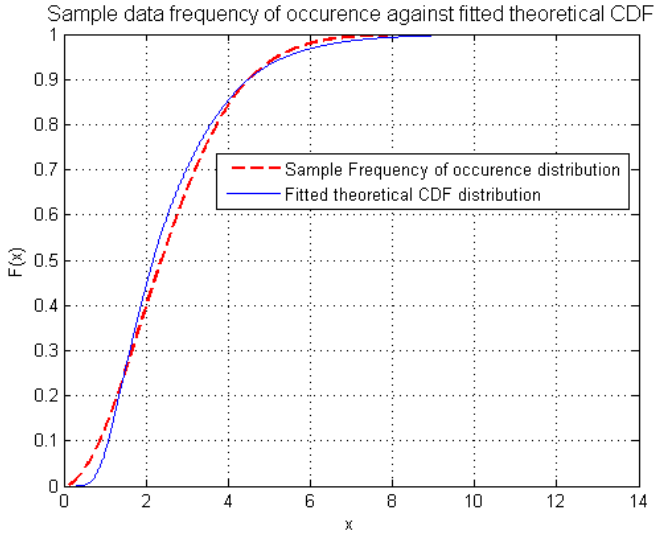

Figure 2-23: Example of the fitting of a theoretical Weibull CDF to the sample cumulative frequency of occurrence.

Once the probability distribution is assumed known, a Monte Carlo simulation is performed in order to reproduce random samples of the H_{m0} population. The size of samples is N as in the original time series.

The Monte Carlo simualtion is run *M* times. Each time, the *m-th* sample of size *N* is binned using the same bin boundaries (i.e. the same numbers of bins N_b) as the original scatter diagram bin boundaries for the variable H_{m0} .

The final outcome of the simulation is a matrix $M \times N_b$ of frequency of occurrence for each bin.

If M is big enough, say at least *M =10000*, the distribution of the frequency of occurrence of each bin follows a normal distribution.

Figure 2-24 shows the normal distribution shape of the frequency of occurrence for *Bin number = 10* corresponding to the interval $4.5\ m \leq H_{m0} < 5.0\ m$.

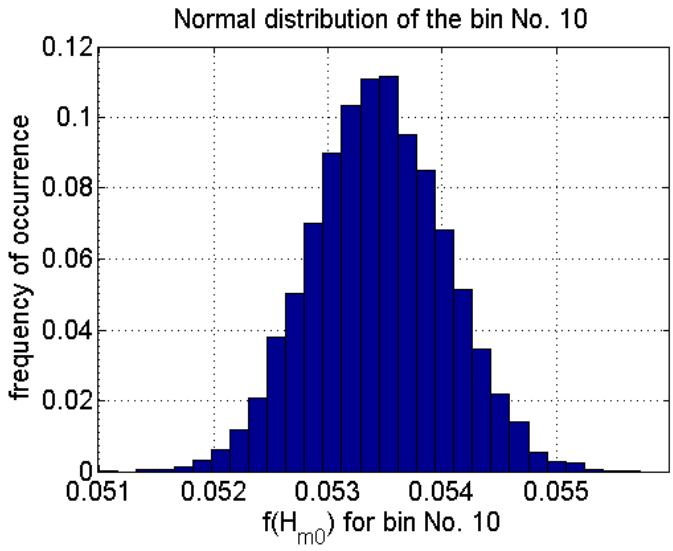

Figure 2-24: Frequency distribution of the frequency of occurrence for bin No. 10 (i.e 4.5 m ≤ Hm0 < 5.0 m) after Monte Carlo simulation

Since the "true" standard deviation of the normal distribution for the frequency of occurrence of each bin is unknown, the Student's-t distribution with *n-1* degree of freedom is applied [10]. A level of significance α can be fixed, and therefore confidence interval (CI) values can be defined for each bin frequency of occurrence. The relationship between the the level of significance α and the confidence interval is as follows :

CI=1- α

Where α ranges between 0 and 1.

Confidence intervals for the mean value of the Student's-t distribution of the frequency of occurrence for each bin can therefore be calculated for different levels of significance α.

When treating metocean data a widely used CI value is 95% (i.e. corresponding to α=5%).

This returns a 95% probability for the mean value of probability of occurrence for each bin bound between an upper value and a lower value of frequency of occurrence (see Figure 2-25).

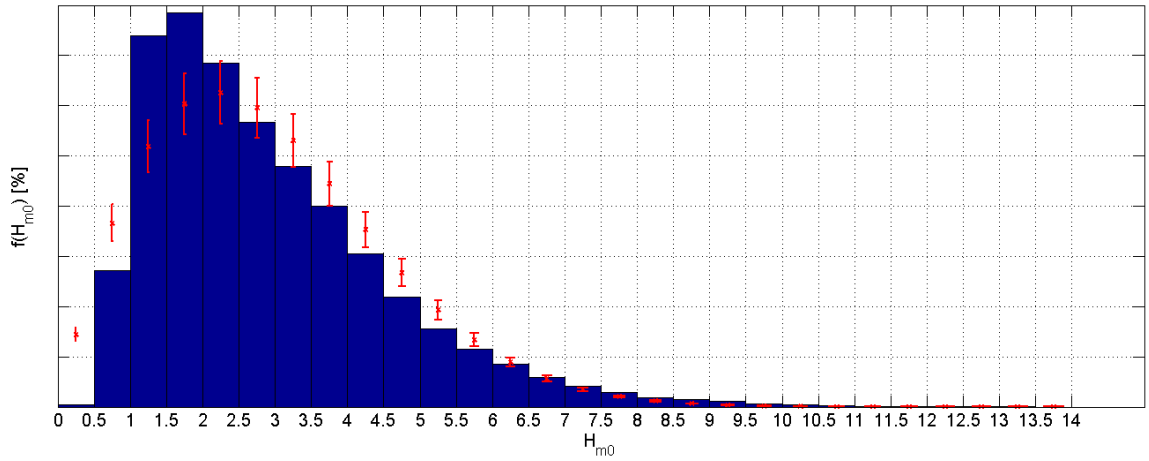

Figure 2-25: Example of the statistical approach applied to the typical Hm0 time series with direction 270°-315° N. The upper and lower boundaries for each bin distribution associated to α=5%. The mean value is represented by a cross.

For completeness, Table 2-6 reports the original time series frequency of occurance, the mean frequency of occurrence, and its related upper and lower boundary for each bin after the Monte Carlo simulation is applied.

Table 2-6: Tabular representation of Figure 22 for the Montecarlo simulation and relative intervals of confidence associated to α=5%.

Bin No.	Hs_{m0} [m]	Freq. of occurrence of "original data"	Mean value of bin normal distributions	Upper boundary of bin normal distributions	Lower boundary of bin normal distributions
1	0 - 0.5	Cannot be shown (-)	0.0289349	0.0318276	0.0260423
2	0.5 -1	-	0.0732298	0.0805515	0.0659082
3	1 - 1.5	-	0.1037370	0.1141092	0.0933649
4	1.5 - 2	-	0.1207261	0.1327971	0.1086552
5	2 - 2.5	-	0.1250951	0.1376030	0.1125873
6	2.5 - 3	-	0.1191529	0.1310666	0.1072393
7	3 - 3.5	-	0.1059799	0.1165764	0.0953835
8	3.5 - 4	-	0.0888525	0.0977363	0.0799687
9	4 - 4.5	-	0.0706231	0.0776841	0.0635621
10	4.5 - 5	-	0.0534531	0.0587972	0.0481089
11	5 - 5.5	-	0.0386370	0.0424997	0.0347743
12	5.5 - 6	-	0.0267304	0.0294026	0.0240582
13	6 - 6.5	-	0.0177189	0.0194901	0.0159477
14	6.5 - 7	-	0.0112886	0.0124169	0.0101602
15	7 - 7.5	-	0.0069039	0.0075939	0.0062139
16	7.5 - 8	-	0.0040692	0.0044758	0.0036626
17	8 - 8.5	-	0.0023064	0.0025368	0.0020760
18	8.5 - 9	-	0.0012567	0.0013822	0.0011312
19	9 - 9.5	-	0.0006628	0.0007289	0.0005966
20	9.5 - 10	-	0.0003363	0.0003699	0.0003028
21	10 - 10.5	-	0.0001643	0.0001807	0.0001479
22	10.5 - 11	-	0.0000782	0.0000860	0.0000704
23	11 - 11.5	-	0.0000356	0.0000391	0.0000321
24	11.5 - 12	-	0.0000159	0.0000174	0.0000143
25	12 - 12.5	-	0.0000067	0.0000074	0.0000061
26	12.5 - 13	-	0.0000028	0.0000031	0.0000025
27	13 - 13.5	-	0.0000011	0.0000012	0.0000010
28	13.5 - 14	-	0.0000004	0.0000005	0.0000004

In order to get a new H_{m0} marginal distribution that represents the sample of size N, it is required that :

$$\sum_{k=1}^{Nb} f_{bin_k} = 1$$

Where f_{bin_k} is the frequency of occurrence of each bin. If the lower boundaries is a negative value, then 0 has to be assumed as a lower boundary.

This allows not one unique combination, but all combinations of frequency of occurrence for each bin within the CI bands that satisfies the equation above.

The new joint frequency of occurrence of H_{m0} and T_e can therefore be simply calculated as the product of the two marginal distributions and a new scatter diagram is available to be fed to the WP2 hydrodynamic module.

For simplicity, the mean value column in Table 2-6 is chosen. Note also that the the summation of the items in that column naturally sum up to 1.

The new scatter diagram is therefore simply recalculated. Figure 2-26 shows the altered scatter diagram expressed in frequency of occurrence (the total number *N* of waves will be the same as the original).

H_{m0} (m) \ T_e (s)	0 - 1	1 - 2	2 - 3	3 - 4	4 - 5	5 - 6	6 - 7	7 - 8	8 - 9	9 - 10	10 - 11	11 - 12	12 - 13	13 - 14	14 - 15	15 - 16	16 - 17	17 - 18	18 -19	19 - 20	20 -21	21 - 22	
0 - 0.5	0	0	0	0	6	48	196	534	719	707	693	598	399	200	119	59	14	5	2	1	0	0	4299
0.5 -1	0	0	0	1	15	121	496	1351	1818	1789	1753	1514	1011	507	302	148	34	13	5	2	0	0	10879
1 - 1.5	0	0	0	1	21	171	702	1913	2576	2534	2484	2145	1432	718	428	210	48	19	6	2	0	0	15412
1.5 - 2	0	0	0	1	25	199	817	2227	2998	2949	2891	2496	1667	836	498	244	56	22	7	3	0	0	17936
2 - 2.5	0	0	0	1	26	206	847	2307	3106	3055	2995	2586	1727	866	516	253	58	23	8	3	0	0	18585
2.5 - 3	0	0	0	1	24	196	807	2198	2959	2910	2853	2463	1645	825	492	241	56	22	7	3	0	0	17702
3 - 3.5	0	0	0	1	22	175	718	1955	2632	2589	2538	2191	1463	733	437	215	49	20	7	2	0	0	15745
3.5 - 4	0	0	0	1	18	147	602	1639	2206	2170	2127	1837	1227	615	367	180	41	16	6	2	0	0	13200
4 - 4.5	0	0	0	1	14	116	478	1303	1754	1725	1691	1460	975	489	291	143	33	13	4	1	0	0	10492
4.5 - 5	0	0	0	0	11	88	362	986	1327	1306	1280	1105	738	370	221	108	25	10	3	1	0	0	7941
5 - 5.5	0	0	0	0	8	64	262	713	959	944	925	799	533	267	159	78	18	7	2	1	0	0	5740
5.5 - 6	0	0	0	0	5	44	181	493	664	653	640	553	369	185	110	54	12	5	2	1	0	0	3971
6 - 6.5	0	0	0	0	4	29	120	327	440	433	424	366	245	123	73	36	8	3	1	0	0	0	2632
6.5 - 7	0	0	0	0	2	19	76	208	280	276	270	233	156	78	47	23	5	2	1	0	0	0	1677
7 - 7.5	0	0	0	0	1	11	47	127	171	169	165	143	95	48	28	14	3	1	0	0	0	0	1026
7.5 - 8	0	0	0	0	1	7	28	75	101	99	97	84	56	28	17	8	2	1	0	0	0	0	605
8 - 8.5	0	0	0	0	0	4	16	43	57	56	55	48	32	16	10	5	1	0	0	0	0	0	343
8.5 - 9	0	0	0	0	0	2	9	23	31	31	30	26	17	9	5	3	1	0	0	0	0	0	187
9 - 9.5	0	0	0	0	0	1	4	12	16	16	16	14	9	5	3	1	0	0	0	0	0	0	98
9.5 - 10	0	0	0	0	0	1	2	6	8	8	8	7	5	2	1	1	0	0	0	0	0	0	50
10 - 10.5	0	0	0	0	0	0	1	3	4	4	4	3	2	1	1	0	0	0	0	0	0	0	24
10.5 - 11	0	0	0	0	0	0	1	1	2	2	2	2	1	1	0	0	0	0	0	0	0	0	12
11 - 11.5	0	0	0	0	0	0	0	1	1	1	1	1	0	0	0	0	0	0	0	0	0	0	5
11.5 - 12	0	0	0	0	0	0	0	0	0	0	0	0	0	0	0	0	0	0	0	0	0	0	2
12 - 12.5	0	0	0	0	0	0	0	0	0	0	0	0	0	0	0	0	0	0	0	0	0	0	1
12.5 - 13	0	0	0	0	0	0	0	0	0	0	0	0	0	0	0	0	0	0	0	0	0	0	0
13 - 13.5	0	0	0	0	0	0	0	0	0	0	0	0	0	0	0	0	0	0	0	0	0	0	0
13.5 - 14	0	0	0	0	0	0	0	0	0	0	0	0	0	0	0	0	0	0	0	0	0	0	0
	0	0	0	9	204	1649	6771	18445	24832	24425	23944	20674	13806	6921	4126	2024	467	184	62	21	2	0	

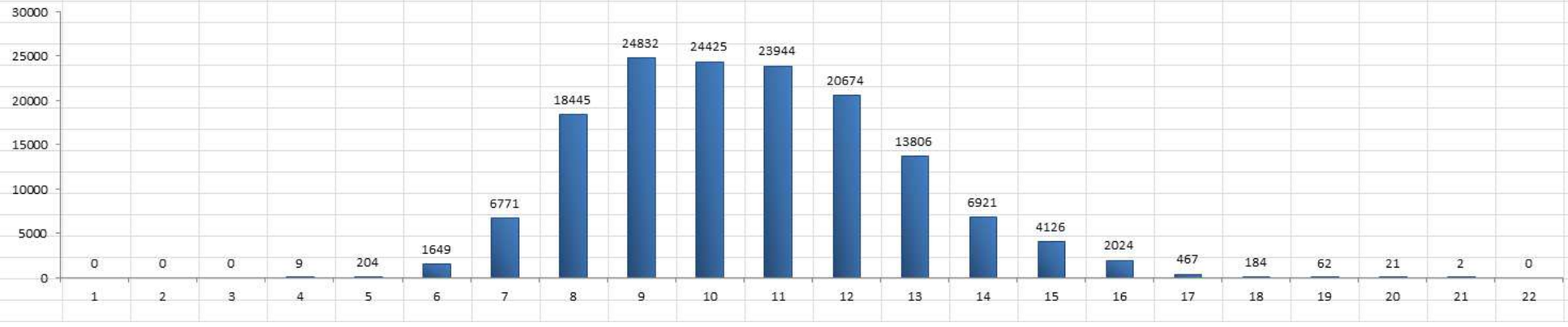

Figure 2-26: 270°-315° N Directional Scatter Diagram resulting from the Monte Carlo simulation with related bar charts of Hm0 and Te. Each bin represents the number of waves

The hydrodynamic wave model can therefore be tested using a scatter diagram as input to the scatter diagram shown in Figure 2-26.

Figure 2-27 shows the farm layout result of the simulation. Similarly to section 2.1.3.1, 20 devices are placed within the lease area. The simulation set up is the same as described in section 2.1.3.1.

The arrow shows the mean direction of the directional scatter diagram simulated, 270°-315° from North.

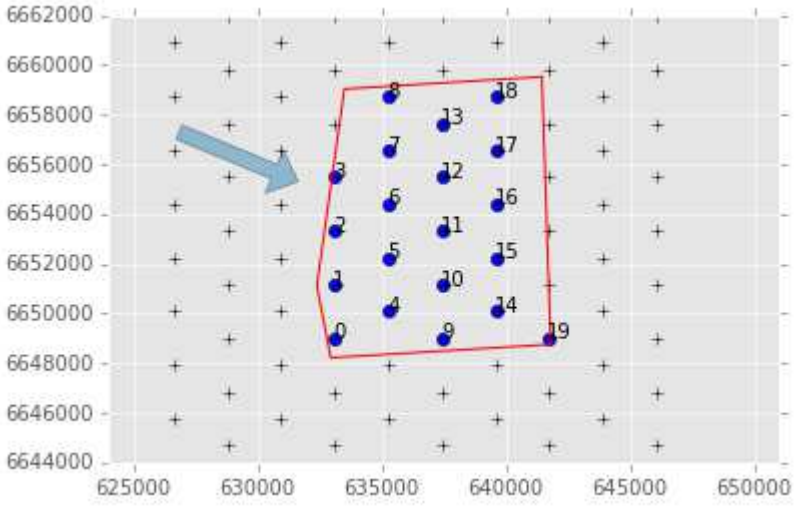

Figure 2-27 Optimal WP2array layout solution found by the wave model.

The result of the original scatter diagram (Figure 2-28) is compared to the new scatter diagram obtained after the statistical manipulation of the original data (Figure 2-26).

It is worth reminding that the total number of sea states is exactly the same for both simulations.

Results in terms of Array energy production is shown in Figure 2-28.

Array Annual Energy Production [MWh]	
Original data	Statistically altered data
63.63	47.07

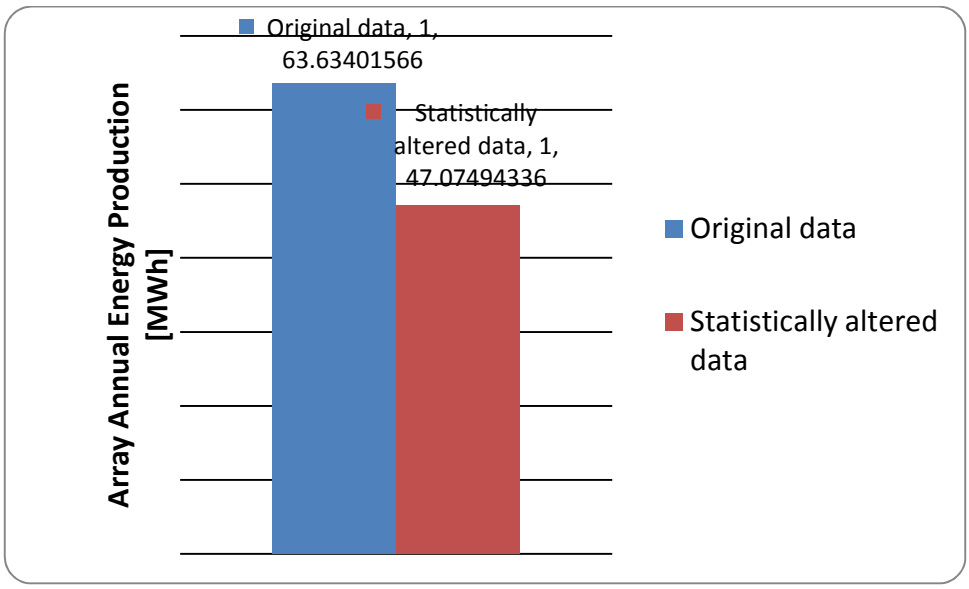

Figure 2-28: Comparison of AAEP resulting from simulation using as input the original scatter diagram (i.e. unaltered) and the one resulting from the statistical computation.

The simulations show a drop in AAEP when the statistically altered scatter diagram is fed as input to the WP2 model. That is due to the different "arrangement "of the seastets within the fixed scatter diagram boundaries as the linear dependency of output from the input has been investigated on section 2.1.3.1. Most likely that is due to the fact that more seastates are redistributed for low H_{m0} bins (i.e. 0-0.5 m and 0.5-1.0 m) where the device energy production is rather low. This energy input for low values of Hm0 are taken out from other bins, since the total number of seastates is fixed, where the wave device would engage more in terms of power production.

2.2 Tidal Model Limitations and Uncertainties

2.2.1 Theoretical limitations

As with the wave submodule, the following text describes the limitations associated with the theories and assumptions implemented in the tidal submodule, and outlines its range of applicability. This qualitative exercise is the first step in the assessment of the tool's uncertainty.

Table 2-7: Limitations on the tidal submodule stemming from the assumptions made in the theoretical formulation

Assumption	**Limitation**
Flow Field Modelling	Simple model of the wake behind the turbine
Wake Interaction	Superposition of wakes based on streamline and parameterised wake profiles
Horizontal-boundary assumptions	No horizontal boundary is considered
Vertical-dimension assumptions	Analytical formulation of the vertical profile
Device yawing	Modification of the wake in function of the yaw angle.

2.2.1.1 Flow Field Modelling

A very simple algebraic axi-symmetric wake model was developed [2] to represent the velocity deficit behind a (wind) turbine. This model was further developed to incorporate a radial velocity profile [3]. These wake models are fairly primitive and neglect many wake flow field characteristics such as upstream effects, and surrounding flow speed up due to conservation of mass. In addition to their shortcomings in modelling these features, they both require some assumptions about the flow before they canprovide a result. The Jensen model requires a decay constant and the Larsen model requires the user to define a known velocity at a downstream location. The resulting flow can be drastically affected by inappropriate assumptions.

Due to the run speed requirements of the DTOcean project, it is not feasible to run high fidelity CFD calculations for the turbine array flow field. The method employed by the current model is to run CFD simulations for characteristic flows and populate a lookup table from this data. By doing this, a simple, fast-running model is created, which is accurate for a large array of cases.

The database is populated with wake flows for a range of turbine thrust coefficients and incoming turbulent intensities.

A barycentric interpolation scheme is employed to extract data from this table for cases which lie in between parametric case points. The output of the database lookup is an axi-symmetric flow field of velocity and turbulence data.

This wake model, however, is not without its own limitations. The database is limited to looking up points within its defined parameter space. There is no extrapolation algorithm. Thus for points outside of the initial database definition, more points would need to be added to the database.

Another limitation of the database method is physical storage space. As points are added to the database, or additional output variables are stored, the database will grow. Currently the database stores stream-wise velocity and turbulence intensity over a spatial field of 20 by 4 turbine diameters. With spatial discretization of 0.025D, the database takes up about 200Mb decompressed. This size will scale linearly with an increased number of variables, discretization and domain size.

2.2.1.2 Wake interactions

The core of the wake interaction model is based on a rather simple Jensen model [10] to which the parametric expression of the wake decay has been substituted with a CFD simulation based dataset and which has been modified to follow streamlines composed of the wakes' trajectories rather than straight lines. Although these two additional features make the model less approximate than a traditional Jensen model, it still has limitations in terms of applicability.

Several wake superimposition schemes will be tested during the model validation phase of this project [13]. Nonetheless, the model, and thus wake interaction, cannot account for non-hydrostatic effects. Consequently, the influences of turbines sitting in near wakes or upstream in the close vicinity of the rotor will not be accurately modelled in the array's performances and wake interactions. In practice however, due to avoidance zones and maintenance ships safety requirements, such configurations are unlikely to occur. Note that this theoretical limitation applies for both momentum and turbulence flow characteristics.

From a hydrodynamics point of view, turbine wakes can be considered as stream tubes [14]. Accordingly, it has been assumed that a wake's centre-lines follow the streamline generated at hub locations in the initial flow. This assumption permits the model to account for the influence of the flow advection on the wake expansion as well as to consider the distance between turbines relative to their wake centre-line. Nevertheless, its numerical implementation may not work in highly rotational flows with recurrent eddies. In practice however, such flows tend to be avoided as they would require complex control of the machines as well as generated "chaotic" input to the drive train and hence enhanced loading and fatigue to the entire converter.

Additionally, structure induced wakes are not accounted for in the present model. Device structure may include a pile, nacelle, foundation, floating structure or any other component apart from the blades themselves. This assumption may impact the overall energy balance assessment of the system and wake interaction characterisation which, respectively, might introduce inaccuracy in modelled impact and resource assessments.

2.2.1.3 Horizontal-boundary assumptions

Lease's horizontal/lateral boundaries/limits are considered open thus, as far as the model is concerned, no horizontal boundary effects are accounted for nor modelled. This assumption may lead to spurious results for configurations where the deployment is close to the edge of a constraint site (such as a channel) or where the upstream row of the array layout densely covers the width of the channel (e.g. approximately less than rotor-diameter lateral spacing between devices). In such cases, blockage effects on the overall array performance will be under-estimated. Yet, in practice, considering maintenance and environmental requirements, this type of configuration is likely to be avoided.

Whelan [15] developed a 1-d analytical solution for an infinite array permitting to investigate the influence of the blockage effects on the percentage reduction in downstream free surface elevation. Based on this model, it has been showed during the PerAWaT project that the downstream impact of an infinite row of turbines at a lateral spacing of two rotor diameters can be considered negligible. Yet this assumption seems valid only when the fluid is subcritical or tranquil, that is when the Froude number Fr < 1, where

$$Fr = \frac{U}{\sqrt{gd}}$$

Nonetheless, and similarly to the current code, the previous example does not address the possibility of upstream flow diversion away from the array and in situations where, for example, an array is situated between an island and the main land, the upstream effect of the array should be considered [15].

2.2.1.4 Vertical-dimension assumptions

The current model does not resolve the velocity vertical profile per se but assumes its shape based on power-law formulas. Therefore, one should expect increased discrepancies in non-ideal sites with, for instance, reverse shear and abnormal vertical stratification due steep density and/or temperature gradients. In addition, wake influences on vertical profiles are not accounted for.

As discussed earlier and due to the open horizontal-boundary assumption, Whelan's correction method for blockage effects cannot be used in this model yet its Froude limit (i.e. Fr < 1) still applies. Potential-flow approach should applied as suggested by the PerAWaT project [16]. However, for the sake of computational time, a purely empirical approach has been chosen. Accordingly, based on Sandia's CFD model series of various vertical blockage ratios (i.e. rotor-diameter divided by the water column height), either a Ct or wake-shape correction formula will be developed.

2.2.1.5 Device yawing

The current model accounts for yawing of devices from both the performance and wake points of view, yet with two different approaches. The influence of yawing on performance is accounted for by correcting the actuator disc surface area to be the "apparent" rotor surface area. This apparent surface

can be defined as the projection of the actuator disc surface onto the plane perpendicular to the inflow velocity vector. The influence of yawing however shall be accounted for in a similar fashion to the vertical blockage effects, that is, through an empirical correction of the Ct and/or turbine diameter. The axi-symmetric wake from the CFD database will be scaled in the span-wise direction to represent the narrower cross section of a yawed turbine and the resulting narrower wake.

Consequently, in the case of performance, limitations will occur for turbines with ducted design and/or yaw-specific control. In the case of the wake, the main assumption here is that the hydrodynamic behaviour and relative shape of the wake shall stay the same and that only its dimensions would change accordingly to Ct and/or turbine diameter. Extensive CFD simulations, experiments and/or in-situ measurements are required to either infirm or confirm such assumptions.

2.2.2 Error analysis for validation

The ETI's PerAWaT project produced results that could be used to evaluate the accuracy of the methods used to account for blockage and turbulence intensity. The test plan therefore follows the PerAWaT format. In particular in the following two cases will be compared.

1. 1 device
2. 2 devices at 1.5 D lateral spacing

The overall aim is to build up a validation dataset to assess the uncertainty of the DTOcean tidal model. This will be done by running a number of cases in CFD and comparing these to the DTOcean tidal module results and the available PerAWaT results.

2.2.2.1 PerAWaT flume experiments

The flume used in the PerAWaT experiments was a rectangular channel 5 meters wide by 12 meters long and with a depth of 0.45 meters. It had a flat bottom and the first row of turbines was 6 meters downstream of the inlet at mid-height in the water column Figure 2-29, Figure 2-30.

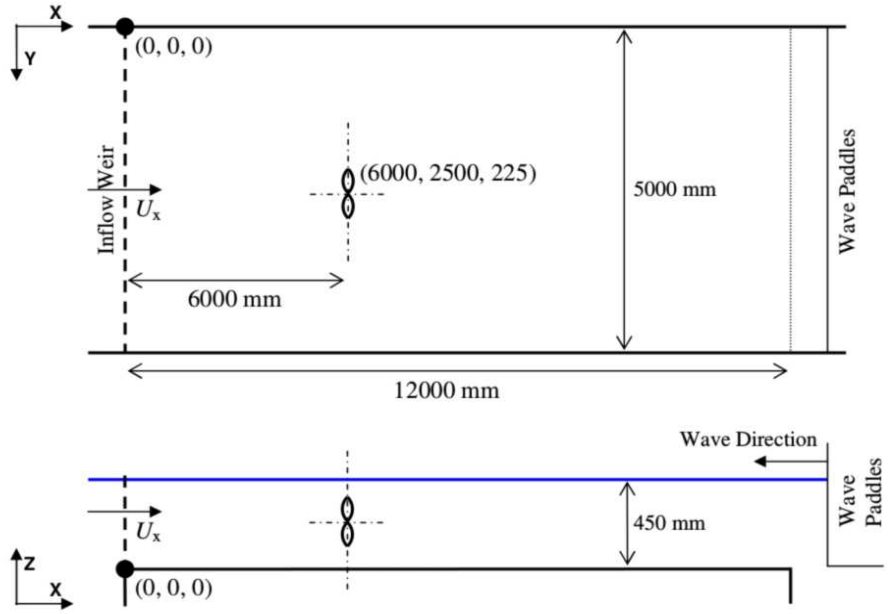

Figure 2-29: Longitudinal arrangement of flume

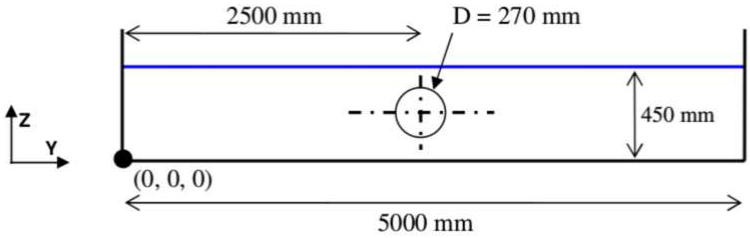

Figure 2-30: Lateral arrangement of flume.

Increased turbulence intensities were achieved by increasing the bed roughness. Large-scale turbulent structures were achieved using a submerged conical island.

2.2.2.2 Turbines

The PerAWaT turbines were designed so that the rotor operated at a similar thrust coefficient and tip speed ratio to a full-scale turbine. Turbine characteristics: Diameter 0.27 meters, Ct = 0.76, Cp = 0.3.

The Reynolds number was $3x10^4$ in these experiments versus 10^7 at full-scale, meaning that more turbulent effects can be expected at full scale. This is a common compromise when scaling in the marine environment.

2.2.2.3 Turbine / Array Layout

Figure 2-31 shows the five layouts used in the PerAWaT flume experiments. They comprised of a number of single and multiple row arrangements, designed to investigate blockage, wake shape and interaction and the effect of different turbulent intensities.

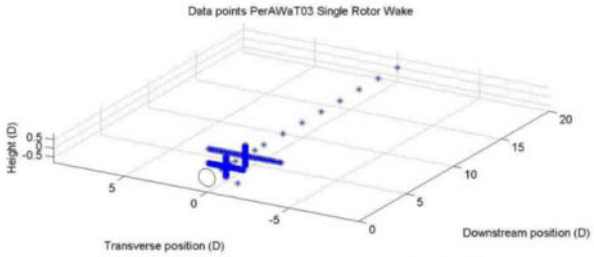

(a) Single wake measurement (see also Section 5)

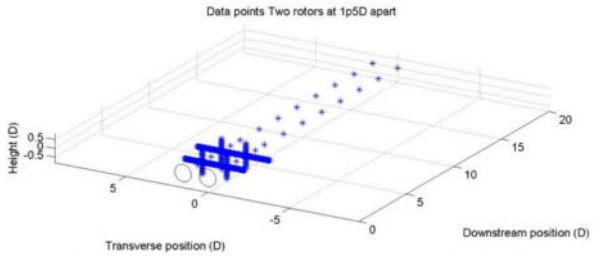

(b) Two rotor blockage study. – lateral spacings of 1.5D, 2D and 3D (see also Section 5.3).

Figure 2-31: Indicative arrangement of measurement positions downstream of the principal array configurations. Velocities are measured downstream of the final row of the array. Longitudinal traverse is conducted over the range 0D<X<10D relative to the rotor plane.

2.2.2.4 Data comparison

In order to compare the data between CFD, PerAWaT and DTOcean datasets, it has been decided to scale all the quantities to the full scale size using a Froud scaling law.

Froud scaling at 1:70 should be used to scale up the turbine and flume described in the PerAWaT experiments:

Froude = U/√(gd) = 0.21

Where U is the mean inflow velocity, g is the acceleration due to gravity and d is the water depth.

U_{full} = 0.21 * √(gd) = 0.21 * √(9.81*31.5) = 3.69 m/s

TI_{full} = 10%

Reynolds number = 1*10^7

2.2.2.4.1 FLUME – FULL SCALE DIMENSIONS

Rectangular channel 350 meters by 840 meters; flat bottom, depth 31.5 meters; first row at 420 meters downstream of the inlet at mid water column.

2.2.2.4.2 TURBINE – FULL SCALE CHARACTERISTICS

Diameter 18.9 meters, Ct = 0.76, Cp = 0.3

2.2.2.4.3 SINGLE ROTOR (LAYOUT A):

Figure 2.26 shows the variation of the velocity deficit in function of x and y coordinates. It is evident that both codes (CFD and DTOcean) highly underestimate the velocity deficit. But it is also interesting to note that the CFD results underestimate the velocity deficit decay in the x-direction, while the DTOcean code can correctly estimate it. From this first set of results it is already possible to foresee an important deviation between the physical and numerical results for the case of interaction. Nevertheless, since the correlation between the results is good enough, as appear for the single machine case, a simple calibration of the numerical model could solve the divergences.

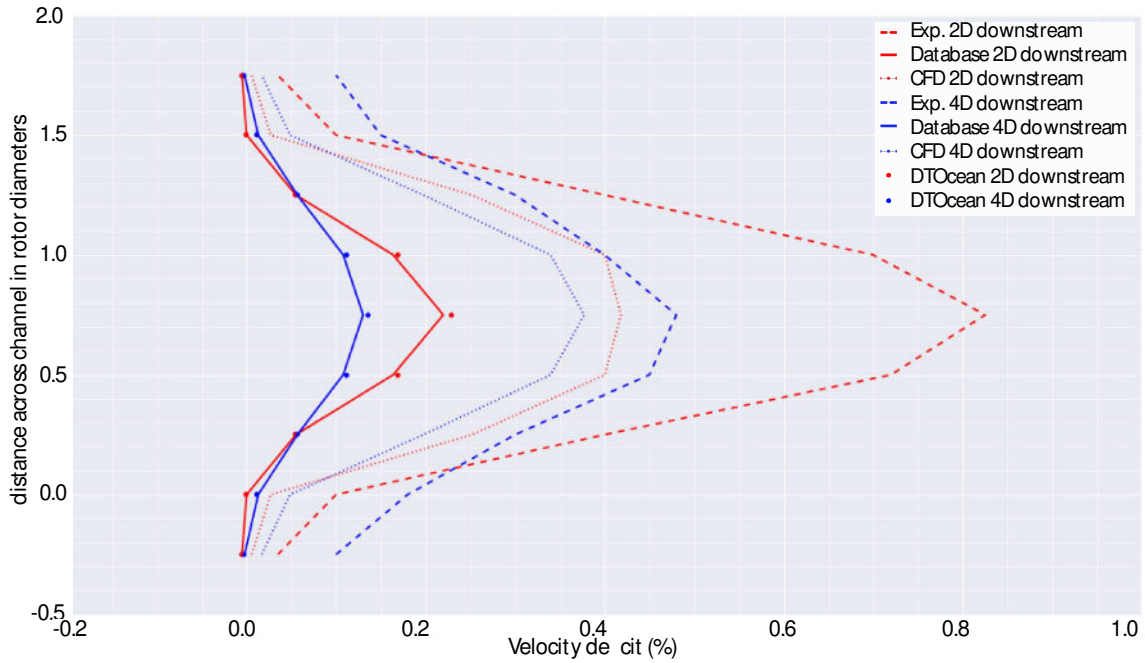

Figure 2-32: Variation of the turbulence intensity in function of x and y coordinates. Comparison between DTOcean, CFD and PeraWatt results.

2.2.2.4.4 TWO ROTOR (LAYOUT B) RESULTS:

Figure 2-31 shows the variation of the velocity deficit in function of x and y coordinates. As for the single turbine case, both numerical results highly underestimate the velocity deficit at the control points. From the results it is possible to see that the wakes do not interact in the short distance, while the interaction becomes tangible 4D downstream. This behaviour seems well captured for both numerical results.

2.2.2.4.5 SUMMARY:

The comparison between CFD, experimental and WP2 data highlighted two major needs:

1) Identification of the sources responsible for the divergence between the WP2 and the CFD results.
2) Reduce the difference between CFD and experimental data if possible and run additional configuration.

The second element of the list is of high importance; it is necessary to understand if either one of the comparison points is reliable. Without achieving this level of confidence the comparison with the WP2 results is somehow meaningless.

A technical addendum of this deliverable will be issued at a later stage when the final verification will be performed.

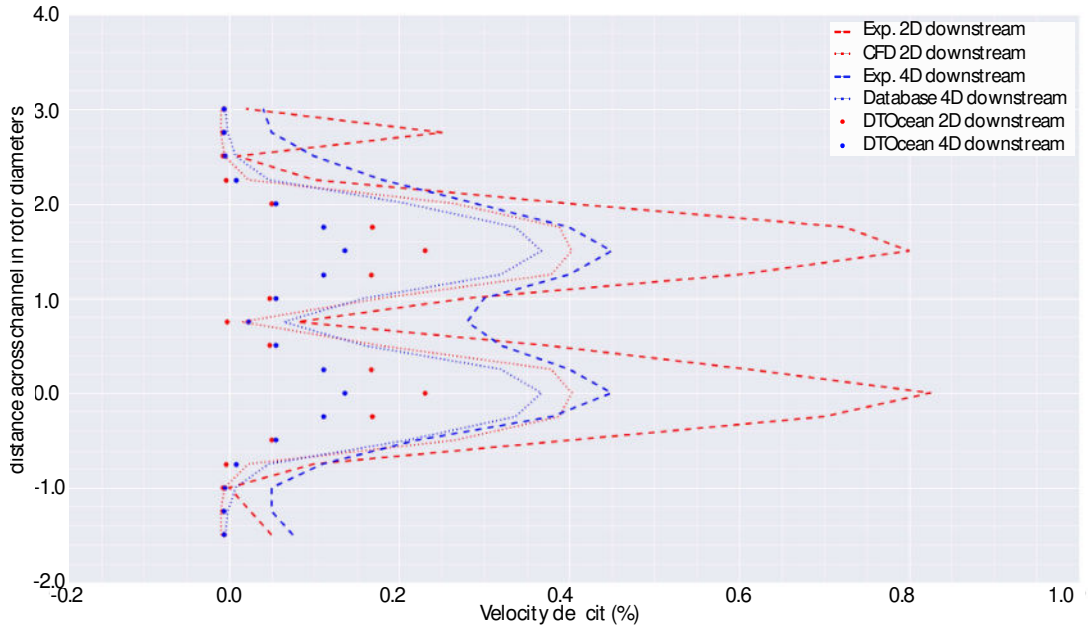

Figure 2-33: Variation of the turbulence intensity in function of x and y coordinates. Comparison between DTOcean, CFD and PeraWatt results.

2.2.3 Input/output uncertainties assessment

Similarly to the wave model (Section 2.1.3.1), the beta version of the tidal hydrodynamic sub-package is subject to a sensitivity analysis on relevant parameters in order to check the reliability of the model at current stage of development. The two key parameters that are deemed as the most significant for the sensitivity analysis are chosen within the list of metocean conditions inputs:

- Turbulence intensity (TI)
- Magnitude of the tidal stream velocity vector (U_t)

It is necessary to mention that simple simulations with a uniform flow field parallel to the turbine have been performed (turbine yaw angle is disabled). A figure of a generic flow field simulated can be found in Figure 2-34. Moreover the sea surface elevation (SSH) with respect to the mean water level is considered constantly null.

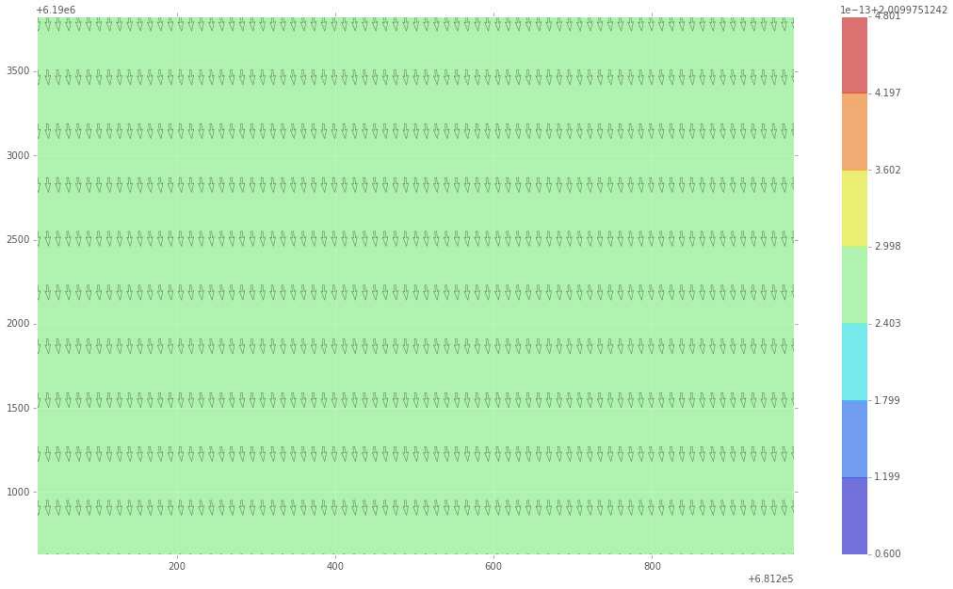

Figure 2-34: Velocity field screen shot from the Beta version of tidal hydrodynamics sub-packages.

The two outputs of the sensitivity analysis that are investigated are:

- Array Annual Energy Production (AAEP)
- Array q-factor

A better description of the simulation protocol, including the range of variation of the parameters, is provided in each sub-section (i.e. *Test 1* and *Test 2* sections).

A generic device with the following characteristics is simulated:

- Generic single horizontal axis turbine;

- Bottom fixed. The hub height is set to 26m from the seabed;
- Power curve : generic power curve Figure 2-35;
- The cut-in and cut-out velocity is set to 1.0 m/s and 2.75 m/s respectively;
- Turbine yaw disabled.

In a similar fashion to the wave model, a generic environment and lease area are chosen:

- Generic Boundary lease area;
- Bathymetry =flat, -60 m ;
- Minimum distance among devices = 80 m;
- Installation depth constraints = Minimum installation depth is set to 52 m. Unlimited boundary is provided for the maximum installation depth;
- Blockage-Ratio = 1;
- Optimisation threshold = 0.85 (The input defines the minimum q-factor allowed for the selected array layout. Any array with average q-factor smaller than this value will be considered unfeasible).

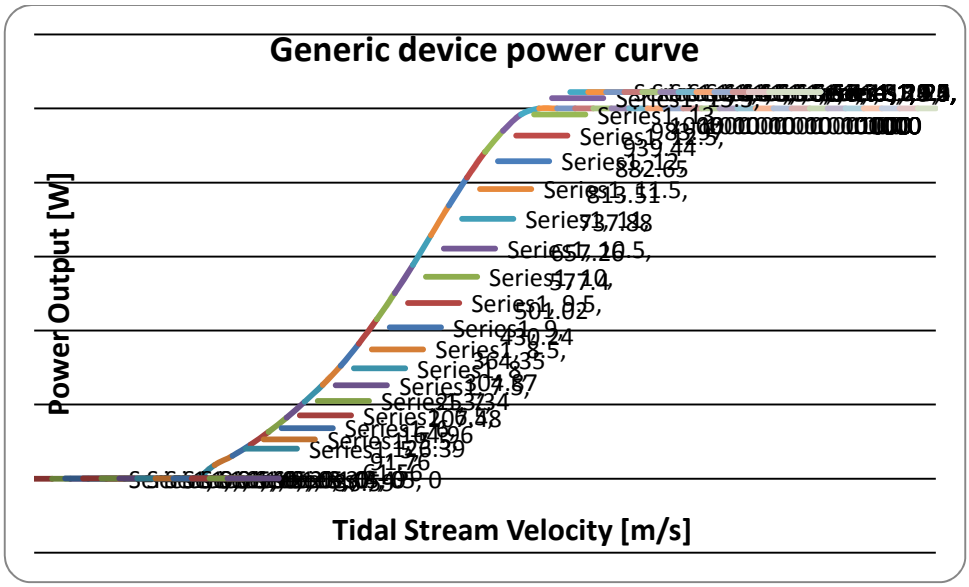

Figure 2-35: Generic device power curve used in the simulations.

The WP2 algorithm provided a solution of 20 tidal devices placed within the lease area as shown in Figure 2-36.

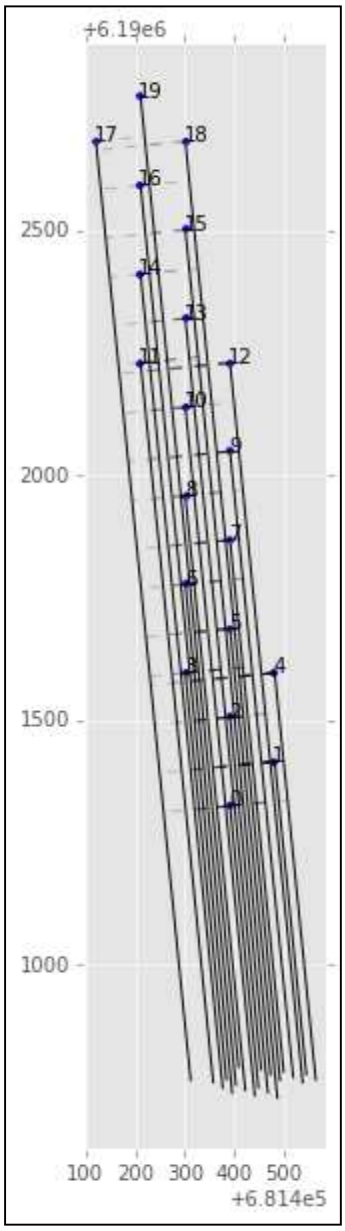

Figure 2-36: Solution found by WP2 algorithm. Streamlines of the 20 tidal devices with relative numbering are shown as well.

Test 1 -Varying Turbulence Intensity (TI):

The first test is performed by varying the turbulence intensity (TI) within a range of 0% and 30% of the tidal stream velocity vector magnitude (U_t) using 5% steps. Table 2-8 sums up the characteristics of the simulation with regard to the metocean conditions.

Table 2-8: Metocean condition for Test 1

Test 1 : Turbulence Intensity (TI)	
U_t	2 m/s. Unchanged throughout the simulations
SSH	0 m w.r.t. MSWL. Unchanged throughout the simulations
TI	**from 0% to 30% of U_t at 5% steps**

The outcome of the simulations is shown in Table 2-9 and Figure 2-37 The similarity of behaviour of AAEP and the Array q-factor can be appreciated. The two curves show a concavity with a minimum at TI=10%. The trend of the curves is in line with what is expected from the WP2 tidal model at the beta development stage.

Table 2-9: Array Annual Energy Production (AAEP) and Array q-factor for different values of turbulence intensity (TI).

TI	Array Annual Energy Production [MWh]	Array q-factor
0%	264.2323431	1.287534428
5%	191.5999019	0.933615724
10%	158.1416983	0.770582733
15%	158.44536	0.772062396
20%	165.2552721	0.8052453
25%	174.07437	0.848218435
30%	195.906213	0.95459924

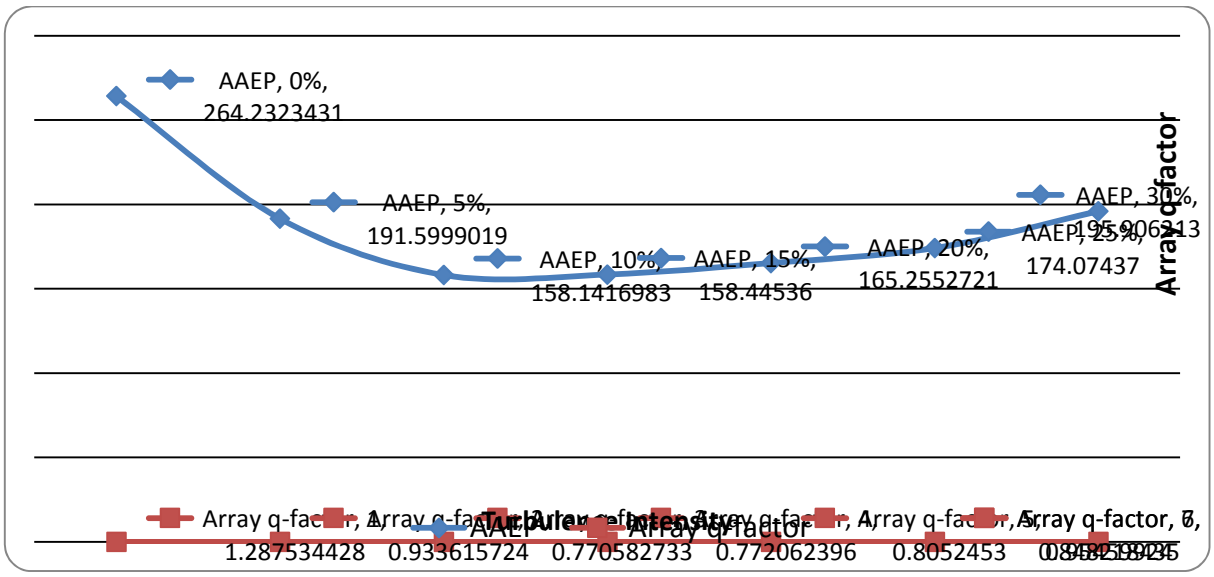

Figure 2-37: Array Annual Energy Production (AAEP) and Array q-factor behavior for different values of turbulence intensity (TI).

Test 2 – Varying tidal stream vector magnitude (U_t):

The second test is performed by varying the tidal stream vector magnitude (U_t) within a range of 0 m/s and 4 m/s using 0.5 m/s steps. Table 2-10 sums up the characteristics of the simulations from a metocean input perspective.

Table 2-10: Metocean condition for Test 2

Test 2: Tidal stream velocity vector (U_t)	
U_t	**from 0 m/s to 4 m/s at 0.5 m/s steps**
SSH	0 m w.r.t. MSWL. Unchanged throughout the simulation
TI	10% of U_t . Unchanged throughout the simulation

The outcome of the simulations is shown in *Table* 2-11 and *Figure* 2-38. As it can be noticed the tidal farm doesn't start producing energy for values of U_t smaller than the cut-in velocity (set to 1 m/s in the simulations). The Array q-factor cannot therefore be computed (i.e. no markers shown in Figure 2-38. As U_t approaches the cut-in velocity some turbines in the array start yielding energy (

Table 2-12). Similarly the array will stop producing energy for value of U_t greater than the cut-out velocity (set to 2.75 m/s in the simulations) and again, the Array q-factor cannot be shown in Figure 2-38.

These behaviours are reflected in the AAEP and Array q-factor curves.

Table 2-11: Array Annual Energy Production (AAEP) and Array q-factor for different values of tidal stream vector magnitude (Ut).

U_t	Array Annual Energy Production [MWh]	Array q-factor
0	0	N/A
0.5	0	N/A
1	0.586284238	0.311820138
1.5	26.66835322	0.763289756
2	152.8518066	0.767316902
2.5	544.0303387	0.802481762
3	48.78080997	0.743423207
3.5	0	N/A
4	0	N/A

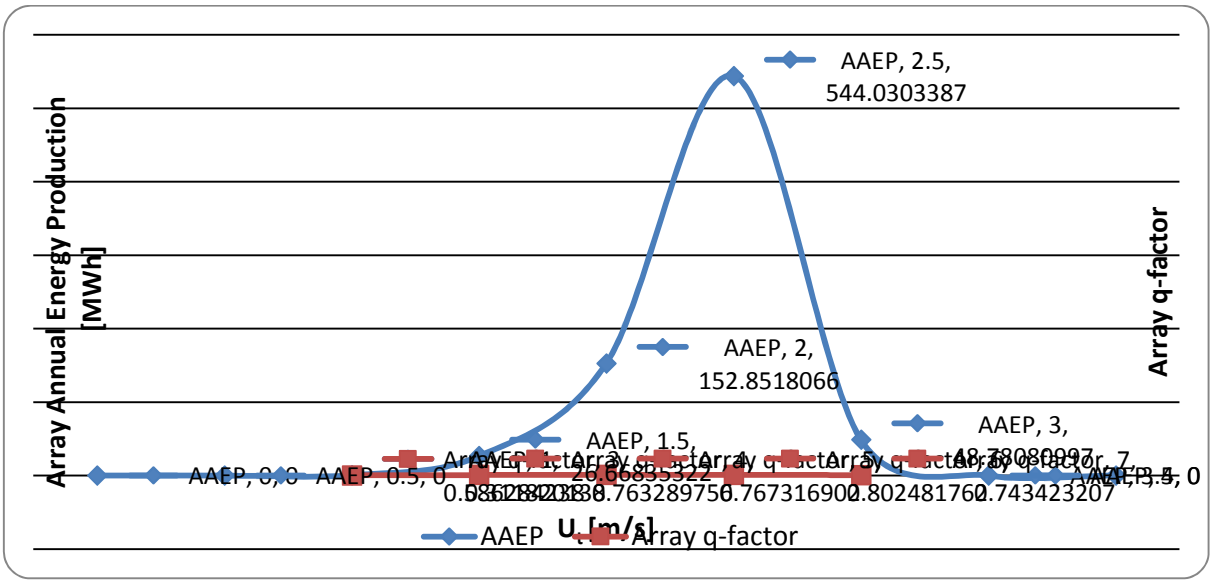

Figure 2-38: Array Annual Energy Production (AAEP) and Array q-factor behaviour for different values of tidal stream velocity (Ut).

Table 2-12: Array Annual Energy Production produced by each turbine in the array at the closest Ut stes to cut-in and cut-out velocity, respectively 1 m/s and 2.75 m/s.

No. Body	U_t = 1 m/s	U_t = 3 m/s
1	0	48780809.97
2	0	0
3	0	0
4	94738.76892	0
5	0	0
6	0	0
7	0	0
8	0	0
9	105180.6202	0
10	0	0
11	94834.73685	0
12	0	0
13	0	0
14	0	0
15	0	0
16	0	0
17	88136.29345	0
18	94010.00242	0
19	109383.8162	0
20	0	0

3 INTRODUCTION TO THE ENVIRONMENTAL ISSUES RELATED TO ARRAY DESIGN

Specifications of environmental conditions and dependencies on array changes can generate uncertainties in power production. Indeed, deployment of wave and tidal arrays can alter the hydraulic environment and change the amount of resource available for extraction. Such deployments also have impacts in terms of environmental issues.

Within the framework of DTOcean, a specific module, called the Environmental Impact Assessment Module (EIAM), is designed to assess the environmental impacts of the various technological choices made to optimize an array of wave or tidal devices.

The following chapter of this document deals specifically with the impacts of the introduction of devices in the marine environment in term of hydrodynamics and array optimization. In that context, several environmental impacts have been selected. The first environmental concern regards the amount of energy extracted by arrays and the direct consequences on the surrounding waters with modification of the flow. Another concern is the modification water turbidity that might directly affect primary production rates, sediment transport and benthic habitats. Noise is also a major environmental concern, especially at array levels. Array optimization and changes will also have major implications in terms of collision risks for marine life. Chemical pollution risks are also a concern with such deployments. Finally, some factors such as reef effects, reserve effects and resting places can be considered beneficial and are also dependent on array choices.

In this report, all the issues cited above are summarized in terms of potential environmental impact. Some general recommendations to minimize environmental effects and specific recommendations based on choices driven by hydrodynamic concerns are also given. Finally, the last section of this document gives a description of each environmental issue and its potential impacts, and of the developed EIAM functions with detailed explanations of calibration choices and values.

4 MAIN ENVIRONMENTAL ISSUES ASSOCIATED TO ARRAY CHANGES

4.1 Environmental background

4.1.1 Energy extraction

Tidal and wave marine energy converter devices operate by using the kinetic energy provided by currents and waves, respectively. This is often done using a turbine unit that will extract energy from the surrounding environment possibly resulting (at least for tidal energy converters) in changes in the water column velocity structure [17]. The flow upstream of a device will be decelerated, and a turbulent wake with a reduction of velocity will appear downstream the device [18]. An acceleration of flow around the device will also usually result. These modifications will directly affect the resuspension, and accumulation of sediment. Overall, the water flow remains a major process of the repartition of species in the water column and any changes can have an effect on marine ecosystems [19]. All sort of habitat can be impacted as shown in the Figure 4-1 which highlights marine habitats which may be altered by a change of the hydrodynamic flow [19].

Table 4-1 : A list of EUNIS marine habitats at level 3 that may be altered by a change of the hydrodynamic conditions *[19]*

A list of EUNIS marine habitats at level 3 that may be altered by a change to hydrodynamics.

Habitat Type Code	Habitat Description
A1.1	High energy littoral rock
A1.2	Moderate energy littoral rock
A2.1	Littoral Coarse sediment
A3.1	Atlantic and Mediterranean high energy infralittoral rock
A3.2	Atlantic and Mediterranean moderate energy infralittoral rock
A4.1	Atlantic and Mediterranean high energy circalittoral rock
A4.2	Atlantic and Mediterranean moderate energy circalittoral rock
A5.1	Sublittoral coarse sediment
A5.6	Sublittoral biogenic reefs
B3.1	Supralittoral rock (lichen or splash zone)

As tidal stream arrays are expected to modify natural water flows, they can affect benthic habitats and substrate, sediment composition and wave structure during both installation and operation phases of multiples turbines [20]. The level of energy reduction can have a direct impact on benthic habitats. These benthic habitats are essential, because some benthic species stabilize the normal sedimentary process. If these natural skills are altered, the long term consequences on the sedimentary process in the area can be important [19].

The different type of impacts that can occur during wave and tidal operational phases in relation to energy extraction are (according to [21], [22]):

- habitat loss
- habitat alteration
- smothering
- contamination

Environmental issues related to the implementation of devices in an offshore area have been described by [23] (potential impact of hydrokinetic and wave energy conversion technologies on aquatic environment). Amongst them was identified the alteration of hydraulic and hydrologic regimes. Movement of the devices may cause localized shear stresses and turbulence that may be damaging to aquatic organisms. On larger scales, extraction of energy from the currents may reduce the ability of streams to transport sediment and debris, causing deposition of suspended sediments and thereby alter bottom habitats.

Frid *et* al. [24]and references therein also reported that the installation and operation of individual or multiple tidal stream devices may directly affect benthic habitats by altering water flows, wave structures, or substrate composition and sediment dynamics. In particular water flow modification may result in localized scour and/or deposition directly affecting bottom habitats. For example, sand

deposition may impact seagrass beds by increasing mortality and decreasing the growth rate of plant shoots [8], while deposition of organic matter in the wakes of tidal farms could encourage the growth of benthic invertebrate communities [25].

The potential water quality impacts of tidal renewable energy systems have also been reviewed by Kadiri et al [26]. This study shows that tidal renewable energy arrays can have significant implications for the aquatic environment. In particular, in estuarine waters, tidal renewable energy arrays tend to modify salinity gradients, dissolved oxygen levels as well as sediment transport with an increase in sediment deposition and sedimentation rates. These changes might lead to different implications in terms of biogeochemistry such as a decrease in suspended sediments and fecal bacteria concentrations in the water column potentially affecting water quality parameters such as dissolved nutrients and metal concentrations.

More recently, Robins *et al* 2014 [27] studied the impact of tidal-stream arrays in relation to the natural variability of sedimentary processes. The authors showed through modeling and measurements of sediment type and bathymetry that tidal energy converter arrays are expected to impact locally and nearby on sediment processes. In particular suspended sediment concentration could be modified, potentially affecting the biological productivity of the area. Changes have been shown to be small compared to natural variability for 10 to 50 MW arrays that only reduce velocities locally by a few percent, and reduce bed shear stress and bed load transport by slightly more (suspended load transport is relatively unchanged, since tidal energy converter arrays induce locally increased turbidity). However, when a considerable proportion of energy was extracted (e.g. arrays greater than 50 MW), sedimentary processes became significantly affected.

Finally, Robins et al 2014 [27] also stated that their modeled flow reduction was not a complete representation (efficiency losses, drag effect, etc. are not taken into account in the model) and therefore the simulations of environmental impact might have been understated.

Wave converters can also reduce the wave action and wave height by the physical presence of the structures in the sea [18]. However, the impact on perturbations of the water flow and their consequences on sedimentary processes are expected to be much less significant than for tidal energy converters.

4.1.2 Collision risks

The collision risk in this report is qualified by the definition [28] “an interaction between a marine vertebrate and a marine renewable energy device that may a result in a physical injury to the organism”.

- Birds

Birds and especially marine species can be impacted by marine renewable devices through the direct effect of collision. Collisions generally occur when birds fly and collide either with devices in the air (mostly for offshore wind farm) or in the water [28]. Carried out till now was dedicated to offshore

wind farms. They show that the risk of collisions is likely to be species and site specific with the implication of the following factors [28]:

- flight behavior (altitude and maneuverability)
- avoidance availability
- proximity of migratory corridors and feeding areas
- weather conditions
- structure lighting

Collision risk related to wave and tidal devices is currently poorly understood [29]. Due to the lack of installed tidal and wave devices and the difficulty of quantifying collision rates, no quantitative studies have been carried out. However, Langthon and Klaus [26], [30] and Wilson et al. 2006 [28] shows that collision risks may be related to species specific parameters including:

- depth attained in the water column
- swimming speed
- diurnal rhythm of foraging
- location and behavior of species
- level of attraction
- effect of scheme turbidity
- effect of scheme on water flow

Figure 4-1 shows the different depth of several tidal devices and the depth attained by diving birds. It shows that most of the birds dive deeper than the tidal devices and therefore collision risks exists.

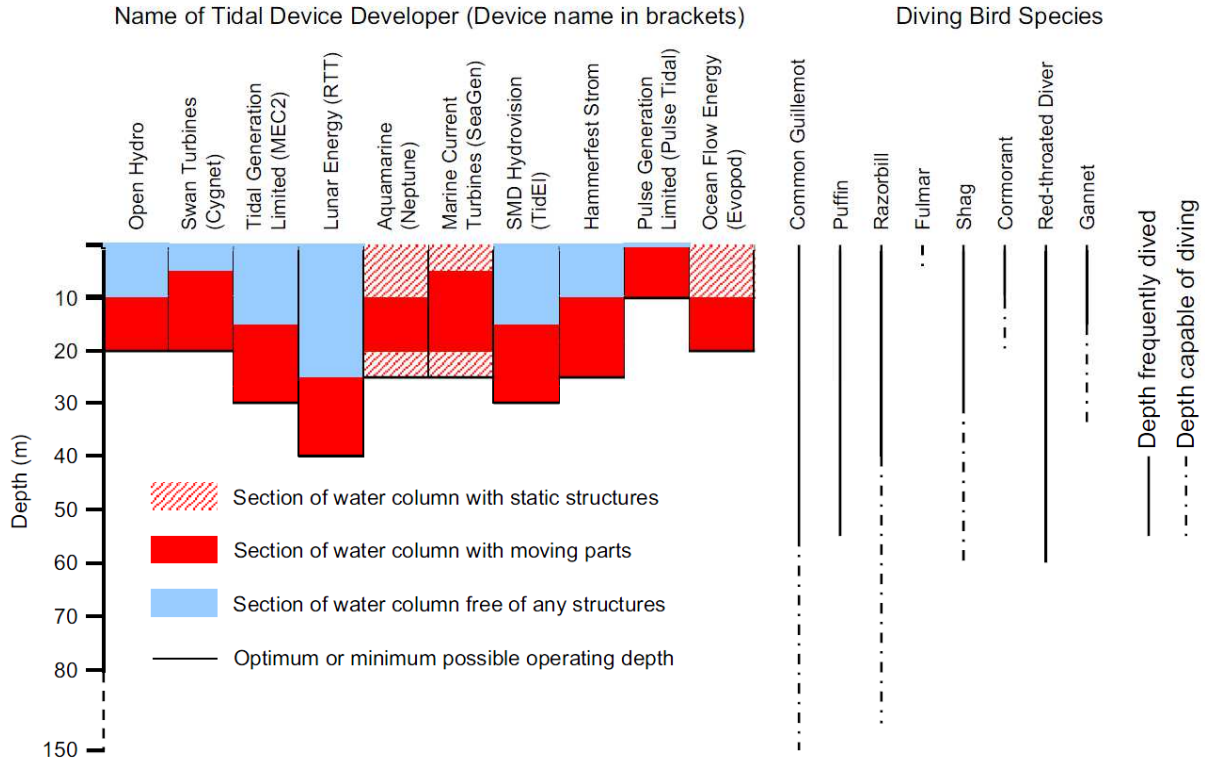

Figure 4-1 :Turbine depths and diving depths of bird species [31].

A few data are available on collision risks between birds and submerged structures other than offshore wind devices [31]. Grecian et al 2010 [32] indicate that there is a link between the type of device and the behavior of diving birds. The following factors affect the risk of collision:

- type of devices (floating or fixed)
- moving part of device (blades, cables)
- depth of device
- Static structure
- horizontal device
- vertical device

According to Grecian et al 2010 [32], the risk of collision between birds and wave devices may be low during flights because wave-powered devices have a small profile outside the water. However, this study highlights the fact that the collision risk is also dependent of several parameters such as:

- bad weather
- reduced visibility
- state of sea
- tide conditions

- Marine mammals

As with birds, marine mammals may be affected by MRE devices, particularly in term of collision and entanglement with tidal and wave devices. European waters are populated by a substantial number of marine mammals including seals and cetaceans. To date, a substantial amount of studies examining the potential impacts of MRE on marine mammals have been carried out, see for example [33], [22], [34], and [35].

Overall the risk of collision is a function of species, body size, swimming behavior and skills, capacity to detect devices as well as device type. The design of devices is also an important factor with regards to collisions. Many devices have a large surface structure and some trap points (ducts, vent devices, floating boxes etc.). Each of these elements can be dangerous for mammals and raise the risk of collision. Inger et al. (2009) [36] indicates that rotating devices from wave and tidal technologies may lead to injury or death.

In conjunction with mammal behavior, the organization of devices in an array as well as the location of the array itself are also important. Collision risks will be depending on depths, array organizations (devices in parallel, series) or location (narrow channels, open waters, sounds, etc). According to Wilson et al 2006 [28], the placing of structures may produce confusion and therefore a behavior modification. The detection of devices by mammals that do not have acoustic detection abilities (or mechanoreceptors) can be affected in highly turbid waters during storm events. Furthermore, large

mammals like whales appear to be more vulnerable than smaller species due to their size and bulk [35], [22]. The age of a mammal has been shown to also be a factor of risk as a preponderance of juveniles is noticed in entanglement observations, probably due to their lack of experience [35], [22]

However, as highlighted [19] there is still a high level of uncertainty regarding whether collision risks might impact mammals at population level. Most of the studies carried out to date are based on model predictions. For example Wilson et al (2006) [28] indicates a prediction of encounter rate of 13 individuals per year per turbine in an area surrounding a commercial deployment on the west coast of Scotland. Carter et al. [37] also modelled the likely encounter rate of marine mammals with marine energy devices and concluded that there is a possible risk for marine mammals only in case of big devices (diameter around 15 to 20 m). Nevertheless, Keenan et al. (2011) [38] showed that no major impacts on marine mammals have been detected across the 3 years of post-installation monitoring of the SeaGen turbine installed in the Narrows of Strangford Lough (Northern Ireland).

4.1.3 Turbidity

Turbidity is the cloudiness or haziness of a fluid caused by large numbers of individual particles. It usually gives an indication of the concentration of suspended particles in water.
MRE developments can modify the turbidity of ecosystems, especially during construction phases, while some activities involve interaction with the sediment. Thus, the concentration of re suspended particulate matter (SPM) can substantially increase locally. During operational phases, higher concentrations of SPM exceeding the natural variability can occur when tidal currents exceed a certain velocity [39] due to the interaction of the current with devices.

The main environmental impact generated by turbid waters is the adsorption of the light that may limit primary production. Indeed, light attenuation by suspended sediments confines the photic zone to a small fraction of the water column, such that light limitation is a major control on phytoplankton production and turnover rate [40].

Turbid waters can also impact benthos animals like filter-feeders and impact the development and growth of different species. SPM concentration increases can cause a decrease in respiration (due to clogging of filtration mechanisms), a behavioral alteration of species and a risk for eggs and larvae [41]. Such impacts are identified in high turbidity due to dredging activity. In contrast, the impact of an increase in turbidity on other species like marine mammals or birds is poorly known. Marine mammals often reside in turbid waters, so significant impacts from turbidity are improbable [41]. However, high turbidities may impact the ability to hunt, and the visual resolution power of diving-birds [42], [41].

Finally, turbid waters can generate high sedimentation rates (often locally) in areas where hydrodynamic conditions are more favorable, thus changing the sediment structure and the associated benthic communities. In general, regularly disturbed habitats characterized by fine sands and fast-

growing opportunistic species are less affected, and recover quicker, than stable habitats monopolized by coarse gravels and slow-growing sessile fauna and flora [43]. In addition to changing community structure, sediment deposition can smother or bury marine organisms associated with the seabed. Non-mobile organisms and early life stages that are unable to move are most at risk [41].

4.1.4 Underwater noise

The quantification of underwater noise due to wave and tidal devices is poorly known. Underwater noise is device specific and also directly related to the number of devices. Each device has a range of associated noise spectra [44]. Sources of noise are multiple. They have been listed by Robinson et al [44] as:

- Noise generated by turbulence and vortex shedding
- Noise from hydraulics, joints and hinges
- Noise from moorings
- Impact of surface waves
- Rotating machinery
- Movement of air or water
- Noise in all operational modes (start-up, braking, stationary)

Noise radiation is created by the moving parts of devices. This movement generates different pressure and turbulence. The variety of designs can then produce a large range of potential noise that can propagate in the water column.

The decibel level of sound is stated in the form of the dB re 1 µPa. The µPa is a unit of pressure [45]. There are different levels of reference to define the underwater noise. The SPL: is the expression of the Sound Pressure Level in decibel (dB). The SEL: Sound Exposure Level metric, sums the acoustic energy over a measurement period, and effectively takes account both the SPL and the duration of the sound in the acoustic environment [46].

Environmental effects related to noise are expected to impact the marine life in different ways. Marine mammals, for example, can adapt to a wide variety of natural sound and have adaptive mechanisms to deal with many anthropogenic sounds. The frequencies that can be heard from marine mammals range from less than 100 Hz up to 180 kHz, making predictions of potential effects challenging. However, when anthropogenic sounds are excessive in level, frequency or even duration, they might exceed the mammal's adaptive capacity and cause the following main effects (see [47] and reference therein):

- Physical injuries: with permanent threshold shifts or loss of hearing sensitivity resulting from either a brief exposure to very intense sounds or a longer duration to moderately intense

sounds, or intermittently but repeatedly to sounds sufficient to cause temporary threshold shifts [48]

- Physiological Reactions: with sound exposure that causes non-auditory physiological effects like stress.
- Masking: when sounds are more difficult to hear because of added noise affecting mammal's detection and interpretation. Masking may affect (1) reproduction if a female cannot hear potential males vocalizing, (2) mother-offspring bonding and recognition if the pair cannot communicate effectively, (3) foraging if animals that hunt cooperatively cannot communicate or if they cannot detect prey , and (4) survival if an animal cannot detect predators or other threats.
- Behavioral responses: following the detection of sounds, mammals can change habitat use to avoid areas of higher sound levels or modify patterns such as diving and surfacing or vocalizing.

As with mammals, fish are characterized by a wide range of hearing structures, resulting in different capacities and sensitivities to noise. They use biological noise to gain information about their surrounding environment in order to locate their prey and predators or even communicate. Noise may generate physical injury, hearing loss and behavioral changes. However, the impact is unknown and will be dependent on the received sound. In their paper review on several European fishes, Gill and Bartlett [49] indicated that fishes that receive high intensity sound pressures (e.g. close proximity to MRE construction) may be negatively be impacted to some degree, whereas those at distances of 100s to 1000s of meters may exhibit behavior responses. During operation there may be more subtle behavioral effects that should be considered over the life time of the MRE development. Slabbekoorn et al. 2010 [50] also stated that very loud sounds of relatively short duration can harm nearby fish.

For birds, noise is considered as an indirect effect. Indeed it may cause a reduction in fish abundance and therefore reduce food resources. For both mammals and fish, displacement is also another potential effect generated by noise where devices are deployed, but this effect is hardly quantifiable.

Different kinds of noise will be generated during construction/installation and operation. However, the construction/installation phase is usually of particular concern due to specific activities such as anchoring and especially pile driving. On that matter and in the absence of large tidal and wave developments, most of the studies carried out on noise are related to wind farms. Bailey et al. 2010 [51] measured pile driving noise at distances of 0.1 km (maximum broadband peak to peak sound level 205 dB re 1 µPa) to 80 km (no longer distinguishable above background noise). These sound levels were related to noise exposure criteria for marine mammals to assess possible effects. For bottlenose dolphins, auditory injury would only have occurred within 100 m of the pile-driving and behavioral disturbance, defined as modifications in behavior, could have occurred up to 50 km away. Harbour porpoises and harbour seals are likely to be able to hear pile driving blows at ranges of more than 80 km and severe injuries in the immediate vicinity of piling activities cannot be ruled out [42]. These

authors also suggested that behavioral responses are possible over many kilometers, perhaps up to ranges of 20 km and that masking might occur in harbour seals up to 80 km.

A review of operational noise record was carried out around MRE test sites [27]. Table 4-2 and Table 4-3 summarize measures for tidal and wave technologies, respectively.

Table 4-2: Underwater noise induced by tidal devices

MRE sites (devices)	Phase	Measurement
Tidal		
Fall of Warness Tidal Energy Test Site (Voith Hydro) 2010	operational	SPL:120-130 dB re 1µPa (500m)
Lynmouth Bristol Channel (Marine Current Turbines MCT)	operational (1 turbine)	166 dB re 1µPa (1m) (calculated)
Strangford Lough (SaeaGen turbine)	operational	SPL: 141 dB re 1µPa (311 m)
Cobscook Bay Tidal Energy Project (TEC)	operational (1 turbine)	100 dB re 1µPa2/Hz (10m)
Roosvelt Island Tidal Energy Project (Verdant Power tidal)	operational (6 turbines)	145 dB re 1µPa (1m)
Admiratly Inlet Tidal Energy Development	operational (2 turbines -6m)	172 dB re 1µPa (1m)

Table 4-3: Underwater noise induced by wave devices

MRE sites (devices)	phase	measurment
Wave		
Billia Croo Wave Energy Test Site (Pelamis)	operational (high sea state:3-4)	181 dB re 1µPa2/Hz (1m) (1KHz))
Wave Energy Test Centre (European Pilot Plant of Wave Energy Oscillating Wter Column device)	operational (8 turbine blades)	SPL: 126 dB re 1µPa (10m)
Lysekil project (Wave energy converters)	operational	SPL average: 129 dB re 1µPa (20m)

Most of the studies emphasized that there is a lack of standardization of survey and analytical methodologies to support future comparisons and assessments [51]. An interesting initiative has been developed by Nedwell et al 2007 [52] with the validation of a frequency weighted scale, the dBht

(Species), as a metric for the assessment of the behavioral and audiological effects on underwater animals of man-made underwater noise.

The dBht (Species) metric has been developed to quantify the potential impact on the marine species behaviours [52] . As any given sound will be perceived differently by different species (since they have different hearing abilities) the species name must be appended when specifying a level.

For instance, the same construction event might have a level of 70 dBht (Salmo salar) for a salmon, and 110 dBht (Tursiops truncatus) for a bottlenose dolphin.

Table 4-4 below summarizes the assessment criteria when using the dBht (Species) process [46]:

Table 4-4: Assessment criteria [50] used in this study to assess the potential behavioral impact of underwater noise on marine species.

Level in dB_{ht}(*Species*)	Effect
90 and above	Strong avoidance reaction by virtually all individuals.
Above 110	Tolerance limit of sound; unbearably loud.
Above 130	Possibility of traumatic hearing damage from single event.

In addition, a lower level of 75dBht has sometimes been used for analysis as a level of “significant avoidance”. At this level, about 85% of individual organisms will react to the noise, although the effect will probably be limited by habituation [46].

Based on the evidence of auditory damage from the public domain, studies [53] propose a set of auditory injury criteria based on peak pressure levels and M-weighted Sound Exposure Levels (Table 4-5) (dB re. 1 µPa2/s (M).

Table 4-5: Proposed injury criteria for various marine mammal groups [53] [46].

	Sound type
Marine mammal group	**Single pulses**
Low Frequency Cetaceans	
Sound Pressure Level	230 dB re 1 µPa (peak)
Sound Exposure Level	198 dB re 1 $\mu Pa_2/s$ (M_{lf})
Mid Frequency Cetaceans	
Sound Pressure Level	230 dB re 1 µPa (peak)
Sound Exposure Level	198 dB re 1 $\mu Pa_2/s$ (M_{mf})
High Frequency Cetaceans	
Sound Pressure Level	230 dB re 1 µPa (peak)
Sound Exposure Level	198 dB re 1 $\mu Pa_2/s$ (M_{hf})
Pinnipeds (in water)	
Sound Pressure Level	218 dB re 1 µPa (peak)
Sound Exposure Level	186 dB re 1 $\mu Pa_2/s$ (M_{pw})
Sound Exposure Level	198 dB re 1 $\mu Pa_2/s$ (M_{pw}) Proposed by Thompson and Hastie (in prep.)

4.1.5 Chemical pollution

The risks of chemical pollution in marine renewable developments related to the devices and vessels are mainly:

- hydraulic fuel leaks causing by unexpected device damage, corrosion, or release of antifouling agents during maintenance operations.
- potential fuel or oil leakages or accidental spillage due to vessel traffic during installation, operation & maintenance and decommissioning phases.

The main impacts related to chemical pollution will be the degradation of water quality surrounding the array. Water quality impacts both directly and indirectly the diversity and abundance of marine communities.

Hydrocarbon pollution in coastal ecosystems is a well-known and growing global problem [54]. Associated harmful effects include organism death, stress for benthic communities [55] and food chain major disturbance [56]. Polmear et al. 2015 [55] have also recently shown evidence of toxicity of lubricants on phytoplanktonic communities. This is confirmed by the study of Hook and Osborn 2013 [57] with long term effects extending over several years.

Anti-fouling paints use a wide range of chemicals which have very different physio-chemical properties and therefore differing environmental impacts, behaviour and effects. Copper has been used as an

anti-foulant for centuries. Biocides have also been widely used over a number of decades, for example Irgarol 1051 and diuron. There are also new or candidate biocides such as triphenylborane pyridine, Econea, capsaicin and medetomidine for which there is very little information in the public domain. The use of antifouling paints can introduce high levels of contamination into the environment, raising some concerns about toxic effects on marine communities. Marine organisms can directly accumulate antifouling contaminants and transfer contaminants to higher trophic levels. If the uptake of the contaminants exceeds the organism's ability for excretion and detoxification, this can reduce normal metabolic functioning [58], [59].

Toxicity is directly related to the properties of the contaminant and especially its bioavailability. Toxicity will increase if a contaminant is more bioavailable. This bioavailability is also driven by the environmental chemical conditions (e.g., temperature and pH) as well as the contaminant affinity for particles (sediment binding). Sediments tend to act as a contaminant sink. The remobilisation of sediments by natural storms or anthropogenic events (e.g. MRE device installation) can be a major source of pollution through the release of contaminants in the water column.

Studies on antifouling paints have shown that plankton is highly sensitive to antifouling substances. Indeed the embryo/larval stages of the mussel, oyster and sea urchin were found to be sensitive, with total dissolved copper EC50 concentrations of 6.8, 12.1 and 14.3 µg L-1, respectively. Fish were more tolerant to copper exposure with EC/LC50 concentrations ranging between 0.12 and 1.5 mg L-1 total dissolved copper. Organic biocides appear to be much more toxic to phytoplankton species than other aquatic animals. Irgarol 1051 appears to be especially toxic to the freshwater diatom (Navicula pelliculosa; (5 day EC50 0.136 µg L-1) [60] and the freshwater macrophytes Chara vulgaris (14 day EC50 0.017 ng L-1) [60]. Table 4-6 provides examples of toxicity effects and levels for different biocides.

Table 4-6: main biocides and toxicity effects.

Toxic effects
Irgarol 1051: blocks the electron transport at photosystem II (inhibiting photosynthesis)
Diuron: blocks the electron transport at photosystem II (inhibiting photosynthesis)
Dichlorofluanid
DCOIT Sean Nine 211: toxic effect: 2,7-32 µg.L-1
CuPT: toxic effect: 2,7-32 µg.L-1
ZnPT: toxic effect: 2,7-32 µg.L-1
Medetomidine: toxic effect: reduce pheromone of amphipod (*Corophium volutator*) at 10µg.L-1

Overall, issues related to water quality may also generate temporary displacement from surrounding areas and affect mammals via their influence on prey or habitat [61]. However, tidal and wave devices will be located in energetic environments and impacts linked to water quality generated by point source pollution will be largely attenuated due to the high dispersive capacity of the area [21].

4.1.6 Beneficial effects: Reef effect

Marine renewable developments on the water bottom can provide new hard substrate to marine organisms for colonization, thus playing the role of "artificial reefs". As such they can generate new or enhance existing habitats with an increased heterogeneity in the area important for species diversity and density. Despite the need for more research about the advantages of these new habitats, there seems to be a consensus about the positive effects for marine organisms. Indeed, new habitats increase the available area for habitat and attract marine life in search of food, hence providing prey for mammals. Langhamer 2012 [62] indicates that a positive reef effect is dependent on the nature and the location of the reef and the characteristics of the native populations.

Figure 4-2 shows examples of colonization on different MRE structures. Pictures in Figure 4-2 show advanced colonisation by mussels (Mytilus Echilij) on protective structures in the Horn Rev offshore wind farm (Denmark) [63].

www.ens.dk/offshorewind Danish Offshore Wind – Key Environmental Issues

Figure 4-2: colonization of offshore wind pile.

This "reef" effect was highlighted on the bases of offshore wind turbines [64]. There may also be a "refuge" effect for some species, which find favorable habitats between the artificial structures. Certain protective structures for laid cables can accommodate benthic species that are of potential interest from a heritage or commercial perspective (e.g. large crustaceans) [65]. Some new investigations at the tidal site of Paimpol-Bréhat (France) seem to show that concrete mattress could be used as a new habitat by crustaceans (Carlier, pers. Comm.).

The positive effect of these new “reefs” has to be tempered soft sediment habitats. The introduction of artificial hard substrates can promote the establishment of hard substrate species and modify the

initial habitat. These new hard substrates can also promote introduced species (including invasive species), and accelerate their geographic expansion by playing the role of "bridgehead" [66].

4.1.7 Beneficial effects: Reserve effect

The physical presence of MRE developments will affect the use of areas with restricted access to these areas. Despite leading to discussions and conflict regarding recreational and commercial activities, these new 'preserved' areas will act as small marine protected areas (MPAs). Inger et al. (2009) [36] highlight the fact that MPAs, where all fisheries and other forms of extraction are excluded, can be used as a fisheries management, conservation and ecological restoration tool.

As well as protecting and enhancing fish stocks, the implementation of such MPAs will also enrich benthic biota, by lifting the pressure from towed bottom fishing gear [67], which has chronic effects on seabed communities and is likely to affect ecosystem functioning [43].

Impact will vary depending on the restriction measures in place but. fishing restriction creates a marine protected area that will have positive impacts on biodiversity, and juvenile's and reproductive adult's protection [68]. These effects have already been observed in offshore windfarms [69]. However, it is important to remember that the location, and hence the habitat protected by this potential reserve effect, could also be valuable in terms of conservation, restoration for surrounding fishery [36].

4.1.8 Resting place

Emerged structure can be used as resting platforms mainly for birds and pinnipeds depending on their accessibility. This positive impact is of course only considered during the operation phase of the project. In open sea where resting places could be rare, these structures will create new habitats. Species such as gulls, terns and cormorants show no avoidance response to emerged MRE structures and may instead be attracted to theses installations through prey aggregation and their use as resting/foraging platforms [65]. This latter study indicates that effects would be species-specific.
The positive impact is however only valuable if it is not dangerous for the animals to stand on the structures.

4.2 General recommendations

4.2.1 Energy modification

- Design devices and arrays in order to minimize the water velocity effect and the bottom substrate effect
- Foster design of devices based on floating platforms (substrate and sediment transport are minimized) [18]
- Minimize power dissipation

4.2.2 *Collision risk*

- Have a good knowledge of the sensitive species (mostly marine mammals) in the project area
- Choose device composition and material that reduce the risk of collision and entanglement, for example: [18], [28]
  - By increasing the detectability of the device by animals (use specific color).
- Locate device in a specific area (bathymetry, etc.)
- Choose appropriate device for the area and species in this area (reducing vertical traps)

4.2.3 *Turbidity*

- Try to choose a low impact design and operation of device regarding sediment disturbance
- Adjust the rotation velocity of the device (tidal)

4.2.4 *Underwater noise*

- Have a good knowledge of the sensitive species in the area
- Use of sound insulation around the device [18]
- Use of acoustic mitigation to exclude animals from the area
- Have a good knowledge of sensitive area and locate the project away from the sensitive area
- Limit the size of the project

4.2.5 *Chemical pollution*

- Design of the device: minimize the volume of lubricants and chemical fluid
- Use of new less toxic antifouling substances

4.2.6 *Reef effect*

- Choose a design that will increase their colonization potential
- Reduce antifouling protection
- Locate device in water deeper than 20 meters [18]

4.2.7 *Reserve effect*

- Adapt activity restriction measures to the project and to the habitats and species found in the area.

4.2.8 *Resting place*

- Secure safe part of device that could be used as resting place by birds or pinnipeds.
- Minimize horizontal surfaces of devices to limit the resting place for marine mammals and birds if these parts of device are dangerous.

4.3 EIAM environmental process

The whole EIAM is based on several scoring principles detailed in Deliverable 7.2. Briefly, the use of the environmental functions allows the EIAM to generate numerical values that will be converted in to environmental scores (Environmental impact score) (Figure 4-3). The conversion from the function scores to the environmental scores is made through calibration matrices. Each function is associated with one calibration matrix (or several depending of the complexity of the function) in order to qualify the pressure score. Calibration matrices are based on literature data.

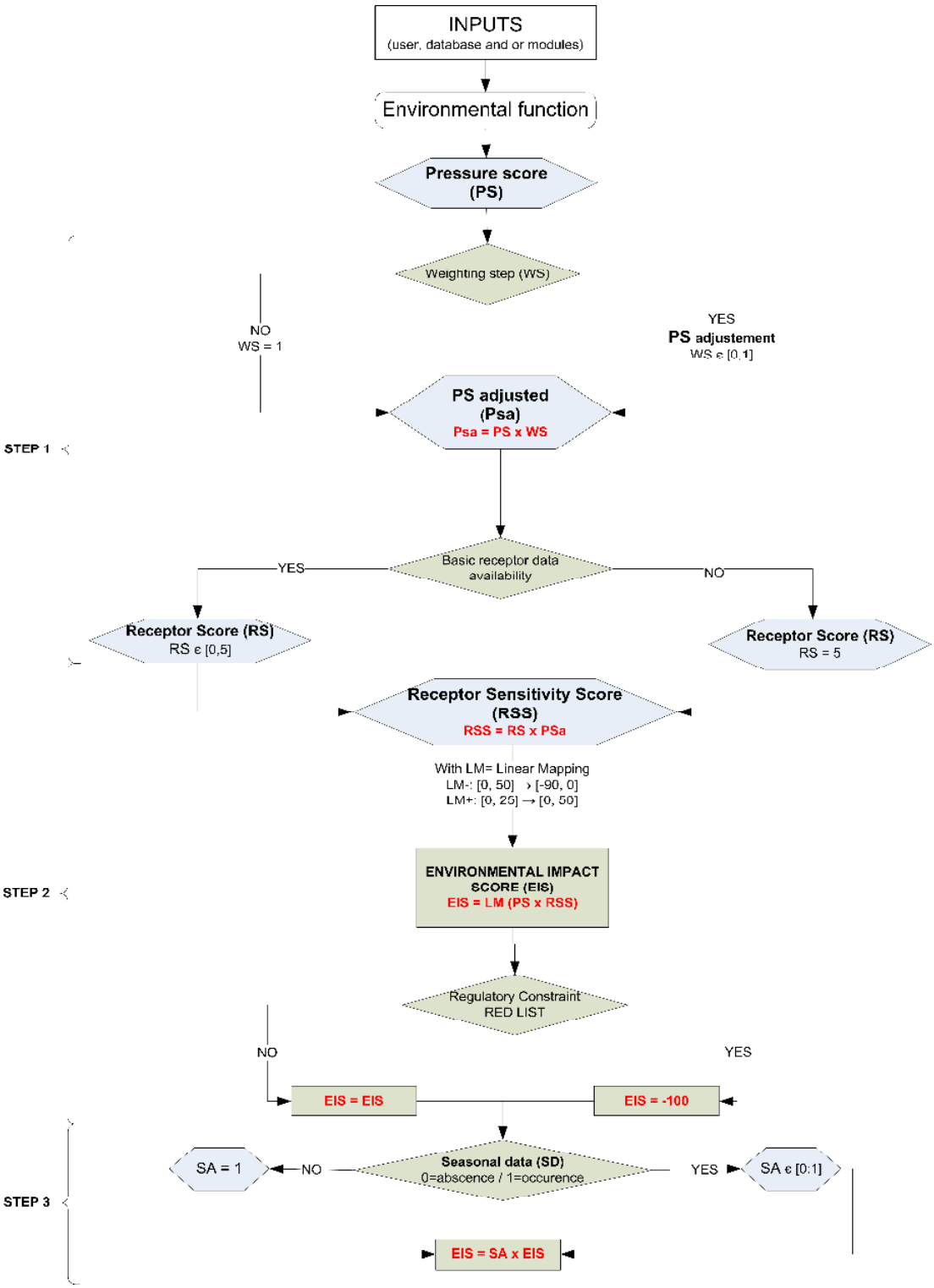

Figure 4-3: flow chart and calibration matrices.

The scoring allocation system developed within the framework of DTOcean is generic for each environmental function and based on three consecutive main steps (as shown in Figure 4-3):

- STEP 1: qualification and quantification of the 'pressure' generated by the stressors.
- STEP 2: basic qualification of the occurrence (or absence) of receptors potentially affected by the stressors. If the chosen receptors in the basic receptor database are also in the red list, the Receptor sensitivity score doesn't use the standard qualification of the score, but takes the maximum score 100.
- STEP 3: qualification refinement of receptors e.g. definition of slot of occurrence during the year where receptors are sensitive (ie nesting seasons for birds, breeding seasons for mammals...).

4.4 EIAM environmental functions associated with hydrodynamics

All the parameters involved in the environmental processes are presented in this section. Stressors create the pressure and receptors are the sensitive animal and vegetal species impacted by the stressors. The environmental function uses inputs to produce a result. As shown in Figure 4-3, a weighting factor can also occur in the first step of the evaluation process to better qualify the pressure.

Some definitions:

- Stressors: Stressors are the physical anthropogenic elements that generate the 'footprint' pressure.
- Receptors: Receptors are all the biological components (animal and vegetal species, habitats) potentially impacted by the stressors.
- Weighting step: The weighting score ranges between 0 and 1. If there is no data for the constraints, the precautionary principle lead to the worst weighting case: 1.
- Inputs: To quantify the pressure and the impact, some parameters or inputs are required. They are provided by the DTOcean database, the other modules or the user.

4.4.1 Environmental function: energy modification

Objective

The aim of this function is to assess the impact of current and wave energy modification due to arrays on biological receptors.

Stressors

In the Array Hydrodynamic issue the energy modification is induced by the extraction of the current and wave energy by the devices. Incoming and outgoing energy from arrays is used to calculate the percentage of energy extracted by arrays.

Receptors

Regarding energy modification the major species that can be impacted are the benthic species (living on the hard and soft substrate).

Required inputs

Extraction of energy by device (WP2) in %

Function

The energy modification function is calculated as written in the equation

$$Energy\ modification = \text{current or wave energy extraction } \% \quad (4.1.)$$

Rule of the function

The higher the percentage of extracted energy, the higher the expected environmental impacts is.

Weighting step

For the energy modification function, the constraint is the type of sediment.

Calibration

Step1

Even if the environmental impact due to the extraction of energy is area specific, the environmental impact is usually qualified as "low" for 1% of the energy extracted and "noticeable" for an extraction around 10% [70]. The bed sediment stress is a function of the current speed (U^2), so small changes of current and waves can readily affect sediment transport.

For the EIAM, several ranges of extracted energy have been defined in Table 4-7:

Table 4-7: Energy extraction range and Pressure score.

Energy extraction range	PS - Pressure score fitting in energy extraction range
[0-10%[	0
[10-20%[	1
[20-30%]	3
>30%	5

Qualification of the sediment feature is important at this stage as it exists a strong relationship between the type and size of the sediment particles and the hydrodynamic pressure. A flow

modification can alter the dynamic sediment erosion/deposition and the size and composition of eroded particles [17]. In order to take that into account to better evaluate the impact of the extracted energy, a weighting score (WS) based on the characterization data of the sediment is used in Table 4-8.

Using this matrix, the environmental impact is better defined with a change of EIS value. For example, EIS value will be lowered for a rocky area as there is a low probability of generating a bed sediment stress. On the other hand, EIS will be increased for sandy areas or other fine sediment particles, as they are easily affected by modification of flow.

Table 4-8: Sediment weighting score.

Constraints : sediments		
Soil group	**Soil types**	**Weighting score**
cohesion less	Loose sand	1
	Medium sand	1
	Dense sand	1
cohesive	Very soft clay	1
	Soft clay	1
	Firm clay	0.5
	Stiff clay	0.5
other	Cemented	0.1
	Soft rock coral	0.1
	Hard glacial till	0.1
	Gravel cobble	0.1
	Hard rock	0.1

At the end of this step the Pressure Score adjusted by the Weighting Score is calculated, the PSa the Pressure Score Adjusted.

Step2

Benthic habitats of hard substrate are potentially more vulnerable than soft substrate because a reduction of the hydrodynamic energy could lead to a sedimentation that will change the habitats. This is the reason why we have assigned the score of 3 for species living in hard substrate and 1 for species in soft substrate. The receptor scores in Table 4-9 are based on the nature of the benthic habitats.

Table 4-9: Receptor Score.

Soil groups	**Soil types**	**RS**

Hard substrate benthic habitats (cemented to hard rock soil types)	Rocky mediolittoral habitats, Rocky infralittoral habitats, Rocky circalittoral habitats (coastal and deep)	3
Soft substrate benthic habitats (cohesion less soil group)	littoral sediment, Infralittoral sediment, Circalittoral sediment (coastal and deep)	1
Particular habitats	Zostera noltii beds, Zostera noltii beds, Maerl beds	4

After selecting the appropriate Receptor Score (RS), The Receptor Sensitive Score (RSS) can be obtained using the equation

$$EIS\ step\ 2 = linear\ maaping\ (PSa\ X\ RS) \quad (4.2.)$$

In the case where the receptor is 'regulatory protected', the DTOcean database should be able to identify it during this STEP and then assign the maximum negative EIS score (-100).

Step3

The final step (STEP 3) takes into account the seasonal distribution of the receptors. If data are available (provided either by the user or the database), EIS step2 will be evaluated to a new value called EIS final using a new matrix containing the information of the receptor monthly absence or occurrence. If the receptor is present and sensitive a score of one is allocated to the seasonal score (SA) and if the receptor is not present or not sensitive the seasonal score will be zero.

Finally, the final Environmental Impact Score is ultimately calculated as:

$$EIS\ final - Environmental\ impact\ score = SA\ X\ EIS\ step\ 2 \quad (4.3.)$$

4.4.2 Environmental function: collision risk

Objective

Evaluation of the collision risk between fauna (marine mammals and birds) and devices.

Stressors

In the Array Hydrodynamic issue only collision is considered and not the entanglement. The presence of devices in the seabed or in the water column can generate a pressure for the species.

Receptors

Regarding the collision risks between animals and devices, the major species that can be impacted are mainly marine mammals and birds. For both species the position of the devices in the water column has to be taken into account.

Required inputs

- cross sectional area of the farm
- Number of devices
- Volume of the device

Function

Work in progress (4.1.)

Rule of the function

0 ≤ ratio ≤ 1
0 = green, increase = goes towards red
The placement of devices and depth are important to determine the collision risk.

Weighting step

For the collision risk function, the constraints are the position and the location of the devices.

Calibration

Step1

To qualify score and calibration, some data found in the literature review have been used. A feedback of this collection is proposed in this chapter. To quantify the collision risk "Pressure Score" PS an arbitrary method was used. After obtaining the result of the function, the data is classified at one of 3 levels.

Above 25% of space occupied by devices, the collision risk is estimated as high. A weight is given for each category dependent on the risk of collision for a specie in Table 4-10.

Table 4-10: Calibration risk range and Pressure Score.

Collision risks range	PS - Pressure score fitting in collision risk range

[0-0.1[	1
[0.1-0.25]	3
>0.25	5

The collision risk depends on the placement of device (location: open ocean, channel etc., and position: in series, in parallel). According to Wilson *et al* 2006 [27] the collision risk between marine mammals and devices disposed in parallel in a channel is higher than in other areas, open ocean for example.
To better evaluate the collision risk, a weighting score (WS) based on the location and the position of the devices is used in the Table 4-11.

- Low weighting score (devices placed in series in open water are qualified are low risk).
- Moderate weighting score (devices placed in parallel in open water or in series in sea loch entrances or in sounds are a potential risk).
- High weighting (devices in parallel in sea loch entrances or sounds are high risk because they occupy more space and severely hinder maneuverability).

Table 4-11: Weighting Score for the collision risk.

weighting parameter	**weigthing score**
open water/ devices in serie	0,25
open water/ devices in parallel	0,5
sea loch entrances/ devices in serie	0,5
sounds / devices in serie	0,5
sea loch entrance/ devices in parallel	1
sounds/ devices in parallel	1

At the end of this step the Pressure Score adjusted by the Weighting Score is calculated, the PSa the Pressure Score Adjusted.

Step2

The next step (STEP 2) is to consider if there are some species in the area and their degree of sensitivity through a coefficient (Receptor score) that will lead to the EIS step 2. Receptor Scores (RS) were obtained from the literature and other European regulations.

According to GHYDRO 2013 [22], in Europe, marine mammals have a specific protected status. Cetaceans and pinnipeds are the object of numerous international regulations and protection texts, such as the Washington convention [71], Berne convention, Convention on migratory species [72], OSPAR etc. They are also directly affected by international agreements such as ASCOBANS [73], ACCOBAMS [74] or the International Whaling Commission [75].

At the European level, the Habitats Directive (Natura 2000) [76] also mentions many species of marine mammals in Annexes IV (species protection) and II (protection of species and their habitats). Finally, the Marine Strategy Framework Directive (MSFD) [77] also shows a close interest in marine mammals and the human activities that threaten them.

Given these protections statuses, it's not pertinent to give the same high score for all marine mammals. It was decided to give a special RS to marine mammals based on their maneuverability, sociability with human activity and feed depth.

An example of RS for marine mammals and birds values are presented in the table below Table 4-12

Table 4-12: Receptor Score Marine Mammals.

Example of species for user	**Score**
Up to 5m - Fulmar	4
5 to30 m - Shag/Cormorant/Gannet	2
> 30 m - Common Guillemot/Puffin/Razorbill	2
Up to 5m - Fulmar	1
5 to30 m - Shag/Cormorant/Gannet	4
> 30 m - Common Guillemot/Puffin/Razorbill	2
Up to 5m - Fulmar	1
5 to30 m - Shag/Cormorant/Gannet	1
> 30 m - Common Guillemot/Puffin/Razorbill	4
Groups Marine Mammals	**score**
Seal	3
Large odontocete, Mysticete or Dolphinids	4
Odontoncete	5

After selecting the appropriate Receptor Score (RS), EIS step 2 can be obtained using the formula:

$$EIS\ step\ 2 = linear\ mapping\ (PSa\ X\ RS) \qquad (4.2.)$$

In the case where the receptor is 'regulatory protected', the DTOcean database should be able to identify it during this STEP and then assign the maximum negative EIS score (-100).

Step 3

The final step (STEP 3) takes into account the seasonal distribution of the receptors. If data are available (provided either by the user or the database), EIS step2 will be evaluated to a new value called EIS final using a new matrix containing the information of the receptor monthly absence or occurrence. If there is data the seasonal score (SA) is allocated with a score of one and if there is no data the seasonal score is allocated of a score of zero.

The final Environmental Impact Score is ultimately calculated as follow

$$EIS\ final - Environmental\ impact\ score = SA\ X\ EIS\ step\ 2 \quad (4.3.)$$

4.4.3 Environmental function: Turbidity

Objective

Evaluation of the impact of the turbidity modification intensity in the water column due to arrays.

Stressors

In the Array Hydrodynamic issue is considered a stressor for the turbidity function, the turbidity created during the operational phase of the devices.

Receptors

The turbidity created during the installation phase is a physical pressure that can affect benthos and the benthic habitats of cohesion less soils, cohesive soils or cemented and rocky soils, but also fishes, marine mammals and sea birds.

Inputs

- initial turbidity
- turbidity measured during the operational phase

Function

$$\text{Turbidity modification} = \text{Comparison between initial turbidity and turbidity} \quad (4.4.)$$

measured during the operational phase

Rule

The rule of this function is to estimate the difference in turbidity between the initial state and the turbidity measured during the operational phase. If the turbidity measured during the operational phase is higher than the initial state, the pressure is considered as major in application of the precautionary principle.

Weighting step

There is no particular constraint for the turbidity function. According to the precautionary principle, the weighting score is calibrated for the worst pressure case with a score of 1.

Calibration

Step 1

The difficulty to quantify this environmental impact is related to the high variability of turbidity in coastal waters [78]. Typical concentrations range from few mg/l to hundreds mg/l during storm events or near estuarine areas. To quantify the turbidity risk we utilize a binary method which consists of comparing the initial turbidity and turbidity during the installation phase in the Table 4-13.

Table 4-13: calibration pressure score for the turbidity risk.

Result of the function	Pressure Score - PS
turbidity stressor < initial turbidity	0
turbidity stressor ≥ initial turbidity	5

Step 2

The hard substrate benthic habitats are potentiality more vulnerable by an increase of turbidity than soft substrate habitats because of the macroalgea. These macroalgea are indeed among the key species of the benthic habitats of hard substrate and the diminution of light induced by the increase of the turbidity directly affects them. That is the reason why we have assigned the score of 3 for species living in hard substrata and 1 for species in soft substrata. Marine mammals and birds can also be impacted by the increase of the turbidity but the lack of data and the low potential risk has led to a score of 1in the Table 4-14.

Table 4-14: calibration Receptor Score for turbidity risk.

Benthic habitats		**Receptor Score - RS**
Hard substrate benthic habitats (Cemented to hard rock soil types)		3
Soft substrate benthic habitats(Cohesion less soil group)		2
Particular habitats (other)		4
Deep sea birds	**Example of species for user**	**Receptor Score - RS**
0-5m	Fulmar	1
5-30m	Shag/Cormorant/Gannet	2
>30m	Common Guillemot/Puffin/Razorbill	3
Fishes and Marine Mammals		**Receptor Score - RS**
Elasmobranch		3
Bony fish		3
Marine mammals		3

After selecting the appropriate Receptor Score (RS), the EIS step 2 can be obtained using the formula

$$EIS\ step\ 2 = linear\ mapping\ (PSa\ X\ RS) \quad (4.5.)$$

In the case where the receptor is 'regulatory protected', the DTOcean database should be able to identify it during this STEP and then assign the maximum negative EIS score (-100).

Step 3

The final step (STEP 3) takes into account the seasonal distribution of the receptors. If data are available (provided either by the user or the database), EIS step2 will be evaluated to a new value called EIS final using a new matrix containing the information of the receptor monthly absence or occurrence. If there is data the seasonal score (SA) is allocated with a score of one and if there is no data the seasonal score is allocated of a score of zero.

The final Environmental Impact Score is ultimately calculated as follow

$$EIS\ final - Environmental\ impact\ score = SA\ X\ EIS\ step\ 2 \quad (4.6.)$$

4.4.4 Environmental function: Underwater noise

Objective

The goal of this function is to evaluate the impact of underwater noise produced by the devices during the operational phase.

Stressors

The noise created during the operational phase of the devices.

Receptors

Underwater noise produced by devices is a physical pressure that can affect marine mammals and fishes.

Inputs

- Initial underwater noise (=background noise).
- Noise produced by the individual devices [unit: dB re 1µPa (1m)].

Function's formula

The 'underwater noise' function consists of a comparison between the initial underwater noise and the underwater noise level produced by the device.

$$Underwater\ noise = comparison\ of\ the\ underwater\ noise\ of\ the\ devices\ with\ the\ iniital\ underwater\ noise\ in\ the\ area \quad (4.7.)$$

Rule

The rule of this function is to estimate the difference between the initial noise and the noise induced by the devices during the operational phase. If the noise measured during the operational phase is higher than the initial state, the pressure is considered as major in application of the precautionary principle.

Weighting step

There is no particular constraint for the underwater noise function. According to the precautionary principle, the weighting score is calibrated for the worst pressure case with a score of 1.

Calibration

Underwater noise is based on the type of device, the movement of the device and the location of the farm. It was decided to use literature review data to create an overview of the underwater noise induced by known wave and tidal devices.

Underwater noises have been studied from experience of test sites. From the data obtained, noise was classified in several categories (Table 4-15).

- Measurement [<; 100 dB re 1µPa]
- Measurement [100 dB re 1µPa; 150dB re 1µPa]
- Measurement [>150dB re 1µPa]

Table 4-15: Pressure Score underwater noise.

Underwater noise Function Score (FS)		**Pressure Score (PS)**
no concordance of data (Noise stressor < initial underwater noise)		0
concordance of data (Noise stressor ≥ initial underwater noise)	[< 100 dB re 1µPa]	1
	[100 dB re 1µPa-150 dB re 1µPa]	2
	[150 dB re 1µPa-200 dB re 1µPa]	3
	> 200 dB re 1µPa	5

Table 4-16: Example of underwater noise produced by devices.

Example of type of devices	**phase**	**measurement**
Fall of Warness Tidal Energy Test Site (Voith Hydro) 2010	operational	148-158dB re 1µPa (1m)
Lynmouth Bristol Channel (Marine Current Turbines MCT)	operational (1 turbine)	166 dB re 1µPa (1m)
Strangford Lough (Sae Gen turbine)	operational (1 turbine)	165 dB re 1µPa (1m)
Roosevelt Island Tidal Energy Project (Verdant Power tidal)	operational (1turbine)	145 dB re 1µPa (1m)
Admiralty Inlet Tidal Energy Development	operational (1 turbine) (6m)	127 dB re 1µPa (1m)

Wave Energy Test Centre (European Pilot Plant of Wave Energy Oscillating Water Column device)	operational (1 turbine)	151 dB re 1µPa (1m)
Lysekil project (Wave energy converters)	operational	158 dB re 1µPa (1m)

Legends: [27]

dB: decibel
SPL: Sound Pressure Level; the level of the RMS sound pressure. SPL is a root mean square (RMS) quantity and averaging time must be defined.
PTS: Permanent Threshold Shift; auditory damage in the form of permanent hearing sensitivity reduction
TTS: Temporary Threshold Shift (recoverable auditory fatigue)

Step 2

To discriminate in term of sensibility, Step 2 involves three expected type of effect:

- behavioral modification of species,
- TTS - temporal threshold shift,
- PTS - permanent threshold shift.

Behavior effect is considered as a moderate effect unlike TTS and PTS that are considered as major effects because of the potential physiological issues they can generate. So receptor scores are based on the following assignment:

- Behavioral modification: score 3
- TTS: score 5
- PTS: score 5

Values in each level (Behavioral, TTS and PTS) are also species specific. Some examples are given in Table 4-17.

Table 4-17: Receptor Score for the underwater noise function.

Sensitivity threshold	**Species**	**Effect**	**RS**
< 143 dB re 1µPa	Large Odontoncete, odontoncetes, Delphinids, Mysticetes	behavioural	3
[143-224] dB re 1µPa		TTS	5
>224 dB re 1µPa		PTS	5

<160dB re 1µPa	Seals	behavioural	3
[160-200] dB re 1µPa		TTS	5
>200 dB re 1µPa		PTS	5

After selecting the appropriate Receptor Score (RS), the EIS step 2 can be obtained using the formula:

$$EIS\ step\ 2 = linear\ mapping\ (PSa\ X\ RS) \quad (4.8.)$$

In the case of a 'regulatory protected' receptor, the DTOcean database should be able to identify it during this STEP and then assign the maximum negative EIS score (-100).

Step 3

The final step (STEP 3) takes into account the seasonal distribution of the receptors. If data are available (provided either by the user or the database), EIS step2 will be evaluated to a new value called EIS final using a new matrix containing the information of the receptor monthly absence or occurrence. If there is data the seasonal score (SA) is allocated with a score of one and if there is no data the seasonal score is allocated of a score of zero.

The final Environmental Impact Score is ultimately calculated as follow:

$$EIS\ final - Environmental\ impact\ score = SA\ X\ EIS\ step\ 2 \quad (4.9.)$$

4.4.5 Environmental function: Reef effect

Objective

The goal of this function is to evaluate the impact of presence of the devices during the operational phase on the flora and fauna. It is a positive function.

Stressors

Devices represent structures that can potentially become artificial reef.

Receptors

The presence of the device creates a reef effect that develops the underwater flora and fauna life.

Inputs

- Surface area of the underwater part of the devices.
- number of device

- Total surface of the lease area

Function's formula

The 'reef effect' function is a ratio between surface area of the underwater part of the device and the total lease surface area.

$$Reef\ effect\ = \frac{(Surface\ area\ of\ the\ underwater\ part\ of\ the\ devices\ X\ number\ of\ device)}{total\ lease\ surface\ area} \quad (4.10.)$$

Rule

This function is positive so if the result is closed to zero the reef effect of the array is not really pronounced. Closed to one the reef effect is maximal.

Weighting step

For the reef effect function, the constraint is the design of the devices.

Calibration

Step1

Turbine systems are currently preferentially located on hard substrates (level bedrock, boulders) and/or very coarse bottoms (pebbles, stones), which host specific benthic communities, mainly composed of fixed and encrusting organisms. This epifauna therefore occupies a predominant place relative to sediment-dwelling organisms (infauna) [22].

The reef effect like the reserve effect is considered as a positive, except if the device is implanted on a soft substrate. Effects less positive should be considered and should be studied more. 4 values for reef effect impact are given as:

- a low reef effect for 0% to 10% recovery:
- a low reef effect for 10% to 30% recovery.
- a moderate reef effect for recovery between 30% and 50%.
- a high reef effect for recovery higher than 50%.

This gives the Pressure Score PS (Table 4-18).

Table 4-18: Pressure Score of the reef effect.

Reef effect range	PS - Pressure score fitting in reef effect range
[0-0.1[	1
[0.1-0.3[	2
[0.3-0.5]	3
>0.5	5

According to Langhamer et al 2009 [79], colonization on artificial reef is influenced by the age, texture, inclination and position in the water column of the reef. Some studies were done on wave devices, and the assemblage of species depends on the design of the structure. In the words of Langhamer et al .2009 [79] "Vertical surfaces were more densely colonized than horizontal surfaces […]".

It is useful to create a Weighting Score (WS) as a function of the design structure (vertical or horizontal) (Table 4-19).

Table 4-19: Weighting Score for the reef effect.

Types of device	Design	WS-Weighting Score
Wave	horizontal	0.5
Wave	vertical	1
Tidal	Horizontal	0.5
Tidal	vertical	1

At the end of this step the Pressure Score adjusted by the Weighting Score is calculated, the PSa the Pressure Score Adjusted.

Step 2

It is considered that all benthic habitats can be affected by reef, so the highest score (5) is given for all organisms. This value is set by default as there is inevitably a reef effect on all structures [56], [62]. This gives the Receptor Score (Table 4-20).

Table 4-20: Receptor Score for the reef effect.

Receptors	RS-Receptor Score
Hard substrate benthic habitats	5
Soft substrate benthic habitats	5

After selecting the appropriate Receptor Score (RS), the EIS step 2 can be obtained using the formula.

$$EIS\ step\ 2 = linear\ mapping\ (PSa\ X\ RS) \quad (4.11.)$$

Step 3

The final step (STEP 3) takes into account the seasonal distribution of the receptors. If data are available (provided either by the user or the database), EIS step2 will be evaluated to a new value called EIS final using a new matrix containing the information of the receptor monthly absence or occurrence. If there is data the seasonal score (SA) is allocated with a score of one and if there is no data the seasonal score is allocated a score of zero.

The final Environmental Impact Score is ultimately calculated as follows:

$$EIS\ final - Environmental\ impact\ score = SA\ X\ EIS\ step\ 2 \quad (4.12.)$$

4.4.6 Environmental function: reserve effect

Objective

Evaluation of the reserve effect of fishery restriction in the tidal and wave arrays. It is a positive function.

Stressors

The array can have a reserve effect depending on the fishery restrictions.

Receptors

Fishery restriction create a reserve effect that can influence all of the ecosystem.

Inputs

- Fishery restriction surface
- Total lease surface area

Function's formula

The 'reserve effect' function is a ratio between the fishery restriction surface and the total lease surface area.

$$Reserve\ effect\ = \frac{Fishery\ restriction\ surface}{Total\ lease\ surface\ area} \quad (4.13.)$$

Rule

This function is positive so if the result is close to zero the reserve effect of the array is not really pronounced. Closed to one the reserve effect is maximal.

Weighting step

In the reserve effect function the weighting step is linked to the level of fishery restriction.

Calibration

Step1

The highest score of 5 is assigned if the result of the function is higher than 0.5 (Table 4-21).

- a low reserve effect for 0% to 10% recovery
- a low reserve effect for 10% to 30% recovery
- a moderate reserve effect for recovery between 30% and 50%
- a high reserve effect for recovery higher than 50%

Table 4-21: Pressure Score Reserve effect.

Reserve effect range	PS - Pressure score fitting in reserve effect range
[0-0.1[	1
[0.1-0.3[	2
[0.3-0.5]	3
>0.5	5

The reserve effect is linked to the fishery restrictions. If fishery activities are completely prohibited in the area, the reserve effect will be potentially higher than for other restrictions. A Weighting Score WS is used to calibrate this data (Table 4-22).

Table 4-22: Weighting Score for the Reserve effect.

Fishery restrictions	WS-Weighting Score
Fishery complete prohibition	1
Cast net fishing and fish traps authorized	0.5
No restriction	0

At the end of this step the Pressure Score adjusted by the Weighting Score is calculated, the PSa the Pressure Score Adjusted.

Step2

The reserve effect touches each category of marine life. The 4 studied categories are:

- Benthos organism
- Birds
- Marine Mammals
- Fish

Reserve effect impacts positively each category the highest score (5) is given for each type of biological components, giving the Receptor Score (Table 4-23).

Table 4-23: Receptor Score for the reserve effect.

Receptors	Receptor Score
Soft substrate benthic habitats	5
Hard substrate benthic habitats	5
Marine mammals	5
Fishes	5
Birds	5

After selecting the appropriate Receptor Score (RS), the EIS step 2 can be obtained using the formula:

$$EIS\ step\ 2 = linear\ mapping\ (PSa\ X\ RS) \quad (4.14.)$$

Step 3

The final step (STEP 3) takes into account the seasonal distribution of the receptors. If data are available (provided either by the user or the database), EIS step2 will be evaluated to a new value called EIS final using a new matrix containing the information of the receptor monthly absence or occurrence. If there is data the seasonal score (SA) is allocated with a score of one and if there is no data the seasonal score is allocated of a score of zero.

The final Environmental Impact Score is ultimately calculated as follow:

$$EIS\ final - Environmental\ impact\ score = SA\ X\ EIS\ step\ 2 \quad (4.15.)$$

4.4.7 Environmental function: Resting Place

Objective

Evaluation of the impact of emerged parts of the devices used as resting place by the fauna.

Stressors

Certain devices have some emerged parts that can be used as a resting place for some species.

Receptors

In the case of the resting place function pinnipeds (marine mammals) and birds are the biological receptors.

Inputs

- surface area of the emerged part of the device
- number of device
- total of the surface lease area

Function's formula

The 'reserve effect' function is a ration between the fishery restriction surface and total of the lease surface area.

$$Resting\ place = \frac{surface\ area\ of\ the\ emerged\ part\ of\ the\ device\ X\ number\ of\ devices}{total\ surface\ lease\ area} \quad (4.16.)$$

Rule

The impact increases with an increase of the surface area of the emerged parts of the devices. Positive or negative impacts: depends on whether it is dangerous or not for the animals to stand on these structures.

Weighting step

In the resting place function, the weighting step is linked to the dangerous part of devices.

4.4.7.1 Step 1

A resting place is considered as a positive effect and so the Pressure Score PS is positive. (Table 4-24).

- a low resting place for 0% to 10% recovery
- a moderate resting place for 10% to 30% recovery
- a high resting place for recovery between 30% and 70%
- a high resting place for a recovery higher than 70%

Table 4-24: Pressure Score Resting Place.

Resting place range	PS - Pressure score fitting in resting place range
[0 -0,1]	1
[0,1-0,30[	2

[0,30-0,70]	3
>0.70	5

The resting place is defined in this report as a positive function, but this effect can be mitigated by the presence of dangerous parts of a device such as traps and moving parts. It was decided to add a weighting score based on this parameter (Table 4-25).

Table 4-25: Weighting Score for the resting place.

Dangerous Part of the devices	WS-Weighting Score
No dangerous part of devices	1
blades	0.1
turbine shroud	0.1
oscillating water column with cavity	0.1
oscillating bodies with translation part	0.1
oscillating bodies with rotating part	0.1
flexible sleeve between each box (Pelamis)	0.1

At the end of this step the Pressure Score adjusted by the Weighting Score is calculated, the PSa the Pressure Score Adjusted.

Step2

With environmental protection status, the majority of birds and all pinnipeds are protected. A specific list of birds sensitive to resting places is expected to be available shortly. For now, RS is defined under two categories (Table 4-26):

- General birds
- Pinnipeds

Table 4-26: Receptor Score for the resting place.

Species	RS-Receptor Score
Birds	5
Pinnipeds	5

After selecting the appropriate Receptor Score (RS), the EIS step 2 can be obtained using the formula.

$$EIS\ step\ 2 = linear\ mapping\ (PSa\ X\ RS) \qquad (4.17.)$$

Step 3

The final step (STEP 3) takes into account the seasonal distribution of the receptors. If data are available (provided either by the user or the database), EIS step2 will be evaluated to a new value called EIS final using a new matrix containing the information of the receptor monthly absence or occurrence. If there is data the seasonal score (SA) is allocated with a score of one and if there is no data the seasonal score is allocated of a score of zero.

The final Environmental Impact Score is ultimately calculated as follows:

$$EIS\ final - Environmental\ impact\ score = SA\ X\ EIS\ step\ 2 \quad (4.18.)$$

4.5 Optimization / Scenario driven

4.5.1 Wave: Scenario 3: Aegir Shetland Wave Farm – Energy modification function example

Technology specific data for the environmental impact assessment

The device used for this scenario is a Pelamis WEC, composed by five cylindrical section of equal length, interconnected by four joints. For the computations of the environmental assessment, formula used the data given in the D2.4. (Table 4-27).

Table 4-27: Pelamis Dimension.

Dimensions	Pelamis (59)
Length	195 m
Diameter	5.5 m
Number of joints	4

According the D2.4, the scenario is run for 5 different cases, by changing the number of devices across the lease area (Table 4-28).

Table 4-28: 5 cases for the Scenario 3.

Array Layout - Scenarios run (5 cases)
2 devices
5 devices
10 devices
20 devices
50 devices

The representation of the location of devices is shown in the

Figure 4-4 below.

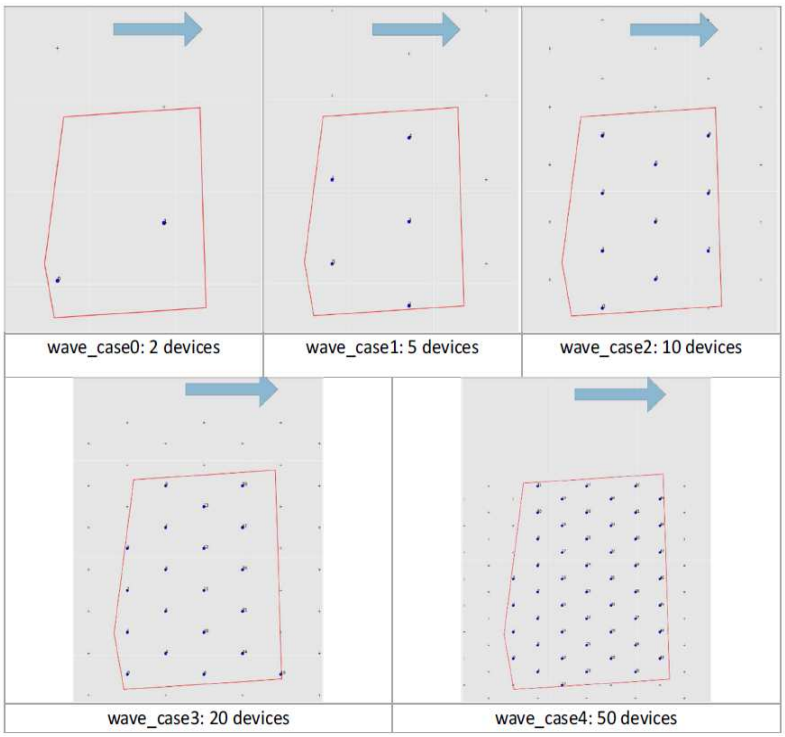

Figure 4-4: Array Layouts for scenario 3.

Environmental specific data from the Aegir EIA scoping [80]:

The wave farm array will be situated within 10km of the south west coast of the Shetland mainland. The position of the devices in the scoping document is located in an area of sandy gravel substrate in the south-west of the lease area. To test the energy modification function in the DTOcean tool for this array we will consequently assume that the Pelamis devices were installed on sandy gravel substrate (Figure 4-5).

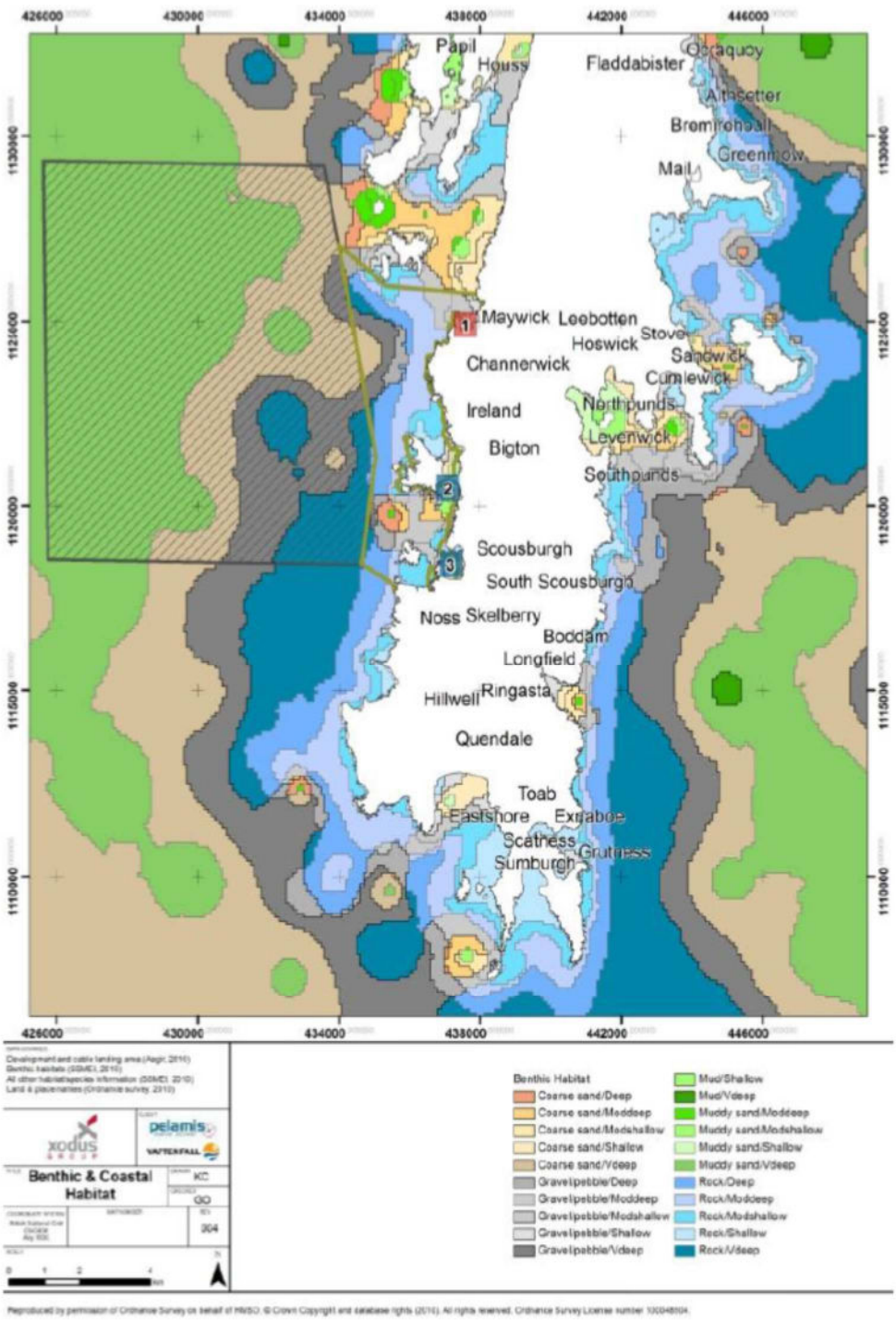

Figure 4-5 : *Map of the benthic habitats in the area of the Aegir Shetland wave farm [80].*

Table 4-29 : Energy modification function general presentation.

General data for the environmental assessment	
Aim	evaluation of the energy modification in the array layout
Stressors	quantity of energy extracted
Receptors	benthic habitats
Inputs	resource reduction
Formula	$Energy\ modification =$ modification of the current (%)
Constraint	Sediment

Step 1: Calibration of the pressure

Table 4-30: Results of energy extraction for the 5 cases of the Scenario 3.

Environmental function : function step	
Cases	**Inputs required : Resource reduction**
Case 0	result of resource reduction: 2.38%
Case 1	result of resource reduction: 3.95%
Case 2	result of resource reduction: 7.01%
Case 3	result of resource reduction: 13.81%
Case 4	result of resource reduction: 29.44%

The tool can compute the formula with the inputs and gives the result. In this case the result is equal to the input (the resource reduction).

$$Energy\ modification = \text{modification of the current } \% \qquad (4.1.)$$

From the result of the function step, the tool automatically takes account the first calibration “the Pressure Score” to give the first Environmental Impact Assessment based on the pressure. The Pressure score is computed from the table of calibration below:

Table 4-7: Energy extraction range and Pressure score.

Function result range	PS-Pressure Score
[0-10%[	0
[10-20%(	1
[20-30%]	3
>30%	5

The results of the first point of the step one (result of the function and calibration associated) is presented in the table below:

Table 4-31: Results of the pressure score of the energy modification function for the 5 cases of the Scenario 3.

Result of the step 1: PS-Pressure Score	
Cases	**PS-Pressure Score**
Case 0	0
Case 1	0
Case 2	0
Case 3	1
Case 4	3

The second point of the step one is to weight the pressure with the environmental constraints, here the sediment type:

Table 4-8: Sediment weighting score.

Constraints : sediments		
Soil group	**Soil types**	**Weighting score**
cohesion less	Loose sand	1
	Medium sand	1
	Dense sand	1
cohesive	Very soft clay	1
	Soft clay	1
	Firm clay	0.5
	Stiff clay	0.5
other	Cemented	0.1
	Soft rock coral	0.1
	Hard glacial till	0.1
	Gravel cobble	0.1
	Hard rock	0.1

In the Aegir Shetland Wave Farm the sediment type is sandy gravel corresponding to the soil group “cohesion less” and a weighting score of 1.

The results of the step one for this example is presented in the table below:

Table 4-32: Results of the pressure score adjusted of the energy modification function for the 5 cases of the Scenario 3.

Result of the step 1: PSa-pressure score adjusted	
Cases	**PSa-pressure score adjusted**
Case 0	0
Case 1	0
Case 2	0
Case 3	1
Case 4	3

Step 2: Qualification of the environmental impact/ RS-receptor score

Table 4-9: Receptor score.

Soil groups	Soil types	RS-receptor score
Benthic habitats of hard substrate (cemented to hard rock soil types)	Rocky mediolittoral habitats, Rocky infralittoral habitats, Rocky circalittoral habitats (coastal and deep)	3
Benthic habitats of soft substrate (cohesion less soil group)	littoral sediment, Infralittoral sediment, Circalittoral sediment (coastal and deep)	1
Particular habitats	Zostera noltii beds, Zostera noltii beds, Maerl beds	4

After selecting the appropriate Receptor Score (RS), The Receptor Sensitive Score (RSS) can be obtained using the equation

$$EIS\ step\ 2 = linear\ maaping\ (PSa\ X\ RS) \qquad (4.2.)$$

Table 4-33: *Results of the EIS step of the energy modification function for the 5 cases of the Scenario 3*

Result of the step 2: EIS step 2	
Cases	**EIS step 2**
Case 0	0
Case 1	0
Case 2	0
Case 3	-13.2
Case 4	-19.6

Step 3: Seasonality of the environmental impact

Finally, the final Environmental Impact Score is ultimately calculated as follows:

$$EIS\ final - Environmental\ impact\ score = SA\ X\ EIS\ step\ 2 \quad (4.1.)$$

Table 4-34: *Seasonal score for the receptor of the energy modification function.*

Soil groups	**SA-Seasonal score**											
	J	F	M	A	M	J	J	A	S	O	N	D
Benthic habitats of hard substrate (cemented to hard rock soil types)	1	1	1	1	1	1	1	1	1	1	1	1
Benthic habitats of soft substrate (cohesion less soil group)	1	1	1	1	1	1	1	1	1	1	1	1
Particular habitats (Zostera beds, Maerl beds)	1	1	1	1	1	1	1	1	1	1	1	1

Table 4-35: *Results of the final EIS step of the energy modification function for the 5 cases of the Scenario 3.*

Result of the step 3: EIS final – Environmental Impact Score												
Cases	J	F	M	A	M	J	J	A	S	O	N	D
Case 0	0	0	0	0	0	0	0	0	0	0	0	0
Case 1	0	0	0	0	0	0	0	0	0	0	0	0
Case 2	0	0	0	0	0	0	0	0	0	0	0	0
Case 3	-13.2	-13.2	-13.2	-13.2	-13.2	-13.2	-13.2	-13.2	-13.2	-13.2	-13.2	-13.2
Case 4	-19.6-	-19.6	-19.6	-19.6	-19.6	-19.6	-19.6	-19.6	-19.6	-19.6	-19.6	-19.6

Considering the scale of impact defined for the environmental impact assessment tool of the DTOcean project , the impact of the energy extraction is considered as null for the cases 0, 1 and 2 and low for the cases 3 and 4.

Figure 4-6 : Scale of impact of the EIAM.

4.5.2 Tidal: Scenario 5: Sound of Islay – Energy modification function example

Technology specific data for the environmental impact assessment

The device used for this scenario is the HS1000, developed by Andritz Hydro Hammerfest. The HS1000 model has a nacelle that can rotate 180° to be face oncoming tides and blades that can reverse their pitch to work with both flood and ebb tides. The 26m diameter rotor is supported via a sloping tower and tripod structure fixed to the seabed using gravity ballast in the legs. For the computations of the environmental assessment, formula used the data given in the D2.4. (**Error! Not a valid bookmark self-reference.**).

Table 4-36 : HS1000 turbine's Dimension.

Dimensions	Andritz Hydro Hammerfest HS1000
Hub height	26 m
Rotor diameter	26 m
Tip height	39 m

According the D2.4, the scenario is run for 5 different cases, by changing the number of devices across the lease area (Table 4-37).

Table 4-37: 5 cases for the Scenario 5.

Array Layout - Scenarios run (5 cases)
2 devices
5 devices
10 devices
20 devices
50 devices

The representation of the location of devices is shown in the Figure 4-7 below.

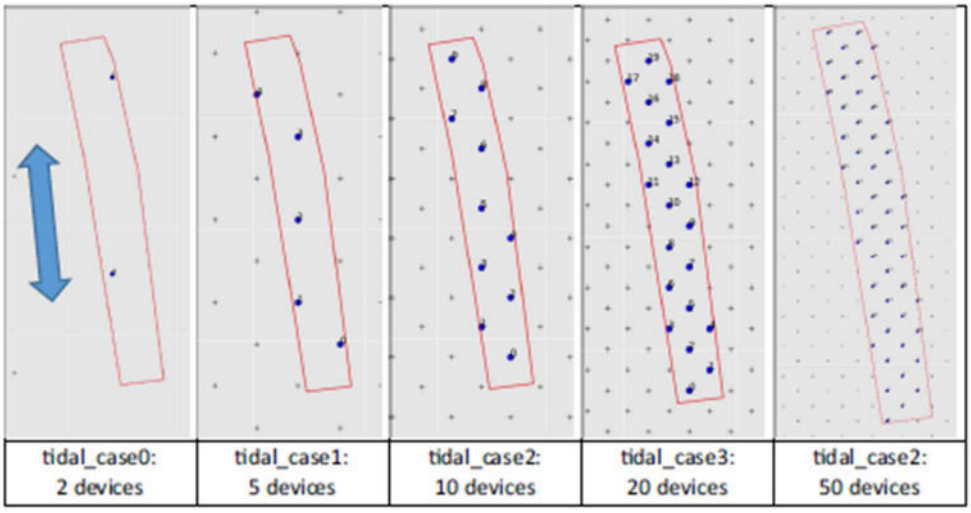

Figure 4-7 : Array Layouts for scenario 5.

Environmental specific data from the environmental impact assessment (EIA) of Sound of Islay tidal array project [81]:

The tidal farm array will be situated on an area of the seabed within the Sound of Islay, just south of Port Askaig. The EIA has shown that the main substrate in the area is a mix of gravelly cobbles and small boulders (Figure 4-8).

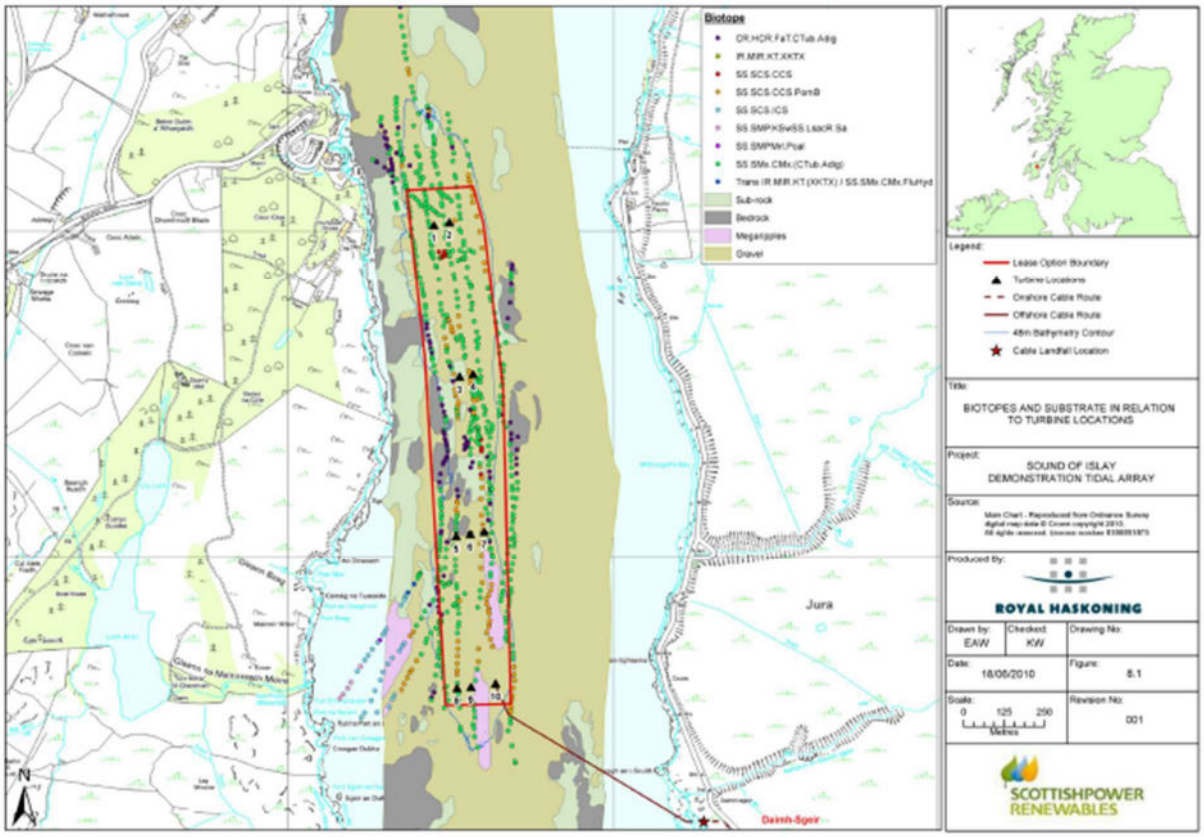

Figure 4-8: Map of the benthic habitats in the area of the Sound of Islay tidal farm *[81]*.

Table 4-29: Energy modification function general presentation.

General data for the environmental assessment	
Aim	evaluation of the energy modification in the array layout
Stressors	quantity of energy extracted
Receptors	benthic habitats
Inputs	resource reduction
Formula	$Energy\ modification =$ modification of the current (%)
Constraint	Sediment

Step 1: Calibration of the pressure

Table 4-38: Results of energy extraction for the 5 cases of the Scenario 5.

Environmental function : function step	
Cases	**Inputs required : Resource reduction**
Case 0	result of resource reduction: 1.49%
Case 1	result of resource reduction: 3.74%
Case 2	result of resource reduction: 7.53%
Case 3	result of resource reduction: 15.35%
Case 4	result of resource reduction: 25.52%

The tool can compute the formula with the inputs and gives the result. In this case the result is equal to the input (the resource reduction).

$$Energy\ modification = modification\ of\ the\ current\ \% \qquad (4.1.)$$

From the result of the function step, the tool automatically takes into account the first calibration "the Pressure Score" to give the first Environmental Impact Assessment based on the pressure. The Pressure score is computed from the table of calibration below:

Table 4-7: Energy extraction range and Pressure score.

Function result range	**PS-Pressure Score**
[0-10%[	0
[10-20%[	1
[20-30%]	3
>30%	5

The results of the first point of the step one (result of the function and calibration associated) is presented in the table below:

Table 4-39: Results of the pressure score of the energy modification function for the 5 cases of the Scenario 5.

Result of the step 1: PS-Pressure Score	
Cases	**PS-Pressure Score**
Case 0	0
Case 1	0
Case 2	0
Case 3	1
Case 4	3

The second point on the step one is to weight the pressure with the environmental constraints, here the sediment type:

Table 4-8: Sediment weighting score.

Constraints : sediments		
Soil group	**Soil types**	**Weighting score**
cohesion less	Loose sand	1
	Medium sand	1
	Dense sand	1
cohesive	Very soft clay	1
	Soft clay	1
	Firm clay	0.5
	Stiff clay	0.5
other	Cemented	0.1
	Soft rock coral	0.1
	Hard glacial till	0.1
	Gravel cobble	0.1
	Hard rock	0.1

In the Sound of Islay Tidal Farm the sediment type is gravel cobble corresponding to a weighting score of 0.1.

The results of the step one is presented in the table below:

Table 4-40: Results of the pressure score adjusted of the energy modification function for the 5 cases of the Scenario 5.

Result of the step 1: PSa-pressure score adjusted	
Cases	**PSa-pressure score adjusted**
Case 0	0
Case 1	0
Case 2	0
Case 3	0.1
Case 4	0.3

Step 2: Qualification of the environmental impact/ RS-receptor score

Table 4-9: Receptor score.

Soil groups	**Soil types**	**RS-receptor score**
Benthic habitats of hard substrate (cemented to hard rock soil types)	Rocky mediolittoral habitats, Rocky infralittoral habitats, Rocky circalittoral habitats (coastal and deep)	3
Benthic habitats of soft substrate (cohesion less soil group)	littoral sediment, Infralittoral sediment, Circalittoral sediment (coastal and deep)	1
Particular habitats	Zostera noltii beds, Zostera noltii beds, Maerl beds	4

After selecting the appropriate Receptor Score (RS), the Receptor Sensitive Score (RSS) can be obtained using the equation

$$EIS\ step\ 2 = linear\ maaping\ (PSa\ X\ RS) \qquad (4.2.)$$

Table 4-41: Results of the EIS step of the energy modification function for the 5 cases of the Scenario 5.

Result of the step 2: EIS step 2	
Cases	**EIS step 2**
Case 0	0
Case 1	0
Case 2	0
Case 3	-11
Case 4	-12.9

Step 3: Seasonality of the environmental impact

Finally, the final Environmental Impact Score is ultimately calculated as follow.

$$EIS\ final - Environmental\ impact\ score = SA\ X\ EIS\ step\ 2 \quad (4.3.)$$

Table 4-42: Seasonal score for the receptor of the energy modification function.

Soil groups	**SA-Seasonal score**											
	J	F	M	A	M	J	J	A	S	O	N	D
Benthic habitats of hard substrate (cemented to hard rock soil types)	1	1	1	1	1	1	1	1	1	1	1	1
Benthic habitats of soft substrate (cohesion less soil group)	1	1	1	1	1	1	1	1	1	1	1	1
Particular habitats (Zostera beds, Maerl beds)	1	1	1	1	1	1	1	1	1	1	1	1

Table 4-43: Results of the final EIS step of the energy modification function for the 5 cases of the Scenario 5.

Result of the step 3: EIS final – Environmental Impact Score												
Cases	J	F	M	A	M	J	J	A	S	O	N	D
Case 0	0	0	0	0	0	0	0	0	0	0	0	0
Case 1	0	0	0	0	0	0	0	0	0	0	0	0
Case 2	0	0	0	0	0	0	0	0	0	0	0	0

Case 3	-11	-11	-11	-11	-11	-11	-11	-11	-11	-11	-11	-11
Case 4	-12.9	-12.9	-12.9	-12.9	-12.9	-12.9	-12.9	-12.9	-12.9	-12.9	-12.9	-12.9

Considering the scale of impact defined for the environmental impact assessment tool of the DTOcean project, the impact of the energy extraction is considered as null for the cases 0, 1 and 2 and low for the cases 3 and 4.

Figure 4-9 : Scale of impact of the EIAM.

5 GENERAL CONCLUSION

In terms of environmental impacts and dependencies on array changes, energy extraction and collision risks are two of the main concerns. Energy extraction can potentially modify sediment transport due to alteration of hydraulics and hydrologic regimes that may reduce the ability of streams to transport sediment and debris, causing deposition of suspended sediments and thereby alter bottom habitats. This can then generate habitat loss, smothering or contamination that directly affects benthic habitats. The impact on perturbations of the water flow and their consequences on sedimentary processes are expected to be much less significant for wave than for tidal energy converters. Collision risks are also directly related to array changes. Currently, collision risks related to wave and tidal devices are still poorly understood due to a lack of installed tidal and wave devices. For birds, collision risks may be mainly related to diving depth attained in the water column, swimming speed, the diurnal rhythm of foraging, location and behavior of species, and sea state in terms of turbidity and water flow. For marine mammals, entanglement is also considered. Overall the risk of collision is in part a function of the mammal's species, but also the body size, swimming behavior and skills, capacity to detect devices as well as the device type. Therefore, the design of devices and array organization are important in preventing collisions and entanglements.

Other impacts considered here include underwater noise, chemical pollution risk, resting places, reef effects and reserve effects. Within the framework of DTOcean, environmental impacts are described through a set of functions that constitute the foundations of the Environmental Impact Assessment Module (EIAM), the purpose of which is to globally assess the environmental impacts generated by the various technological choices to optimize an array of wave or tidal devices. General and specific (based on scenario) recommendations have been proposed for each impact. However, due to the lack of data and feedback from recent developments, these recommendations should be taken with caution. Besides, little is known about the long term effects. As knowledge about environmental impacts will progress in the coming years of MRE array development, the DTOcean EIAM will be able to be updated, thanks to its open source policy, in order to better assess environmental impacts.

6 REFERENCES

[1] DHI, *Mike 21 User Manuel*. 2011.
[2] M. . Longuet-Higgins, "On the joint distribution of the periods and amplitudes of sea waves," *J. Geophys. Res.*, no. 80, pp. 2688–2694, 1975.
[3] Det Norske Veritas, "Environmental Conditions and Environmental Loads: DNV-RP-C205," DNV-RP-C205, 2010.
[4] J. Cruz, *Ocean Wave Energy, Current Status and Future Perspective*, Springer. .
[5] IEC TS 62600-101, "Wave, tidal and other water current converters," *Mar. Energy*.
[6] L. Zhou and P. Frigaard, "Generation and Analysis of Random Waves," 2001.
[7] DTOcean Project, "DTOcean, Deliverable 1.1, 'Detailed deployment scenarios for wave and tidal energy converters'," 2014.
[8] DTOcean Project, "Deliverable 2.2, "Pre-evaluation of array layouts, identified key parameters and their relevant ranges," 2014.
[9] G. Yoshimi, *Random Seas and Design of Maritime Structures*, World Scientific. .
[10] N. Kottegoda and R. Rosso, *Applied Statitiscs for Civil and Environmental Engineers*. Blackwell Publishing, 2008.
[11] I. Katic, J. Hojstrup, and N. . Jensen, "A Simple Model for Cluster Efficiency. In Proc. of the BWEA Conference," 1986, pp. 407–410.
[12] G. . Larsen, *A Simple Wake Calculation Procedure*. 1988.
[13] G. Habenicht, . *Comparison of Different Wake Combination Methods for Offshore Wake Modelling*. 2008.
[14] T. Burton, *Wind Energy Handbook, 2nd Edition*, 2nd ed. 2011.
[15] J. . Whelan, "Modelling of Free Surface Proximity and Wave Induced Velocities around an Horizontal Axis Tidal Stream Turbine. In 7th European Wave and Tidal Energy Conference," Porto, 2007.
[16] M. . Thomson and D. McCowen, *WG3WP4 D1 GH BLOCKAGE MODELLING*. 2010.
[17] S. C. James, E. Seetho, C. Jones, and J. Roberts, "Simulating environmental changes due to marine hydrokinetic energy installations," *OCEANS 2010*, pp. 1–10, 2010.
[18] US Department of Energy, "Report to Congress on the potential environmental effects of marine and hydrokinetic energy technologies," 2009.
[19] M. A. Shields, D. K. Woolf, E. P. Grist, S. A. Kerr, A. Jackson, R. E. Harris, M. C. Bell, R. Beharie, A. Want, E. Osalusi, and others, "Marine renewable energy: the ecological implications of altering the hydrodynamics of the marine environment," *Ocean Coast. Manag.*, vol. 54, no. 1, pp. 2–9, 2011.
[20] C. Frid, E. Andonegi, J. Depestele, A. Judd, D. Rihan, S. I. Rogers, and E. Kenchington, "The environmental interactions of tidal and wave energy generation devices," *Environ. Impact Assess. Rev.*, vol. 32, no. 1, pp. 133–139, 2012.
[21] G. Saunders, G. . Bedford, J. . Trendall, and I. Sotheran, "Guidance on Survey and Monitoring in Relation to Marine Renewables Deployments in Scotland Volume 3: Seals," Scottish Natural Heritage and Marine Scotland, 2011.
[22] M. Lejart, M. Boeuf, A. Barillier, J.-M. Loaec, C. Giry, J. Prevot, C. Auvray, T. Folegot, A. Carlier, J.-P. Delpech, L. Martinez, and B. Cadiou, "Guide to the environmental impact evaluation of tidal stream technologies at sea : GHYDRO," France Energies Marines, 2013.

[23] G. Cada, J. Ahlgrimm, M. Bahleda, T. Bigford, S. D. Stavrakas, D. Hall, R. Moursund, and M. Sale, "Potential impacts of hydrokinetic and wave energy conversion technologies on aquatic environments," *Fisheries*, vol. 32, no. 4, pp. 174–181, 2007.
[24] C. Frid, E. Andonegi, J. Depestele, A. Judd, D. Rihan, S. I. Rogers, and E. Kenchington, "The environmental interactions of tidal and wave energy generation devices," *Environ. Impact Assess. Rev.*, vol. 32, no. 1, pp. 133–139, 2012.
[25] Widdows and Brinsley, 2002.
[26] M. Kadiri, R. Ahmadian, B. Bockelmann-Evans, W. Rauen, and R. Falconer, "A review of the potential water quality impacts of tidal renewable energy systems," *Renew. Sustain. Energy Rev.*, vol. 16, no. 1, pp. 329–341, 2012.
[27] P. E. Robins, S. P. Neill, and M. J. Lewis, "Impact of tidal-stream arrays in relation to the natural variability of sedimentary processes," *Renew. Energy*, vol. 72, pp. 311–321, 2014.
[28] B. Wilson, R. Batty, F. Daunt, and C. Carter, "Collision risks between marine renewable energy devices and mammals, fish and diving birds: Report to the Scottish Executive," 2006.
[29] Bicknell, Votier, Inger, and Atrill, "' The impact of marine renewable energy on birds'.," *Mar. Renew. Biodivers. Fish. Mar. Inst.*, pp. 22–25, 2013.
[30] K.-M. Exo, O. Huppop, and S. Garthe, "Birds and offshore wind farms: a hot topic in marine ecology," *Bull.-Wader Study Group*, vol. 100, pp. 50–53, 2003.
[31] Langton, Davies, and Scott, "Seabird conservation and tidal stream and wave power generation: Information needs for predicting and manging potential impacts.," *Marine Policy*, Aberdeen, p. 8, 2011.
[32] W. J. Grecian, R. Inger, M. J. Attrill, S. Bearhop, B. J. Godley, M. J. Witt, and S. C. Votier, "Potential impacts of wave-powered marine renewable energy installations on marine birds," *Ibis*, vol. 152, no. 4, pp. 683–697, 2010.
[33] S. Dolman and M. Simmonds, "Towards best environmental practice for cetacean conservation in developing Scotland's marine renewable energy," *Mar. Policy*, vol. 34, no. 5, pp. 1021–1027, 2010.
[34] C. Sparling, M. Lonergan, B. Mackey, C. Booth, G. Hastie, D. Gillespie, and J. MacAulay, "Marine Mammals and Tidal Turbines: Understanding true collision risk."
[35] S. Benjamins, V. Harnois, H. Smith, L. Greenhill, L. Johanning, C. Carter, and B. Wilson, "Understanding the potential for marine megafauna entanglement risk from renewable marine energy developments.," Scottish Natural Heritage Commissioned Report, 791, 2014.
[36] R. Inger, M. Attrill, S. Bearhop, A. Broderick, W. James Grecian, D. Hodgson, C. Mills, E. Sheehan, S. Votier, and M. Witt, "Marine renewable energy: potential benefits to biodiversity? An urgent call for research.," *J Appl Ecol*, vol. 46(6), pp. 1145–1153, 2009.
[37] Carter, Wilson, and Black, "Marine renewable energy devices: a collision risk for marine mammals? Proceedings of the ASCOBANS/ECS workshop: offshore wind farms and marine mammals: impacts & methodologies for assessing impacts. San Sebastian," *ECS special publication series*, Spain, 2008.
[38] G. Keenan, C. Sparling, H. Williams, and F. Fortune, "SeaGen Environmental Monitoring Programme Final Report," Royal Haskoning, 2011.

[39] M. Baeye and M. Fettweis, “In situ observations of suspended particulate matter plumes at an offshore wind farm, southern North Sea,” *Geo-Mar. Lett.*, pp. 1–9, 2015.
[40] J. E. Cloern, “Turbidity as a control on phytoplankton biomass and productivity in estuaries,” *Cont. Shelf Res.*, vol. 7, no. 11, pp. 1367–1381, 1987.
[41] V. L. Todd, I. B. Todd, J. C. Gardiner, E. C. Morrin, N. A. MacPherson, N. A. DiMarzio, and F. Thomsen, “A review of impacts of marine dredging activities on marine mammals,” *ICES J. Mar. Sci. J. Cons.*, vol. 72, no. 2, pp. 328–340, 2015.
[42] T. Strod, Z. Arad, I. Izhaki, and G. Katzir, “Cormorants keep their power: visual resolution in a pursuit-diving bird under amphibious and turbid conditions,” *Curr. Biol.*, vol. 14, no. 10, pp. R376–R377, 2004.
[43] H. Tillin, J. Hiddink, S. Jennings, and M. Kaiser, “Chronic bottom trawling alters the functional composition of benthic invertebrate communities on a sea-basin scale,” *Mar. Ecol. Prog. Ser.*, vol. 318, pp. 31–45, 2006.
[44] S. . Robinson and P. . Lepper, “Scoping sudy: review of current knowledge of underwater noise emissions from wave and tidal stream energy devices.,” The Crown Estate, 2013.
[45] D. R. Ketten, “Marine mammal auditory systems: a summary of audiometric and anatomical data and implications for underwater acoustic impacts,” *Polarforschung*, vol. 72, no. 2/3, pp. 79–92, 2004.
[46] J. Nedwell, A. Brooker, and R. BArham, “Assessment of underwater noise during the installation of export power cables at the Beatrice Offshore Wind Farm. Subacoustech Environmental Report.,” Subacoustech Environmental, E318R0106, 2012.
[47] M. . Commission, “Marine mammals and noise: a sound approach to research and management,” Report to Congress from the Marine Mammal Commission, 2007.
[48] W. W. Clark, “Recent studies of temporary threshold shift (TTS) and permanent threshold shift (PTS) in animals,” *J. Acoust. Soc. Am.*, vol. 90, no. 1, pp. 155–163, 1991.
[49] A. B. Gill and M. D. Bartlett, “Literature review on the potential effects of electromagnetic fields and subsea noise from marine renewable energy developments on Atlantic salmon, sea trout and European eel. Scottish Natural Heritage Commissioned Report,” 2010.
[50] H. Slabbekoorn, N. Bouton, I. van Opzeeland, A. Coers, C. ten Cate, and A. N. Popper, “A noisy spring: the impact of globally rising underwater sound levels on fish,” *Trends Ecol. Evol.*, vol. 25, no. 7, pp. 419–427, 2010.
[51] H. Bailey, B. Senior, D. Simmons, J. Rusin, G. Picken, and P. M. Thompson, “Assessing underwater noise levels during pile-driving at an offshore windfarm and its potential effects on marine mammals,” *Mar. Pollut. Bull.*, vol. 60, no. 6, pp. 888–897, 2010.
[52] J. Nedwell, A. Turnpenny, J. Lovell, S. Parvin, R. Workman, J. Spinks, and D. Howell, “A validation of the dBht as a measure of the behavioural and auditory effects of underwater noise.,” Department for Business, Enterprise and Regulatory Reform., E318R0106, 2007.
[53] B. Southall, A. Bowles, W. Ellison, J. Finneran, R. Gentry, C. Greene, D. Kastak, D. Ketten, J. Miller, P. Nachtigall, W. Richardson, J. Thomas, and P. Tyack, “Marine Mammal Noise Exposure Criteria. Aquatic Mammals,” vol. 33, p. 4, 2007.
[54] M. Vikas and G. Dwarakish, “Coastal Pollution: A Review,” *Aquat. Procedia*, vol. 4, pp. 381–388, 2015.

[55] R. Polmear, J. Stark, D. Roberts, and A. McMinn, "The effects of oil pollution on Antarctic benthic diatom communities over 5years," *Mar. Pollut. Bull.*, vol. 90, no. 1, pp. 33–40, 2015.
[56] M. S. Islam and M. Tanaka, "Impacts of pollution on coastal and marine ecosystems including coastal and marine fisheries and approach for management: a review and synthesis," *Mar. Pollut. Bull.*, vol. 48, no. 7, pp. 624–649, 2004.
[57] H. L. Osborn and S. E. Hook, "Using transcriptomic profiles in the diatom Phaeodactylum tricornutum to identify and prioritize stressors," *Aquat. Toxicol.*, vol. 138, pp. 12–25, 2013.
[58] P. S. Rainbow, "Trace metal bioaccumulation: models, metabolic availability and toxicity," *Environ. Int.*, vol. 33, no. 4, pp. 576–582, 2007.
[59] K. A. Dafforn, J. A. Lewis, and E. L. Johnston, "Antifouling strategies: history and regulation, ecological impacts and mitigation," *Mar. Pollut. Bull.*, vol. 62, no. 3, pp. 453–465, 2011.
[60] S. Lambert, K. Thomas, and A. Davy, "Assessment of the risk posed by the antifouling booster biocides Irgarol 1051 and diuron to freshwater macrophytes," *Chemosphere*, vol. 63, no. 5, pp. 734–743, 2006.
[61] Mark et al., *Marine Renewable Energy technology and Env*. Springer, 2014.
[62] O. Langhamer, "Artificial reef effect in relation to offshore renewable energy conversion: state of the art," *Sci. World J.*, vol. 2012, 2012.
[63] S. Thanner, T. McIntosh, and S. Blair, "Development of benthic and fish assemblages on artificial reef materials compared to adjacent natural reef assemblages in Miami-Dade County, Florida.," *Bull. Mar. Sci.*, vol. 78, pp. 57–70, 2006.
[64] E. Linley, T. Wilding, K. Black, A. Hawkins, and S. Mangi, "Review of the reef effects of offshore wind farm structures and their potential for enhancement and mitigation. Report from PML Applications Ltd and the Scottish Association for Marine Science to the Department for Business, Enterprise and Regulatory Reform (BERR)," PML Applications Ltd and the Scottish Association for Marine Science to the Department for Business, RFCA/005/0029P, 2007.
[65] O. Langhamer, "The Scientific World Journal Artificial Reef Effect in relation to Offshore Renewable Energy Conversion: State of the Art," 2012.
[66] D. Sheehy and Vik, "The role of constructed reefs in non-indigenous species introductions and range expansions," *Ecol. Eng.*, vol. 36, pp. 1–11, 2010.
[67] M. Kaiser, K. Clarke, H. Hinz, M. Austen, P. Somerfield, and I. Karakassis, "Global analysis of response and recovery of benthic biota to fishing," *Mar. Ecol. Prog. Ser.*, vol. 311, pp. 1–14, 2006.
[68] A. Carlier and J.-P. Delpech, "Synthèse bibliographique: Impacts des câbles sous-marins sur les écosystèmes côtiers.," IFREMER, Synthèse bibliographique, 2011.
[69] H. Lindeboom, H. Kouwenhoven, M. Bergman, S. Bouma, S. Brasseur, R. Daan, R. Fijn, D. de Haan, S. Dirksen, R. van Hal, R. , Hille Ris Lambers, R. ter Hofstede, K. Krijgsveld, M. Leopold, and M. Scheidat, "Short-term ecological effects of an offshore wind farm in the Dutch coastal zone ; a compilation.," *Environ. Re-Search Lett.*, 2011.
[70] S. P. Neill, J. R. Jordan, and S. J. Couch, "Impact of tidal energy converter (TEC) arrays on the dynamics of headland sand banks," *Renew. Energy*, vol. 37, no. 1, pp. 387–397, 2012.

[71] CITES, “Convention on International Trade in Endangered Species of Wild Fauna and Flora.” .
[72] CMS, “Convention on the Conservation of Migratory Species of Wild Animals.” 2015.
[73] ASCOBANS, “Agreement on the Conservation of Small Cetaceans in the Baltic, North East Atlantic, Irish and North Seas.” .
[74] ACCOBAMS, “Agreement on the Conservation of Cetaceans of the Black Sea, Mediterranean Sea and contiguous Atlantic Area.” .
[75] International Whaling Commission, “The International Whaling Commission (IWC).” 2015.
[76] European Commission, “Natura 2000 network.” 2015.
[77] M. Tasker, M. Amundin, M. Andre, A. Hawkins, W. Lang, T. Merck, A. Scholik-Schlomer, J. Teilmann, F. Thomsen, S. Werner, and others, “MARINE STRATEGY FRAMEWORK DIRECTIVE Task Group 11 Report Underwater noise and other forms of energy,” *Eur. Com.*, 2010.
[78] Commission OSPAR, “Lignes directrices sur la meilleure pratique environmentale (BEP) pour la pose et l’exploitation de câbles.,” 2012.
[79] O. Langhamer, D. Wilhelmsson, and J. Engström, “Artificial reef effect and fouling impacts on offshore wave power foundations and buoys–a pilot study,” *Estuar. Coast. Shelf Sci.*, vol. 82, no. 3, pp. 426–432, 2009.
[80] Aegir Wave Power Ltd, “Aegir EIA scoping Proposed 10MW Wave Energy Farm Scoping Report.,” Edinburgh, A-30351-S00-REPT-01-R08, 2011.
[81] ScottishPower Renewables, “Sound of Islay Demonstration Tidal Array Environmental Statement,” 2010.

ACRONYMS:

H_{m0}	Significant wave height
T_p	Peak Period
T_e	Energy period
PDF	Probability density function
CDF	Cumulative distribution function
N	Size of the sample
N_b	Number of bins
TI	Turbulence intensity
SSH	Sea Surface Elevation
U_t	Magnitude of the tidal stream velocity vector
AAEP	Array Annual Energy Production
CFD	Computational fluid dynamics
Fr	Froude number
MRE	Marine Renewable Energy
EIAM	Environmental Impact Assessment Module
EIS	Environmental Impact Score
PS	Pressure Score
PSa	Pressure Score Adjusted
WS	Weighting Score
WP	Work Package
CITES	Convention on International Trade in Endangered Species of Wild Fauna and Flora
CMS	Convention on Migratory Species
ASCOBANS	Agreement of the Conservation of Small Cetaceans in the Baltic North East Atlantic Irish and North Seas
ACCOBAMS	Agreement of the Conservation of Cetaceans of the Black Sea, Mediterranean Sea and contiguous Atlantic Sea
MSFD	Marine Strategy Framework Directive